Title
Mechanobiology of TGFβ receptor dynamics and signaling in chondrocytes

Author
Rys, Joanna

Publication Date
2015

Peer reviewed|Thesis/dissertation

Mechanobiology of TGFβ receptor dynamics and signaling in chondrocytes

by

Joanna P. Rys

DISSERTATION

Submitted in partial satisfaction of the requirements for the degree of

DOCTOR OF PHILOSOPHY

in

Bioengineering

in the

GRADUATE DIVISION

of the

UNIVERSITY OF CALIFORNIA, SAN FRANCISCO

AND

Acknowledgments

This work and my completion of a PhD would not have been possible without the scaffold of support built by my mentors, coworkers, family, and friends.

I would like to acknowledge faculty members that served on my committees and played instrumental roles in this work – Dr. Sanjay Kumar, Dr. Zev Gartner, Dr. Alfred Kuo, Dr. Jeffrey Lotz, Dr. Ralph Marcucio, and Dr. Rich Schneider. You all helped shape my project and challenged me to tackle the most exciting and daunting questions. It was always a pleasure to discuss my research with such intellectual and scientifically passionate individuals.

I absolutely want to thank my friends and family. My friends – Connie, Paul, Aaron, Katie, Alec, Aditya, Sarah, John-Michael – you joined me at my low points and high points, and always made me laugh. Each of you contributes to my life in such a unique and meaningful way, and I am excited to share the next steps of my journey with all of you. My family – Mom, Dad, Tomek, and Brittany – you have challenged me from the very beginning to be my best and this experience was no different. Thank you for pushing me to succeed and for taking so much pride in my accomplishments. I would not have made it to the end without you.

Last but certainly not least, thank you to all Ortho lab members and my mentor, Tamara Alliston. It has been awesome working with all of you. You shaped me into the scientist I am today, and you made the journey so entertaining along the way. You helped me excel at science and push knowledge boundaries, all while encouraging me to be my goofy self. Those late nights and weekends in lab are so much easier when you have someone like Tamara cheering you on and someone like Dave to say “I feel like I caught a rare animal” after a successful experiment. To Tamara – I cannot believe how much we conquered and accomplished together! You helped me

realize how tough and persistent I can be, and I truly feel like I can take on anything now. Your approach to and excitement for science are so unique, and you have this incredible way of making me feel like a superstar even when I'm in a rut – thank you for everything! Thanks to Jeannie, Jennifer, Faith, Britta, Annie, Kate, Courtney, and Neha for coffee dates, happy hours, laughs, and for being kickass female scientists.

And if you are reading this, then thank you too! I hope you enjoy reading about my journey.

Abstract

The ability of cells to generate a coordinated response to the biochemical and physical cues in the microenvironment is fundamental to development and disease. Signaling pathways integrate these cues through physical and functional interactions among ligands, receptors, and effectors. Cell surface receptors, in particular, undergo spatially regulated organization and multimerization to calibrate the quality, intensity, and duration of the signal and response. However, the mechanisms by which receptors enable the cell to achieve a concerted response to diverse biochemical and physical cues remain unclear. Elucidating these mechanisms is essential for understanding how the cellular microenvironment regulates growth factor signaling. To investigate these spatial and molecular mechanisms, we optimized novel high-resolution and single particle tracking imaging techniques and utilized established biochemical assays to examine TGFβ signaling. TGFβ receptors type I and II are discretely localized to segregated spatial domains at the cell surface. Interestingly, integrin-rich focal adhesions organize TβRII around TβRI, altering receptor mobility and limiting the integration of TβRII while sequestering TβRI at these sites. Disruption of cellular tension leads to a collapse of this highly ordered and unique spatial organization of TGFβ receptors at sites of adhesions. Furthermore, a change in cellular tension through ROCK inhibition or culturing cells on compliant substrates drives the formation of heteromeric TβRI/TβRII complexes and the phosphorylation of downstream TGFβ effector Smad3. This work details a novel mechanically-regulated mechanism whereby focal adhesions and cell tension control the spatial organization, multimerization, and signaling of growth factor receptors in the TGFβ pathway, providing new insight into the cellular mechanisms that integrate biochemical and physical cues.

Table of Contents

List of Figures and Tables

Chapter 1

Mechanobiology of TGFβ signaling in the skeleton

Joanna P. Rys[a,b], David A. Monteiro[a,b], and Tamara Alliston[a,b,c,1].

[a]University of California, Berkeley–University of California, San Francisco Graduate Program in Bioengineering, University of California, Berkeley, CA 94720

[b]Department of Orthopaedic Surgery, University of California, San Francisco, CA 94143

[c]Department of Bioengineering and Therapeutic Sciences, Department of Otolaryngology–Head and Neck Surgery, and Eli and Edythe Broad Center of Regeneration Medicine and Stem Cell Research, University of California, San Francisco, CA 94143

[1]To whom correspondence should be addressed. Email: tamara.alliston@ucsf.edu

The authors declare no conflict of interest.

Abstract

Physical and biochemical cues play fundamental roles in the skeleton at both the tissue and cellular levels. The precise coordination of these cues is essential for skeletal development and homeostasis, and disruption of this coordination can drive disease progression. The growth factor TGFβ is involved in both the regulation of and response to the physical microenvironment. It is essential to summarize the current findings regarding the mechanisms by which skeletal cells integrate physical and biochemical cues so that we can identify and address remaining gaps that could ultimately improve skeletal health. In this review, we describe the role of TGFβ in mechanobiological signaling in bone, cartilage, and tendon at the tissue and cellular levels. We provide detail on how static and dynamic physical cues at the macrolevel are transmitted to the microlevel, ultimately leading to regulation at each level of the TGFβ pathway and to cell differentiation. The continued integration of engineering and biological approaches is needed to answer many remaining questions, such as the mechanisms by which cells generate a coordinated response to physical and biochemical cues. We propose one such mechanism, through which an optimal physical microenvironment regulates TGFβ signaling to induce skeletal cell differentiation.

Overview

Among their many essential roles, skeletal tissues routinely encounter mechanical forces as part of their structural, locomotor, and protective functions. The unique extracellular matrix (ECM) of each skeletal tissue is central to this mechanical behavior. Lest we view the skeleton as the static infrastructure of the body, this ECM is dynamic and biologically regulated. For example, changes in either metabolism or mechanics profoundly impact bone mass and quality (1,2). Likewise, biological and physical cues are able to direct the composition and organization of the ECM of bone, cartilage, tendon, and other musculoskeletal tissues. Through cellular and molecular mechanisms that are becoming increasingly clear, a feedback loop continuously balances the mechanical integrity of these tissues with ever-changing physical demands.

Recent advances in cellular mechanobiology highlight the role of transforming growth factor-beta (TGFβ) in both arms of this feedback loop. On one side, TGFβ is a well-known regulator of ECM synthesis and remodeling that can specify the material quality of the ECM (3,4). On the other, TGFβ signaling is integral to the cellular response to physical cues (5). Therefore, this review focuses on TGFβ in the mechanobiological mechanisms by which skeletal cells and extracellular matrices integrate physical and biochemical cues to support skeletal function. These mechanisms are essential for skeletal homeostasis and their deregulation contributes to diseases ranging from post-traumatic osteoarthritis to bone fragility, both of which have been integrally linked to defects in TGFβ signaling (6-8). This mechanistic understanding has the potential to reveal novel molecules and pathways that can be targeted therapeutically to improve skeletal health.

TGFβ signaling in the skeleton

TGFβ is the prototype of a large family of growth factors that also includes BMPs, activins, and GDFs. Like other family members, TGFβ itself regulates diverse cellular behaviors ranging from fate specification, lineage selection, and differentiation, to epithelial-mesenchymal transition, migration, proliferation, and apoptosis (9). At a high level, TGFβ signals through a complex of heterotetrameric transmembrane receptor serine/threonine kinases. Once the TGFβ ligand is activated from its latent form – via integrin-mediated activation, cellular tension, or acid- or protease-mediated cleavage – it binds directly to a pair of type II receptors (10-14). The ligand-bound TβRII complex recruits and phosphorylates two type I receptors (TβRI) – either Alk5 or Alk1 (15,16). TβRI, in turn, phosphorylates and activates Smad2/3 proteins and multiple non-canonical effectors, such as Smad1/5/8, RhoA, TAK1, and Akt (17,18). In complex with Smad4, phosphorylated Smads translocate to the nucleus where they interact with sequence-specific transcription factors, coactivators, and corepressors to modulate gene expression.

The effect of TGFβ signaling on cell behavior is highly context-dependent. TGFβ activity depends on cell-intrinsic factors, such as the composition of cell-surface receptor complexes or the availability of specific transcription factors, as well as cell-extrinsic factors, such as the activity of other signaling pathways or the physical features of the ECM (19). This complexity is evident in TGFβ-mediated control of mesenchymal differentiation into chondrogenic and osteogenic lineages. TGFβ-activated Smad3 promotes chondrogenic differentiation by facilitating recruitment of the coactivator CBP to transcriptional complexes containing the chondrogenic transcription factor Sox9 (20,21). On the other hand, TGFβ inhibits osteogenic differentiation through Smad3 recruitment of the corepressor histone deacetylase 4 to repress

Runx2-inducible osteogenic gene expression (22,23). As will be discussed later, cell-extrinsic differences in ECM stiffness or topography further influence the ability of TGFβ to promote chondroinduction of MSCs (24). Thus, the combination of cell-intrinsic factors and cues presented in the cellular microenvironment dramatically alter the activity of the TGFβ pathway in skeletal cell differentiation.

In addition to influencing cell differentiation, another key function of TGFβ is its ability to control ECM synthesis and remodeling. TGFβ regulates the expression of various ECM proteins, such as fibronectin, collagens, and other matrix glycoproteins (9). Depending on the cell type and context, TGFβ also controls the expression of proteases such as matrix metalloproteases (MMPs) and their inhibitors (TIMPs) (25,26). In this way, TGFβ can stimulate or limit ECM remodeling. The ECM, in turn, regulates TGFβ signaling. Heparan sulfate domains of many ECM proteins such as fibronectin bind and sequester TGFβ in the ECM (27). Small leucine-rich proteoglycans such as biglycan and decorin sequester TGFβ in the skeletal ECM, coordinating the control of bone marrow stromal cell fate (28). Not only do these protein/protein interactions provide spatial control of ligand availability, but they also regulate the activation of latent TGFβ. The ECM of the skeleton, in particular, has high local concentrations of TGFβ (29).

In part because of its role in regulating skeletal cell differentiation and ECM synthesis, TGFβ plays a vital role in the development and homeostasis of many skeletal tissues. TGFβ, let alone the other TGFβ family members, has been implicated in over one dozen human skeletal diseases, most recently in the bone fragility associated with osteogenesis imperfecta (6,30). Many *in vitro* and *in vivo* studies have elucidated cellular and molecular mechanisms that underlie these

actions. This insight has motivated the development of pharmacologic agents to manipulate TGFβ signaling therapeutically. Several clinical trials are currently exploring the utility of these agents for a variety of conditions, including those in the skeleton (31). Because of the scope of this topic, we refer readers to other articles that review the important role of TGFβ signaling in the skeleton and in skeletal disease (3,30,32,33). Here we focus on the role of TGFβ in the regulation of skeletal extracellular matrices and in the response of skeletal cells to macromechanical physical cues and to physical cues within the extracellular matrix.

Multi-scale mechanobiology of the skeleton

Distinct features of the ECM, comprised of fibers and ground substance, support the mechanical function of each skeletal tissue. Almost all skeletal tissues utilize collagen fibers to provide toughness and resistance to tension, most notably the tendons and ligaments. The ground substance of skeletal extracellular matrices is more variable. Hard tissues such as bone, dentin, and enamel rely on mineral to provide resistance to deformation, whereas viscoelastic tissues such as cartilage and intervertebral disc employ proteoglycans to provide resistance to compression. Progress in understanding the mechanobiology of bone, cartilage, and tendon can serve as a foundation for more detailed analyses of dentin, intervertebral disc, and other less well-studied skeletal tissues.

Each skeletal tissue senses and responds to physical cues at multiple hierarchical scales. Locomotion produces macromechanical forces that bone experiences as compressive and tensile strains, depending on the specific local geometries of each bone (34). The same motion is able to produce compression and osmotic pressure in cartilage and tension in tendon. The fibers and

ground substance of the skeletal ECM and skeletal cells respond to these forces in a variety of ways (Figure 1.1). For example, skeletal loading forces fluid through canalicular networks in bone that osteocytes sense as shear flow (35). Upon compression of cartilage, water is depleted from the proteoglycan-rich ECM, resulting in osmotic pressure changes in chondrocytes (36-38). Tenocytes experience stretch-induced changes in cellular tension (39).

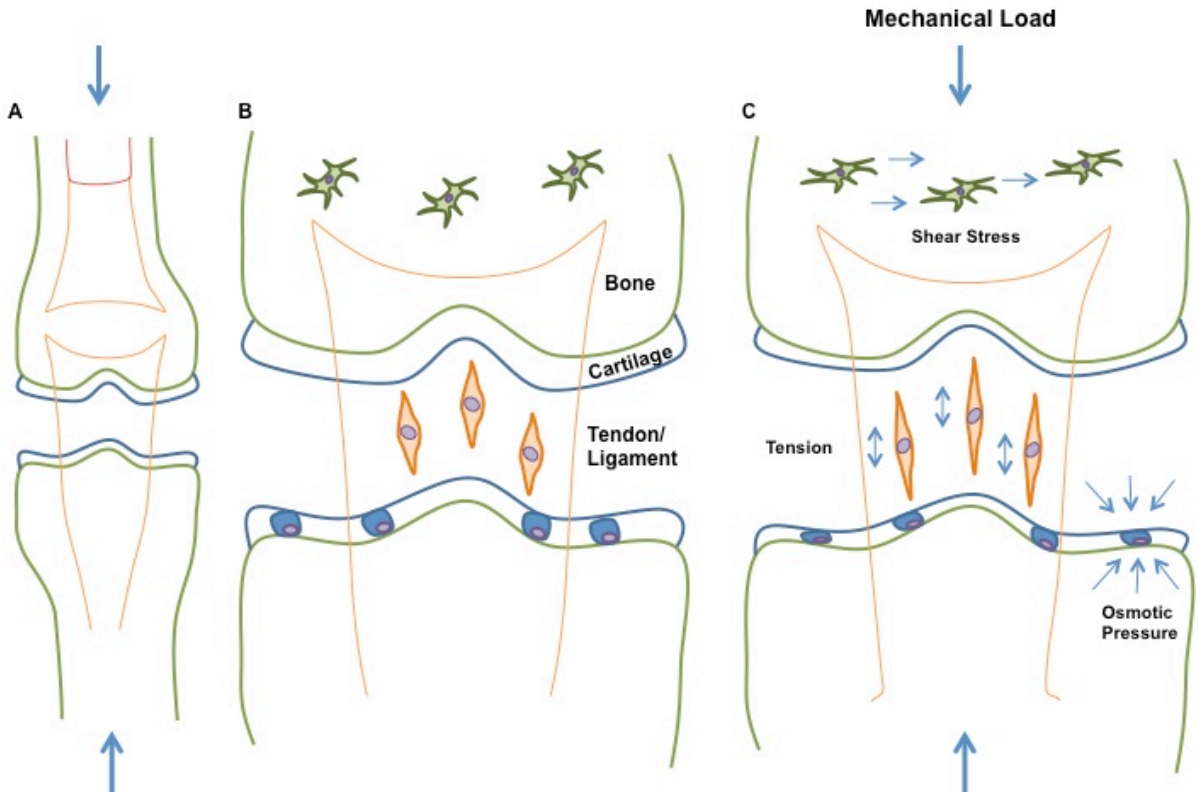

Figure 1.1 Transmission of load from macromechanical forces to the cellular level. Mechanical forces produced by locomotion uniquely affects each tissue (bone, cartilage, tendon, A) at the macroscale and microscale levels (B). Loading forces fluid through the canalicular networks in bone, where osteocytes reside and sense this load as shear stress (C). During the same loading regimen, cartilage experiences compression and water is depleted from its proteoglycan-rich matrix, resulting in osmotic pressure differences in chondrocytes (C). Mechanical loading of the joint increases tension of the patellar ligament/tendon and the tenocytes within experience stretch-induced changes in cell tension (C).

Even at rest, changes in the material properties and organization of the ECM alter cellular tension. Through actomyosin contractility, cells generate cellular tension by pulling on the ECM at integrin-rich focal adhesions. This process initiates a host of molecular responses which reveal the effect of physical cues at the molecular scale, for example by stretching proteins to expose hidden domains that alter binding or enzymatic activity (40,41). These changes impact cellular behaviors from migration to differentiation (42). Critical studies examining skeletal differentiation of mesenchymal progenitors (MSCs) revealed the profound effect of ECM stiffness and shape on lineage selection (43,44). For example, McBeath et al. showed that substrate shape and cell spreading directs lineage selection between osteoblast or adipocyte fates by modulating Rho activity (45).

Micrometer-sized topographical features, such as the roughness of a titanium surface, influence cell behaviors including osteoblast attachment and the expression of osteoinductive transcription factors (46). Dalby et al. further demonstrated that osteoprogenitors on disordered nanoscale features preferentially expressed bone-specific ECM proteins, osteopontin and osteocalcin, and formed bone nodule-like structures (47). Such microstructures also regulate chondrocyte proliferation (48). Furthermore, these physical cues alter the cellular response to growth factor signaling, such that specific cues enhance the chondroinductive effects of TGFβ (24,49). Thus, physical cues intersect with biological systems at each of these length scales.

Additional studies are needed to span these length scales to answer fundamental questions. Among the questions are “What are the mechanisms by which cells discriminate among the many types of macromechanical cues present in the skeleton?” and “How do cells integrate

signaling by physical and biochemical cues?". Disciplinary gaps present challenges to finding these answers, in part because our insight into the macro-level derives more heavily from engineering and materials science, whereas cellular biology and biophysics inform our understanding of molecular scale mechanobiology. Therefore, this review seeks to provide macromechanical context for mechanobiological observations in skeletal biology.

Tissue-level roles of TGFβ in skeletal mechanobiology

Static and dynamic physical cues regulate skeletal tissue development and homeostasis, influencing material and mechanical properties. These properties deteriorate during disease, altering the ability of these tissues to withstand and respond to mechanical load. TGFβ signaling is essential throughout all of these processes. It contributes to the regulation and response to physical cues, such that disruption of TGFβ signaling impacts tissue development and activity. TGFβ is also deregulated during disease processes, which can further drive skeletal disease progress. Understanding the coupling of physical cues and TGFβ at the macroscale level is important for tissue regeneration efforts.

Bone

Bone exists in a state of dynamic equilibrium, undergoing competing processes of formation and resorption. Crosstalk among osteoblasts, osteoclasts, and osteocytes maintains bone mass even in the face of changing mechanical or metabolic demands (1,2). In particular, mechanical loads stimulate an increase in bone mass through a Wnt-dependent mechanism (50). Mechanical load represses osteocyte expression of sclerostin, a secreted antagonist of the osteoinductive Wnt pathway (51). TGFβ also plays a critical role in the anabolic response of bone to mechanical

load, such that ablation of TGFβ receptors prevents load-induced bone formation and repression of sclerostin expression (50). This occurs in part through mechanosensitive regulation of Smad3 phosphorylation. Therefore, mechanical load regulates the activity of the two key pathways that regulate bone homeostasis - TGFβ and Wnt - through mechanisms that are coupled but remain to be fully elucidated.

Many other factors in addition to bone mass influence the ability of bone to resist fracture. These factors, collectively considered 'bone quality', include bone geometry, trabecular microarchitecture, and ECM material properties, among others (52). The material properties of bone ECM are site-specific, biologically regulated, and functionally essential, and are controlled by TGFβ signaling through a TGFβ, TβRI/TβRII, Smad3, and Runx2 dependent mechanism (36). They can be regulated postnatally by pharmacologic antagonists of TGFβ signaling (37,38). This TGFβ-dependent control of bone quality may contribute to the fragility in patients with osteogenesis imperfecta, in which collagen mutations deregulate the activity of the TGFβ pathway (6). Though TGFβ is clearly mechanosensitive in bone and in other tissues, the extent to which bone quality is mechanoregulated through a TGFβ-dependent pathway remains to be determined.

Cartilage

Cartilage serves as a viscoelastic, lubricated cushion allowing for joint articulation with minimal wear. Though 80% water, the cartilage ECM is mainly comprised of proteoglycans such as aggrecan and hyaluronic acid and both fibrillar and non-fibrillar collagens. The integrity of articular cartilage ECM is regulated in part by mechanical loading. While healthy loads promote

cartilage homeostasis, excessive loads can also be harmful (53). During loading, water is forced out of the ECM, imparting direct strain to chondrocytes in addition to generating secondary physical cues such as fluid shear stress and hydrostatic and osmotic pressures (54-56). Chondrocytes respond to these physical cues through multiple mechanisms including ion channels, focal adhesions, and primary cilia (57-59). For example, O'Conor et al. identified TRPV4 as an osmotically sensitive transducer of mechanical loading that regulates cartilage ECM synthesis (60).

These mechanotransduction participants are important for growth factor signaling, such that integrins modulate mechanosensitive chondroinduction by TGFβ (24,61) and primary cilia support the chondrocyte response to hedgehog signaling (62). Indeed, deregulation of either TGFβ or hedgehog signaling has been implicated in osteoarthritic degeneration of articular cartilage (7,63). As cartilage degrades, the material properties of cartilage also change (64). The extent to which these physical changes in the cellular microenvironment contribute to the loss of chondrocyte homeostasis in arthritis remains to be determined. Additional research into these mechanobiologic mechanisms is needed to improve our understanding of and ability to prevent or treat this widespread debilitating disease. Already this insight has been applied to advance the use of stem cells for cartilage tissue regeneration, as discussed below.

Tendon

The closely-packed parallel collagen fibers within tendons affords them the ability to withstand and transfer large tensile forces from muscle to bone (65). Mechanical loading and exercise each modulate tendon ECM synthesis and remodeling. For example, Langberg et al. showed that

human physical training boosted type I collagen turnover in Achilles' tendons (66). In mice, treadmill running was shown to increase the presence of myofibroblasts in patellar tendons, suggesting that tendons are actively repaired and remodeled under high loads (67). In addition, chronic exercise alters the expression of TGFβ3 in supraspinatus tendon as well as in ligaments (68,69). This increase is coincident with an increase in circulating TGFβ following exercise, though this could come from a variety of non-skeletal sources such as platelets (70,71). Disruption of TGFβ signaling results in the complete loss of tendon tissue (72,73). TGFβ coordinates tenocyte differentiation in the developing limb, in part by inducing expression of the tendon lineage-specific transcription factor, scleraxis (74). Tendon homeostasis also requires the TGFβ effector Smad3, which binds scleraxis and Mohawk, another key tenocyte transcription factor (75). TGFβ also participates in development of the tendon insertion, which itself is a mechanosensitive process (76).

Development and regeneration

As for the tendon insertion, physical cues are essential for the development and maintenance of skeletal tissues. The critical role of mechanical cues in developing the correct size and shape of skeletal elements, especially in the integration of musculoskeletal tissues at tendon insertions, is well-known (76-78). Postnatal mechanical forces also participate in defining bone shape, as exemplified by the increasing angle of the femoral head relative to the diaphysis in humans throughout early childhood (79). Insight derived from the study of physical cues in skeletal development and homeostasis has been applied practically to promote the directed differentiation of progenitor cell populations for skeletal tissue regeneration. A common approach has been to compare chondroinduction of stem cells in response to inductive physical and biochemical cues,

both alone and in combination. The combination of physical and biochemical cues often has a synergistic effect on chondrocyte differentiation and articular cartilage ECM synthesis. For example, treatment of bovine cartilage explants with dynamic compression and insulin-like growth factor (IGF-I) increased protein and proteoglycan synthesis significantly more than either stimulus alone (80). Elder et al. showed that the combination of hydrostatic pressure and TGFβ treatment increased Young's modulus and collagen content in bovine articular cartilage over levels resulting from application of hydrostatic pressure or treatment with TGFβ alone (81). While it is clear that physical cues can prime cells for a more robust response to growth factor stimulation, the mechanisms by which cells integrate these diverse stimuli remain to be determined.

Cellular and molecular roles of TGFβ in skeletal mechanobiology

The effect of static and dynamic physical cues on TGFβ signaling has been examined in multiple tissues, including in the skeleton. Collectively, these studies reveal the mechanosensitive regulation of the TGFβ pathway from ligands and receptors to transcription factors in the nucleus (Table 1). These mechanisms have proven relevant for diverse cell types in and out of the musculoskeletal system and represent molecular solutions to the fundamental cellular challenge of integrating diverse biochemical and physical cues to generate a coordinated cellular response.

TGFβ mRNA and protein expression

The expression and activity of the TGFβ ligands are sensitive to a wide variety of physical stimuli. It has long been established that physical cues regulate TGFβ1 expression at the mRNA and protein levels in both cartilage and bone. In 1994, Raab-Cullen et al. found that the application of mechanical load to tibial periosteal bone rapidly induces TGFβ mRNA levels (82). Sakai et al. demonstrated that physiological levels of fluid shear stress increase TGFβ1 protein expression in osteoblast-like Saos-2 cells (83). Since osteocytes sense shear stress following macromechanical load, the effect of shear stress on TGFβ expression helps to couple physical and biological signals to control of bone remodeling. In cartilage, cyclic compression on hMSCs in scaffolds stimulates mRNA and protein expression of TGFβ1 and TGFβ3, both of which can promote chondrogenesis (84). Static physical cues such as ECM stiffness, shape, or topography also regulate TGFβ1 ligand expression. TGFβ1 mRNA is increased as chondrocytes grow on an inductive substrate stiffness that promotes chondrogenic gene expression, and this autocrine TGFβ induction accounts for a significant fraction of the functional benefit of these physical cues (24). TGFβ1 expression is also sensitive to topography cues in bone implants, such that

production is higher on rough surfaces than on smooth surfaces (85). Therefore, regulation of TGFβ ligand expression is a key mechanism by which cells respond to physical cues.

Activation of latent TGFβ ligand

Not only is the TGFβ ligand regulated at the transcriptional level, but it is also undergoes post-translation control. TGFβ is synthesized in an inactive form that is covalently linked to the latency-associated protein (LAP) (86). This small latent complex prevents the recognition of the TGFβ ligand by its receptors and therefore prevents induction of downstream signaling. In the majority of cells, the small latent TGFβ complex is bound by latent TGFβ-binding protein to form the large latent complex. This large latent complex is sequestered within the ECM, essentially providing cells with a reservoir of latent TGFβ (77,87). Depending on the cell or tissue type and the physiological context, multiple mechanisms activate latent TGFβ, including integrin-mediated activation, cellular tension, or proteolytic cleavage (10-13). In bone, osteoclast protease and acid secretion are involved in the activation of latent TGFβ. The mildly acidic environment formed during bone resorption to help dissolve the bone matrix is thought to denature LAP and disrupt the interaction between LAP and TGFβ (14). In myofibroblasts, generation of cellular tension directly activates latent TGFβ1 bound within a rigid ECM (13). One proposed mechanism for this activation is transmission of high cellular tension through integrins to TGFβ via the RGD sites in LAP. Cellular tension transmitted through these protein-protein complexes induces a conformational change to release active TGFβ from LAP (13).

Whether tension-dependent activation of latent TGFβ operates in other skeletal cell types remains to be determined. Nonetheless, important findings in cartilage and tendon suggest the

role of similar mechanisms. Albro et al. demonstrated that mechanical shearing of synovial fluid can activate a substantial amount of latent TGFβ, which then remains stable in synovial fluid (88). In addition, mechanical stretching of tendon fibroblasts increases secretion of TGFβ (89). Maeda et al. found that tendon transection *in vivo* increases activated TGFβ levels (90). *In vitro*, when exposed to mechanical force by fluid shear stress, tenocytes express much higher levels of TGFβ1. Together, these results suggest that sudden interruption of tensile loading by complete tendon transection might destabilize the surrounding structure of the ECM, releasing active TGFβ (90). A precise mechanism for activation in these contexts is not yet fully understood. In bone, deregulation of latent-TGFβ activation results in Camurati-Engelmann disease (91-94). Therefore, it will be especially important to determine the extent to which these mechanosensitive mechanisms of latent TGFβ activation occur in bone at the tissue or cellular level.

TGFβ signaling at the receptor level

For TGFβ and for other signaling pathways, the regulation of receptor clustering, multimerization, and internalization affects ligand binding and effector recruitment as well as downstream signal intensity and duration (95-98). For example, the internalization and endocytosis pathways of TGFβ receptors influence receptor function and activity (96). Receptor internalization through clathrin-coated pits promotes downstream TGFβ activity, as the Smad2 anchor SARA is enriched. In contrast, internalization through lipid raft-caveolar pathways leads to receptor degradation by interactions with Smad7-Smurf2 (99). TGFβ receptors have also been shown to interact with integrins (100), a key component of the mechanotransduction pathway, such that an active integrin β1 subunit is required for collagen-induced Smad activation.

Nonetheless, a direct link between physical cues and TGFβ receptor organization and activity has only recently been established.

We recently demonstrated for the first time that cellular tension regulates the spatial organization and multimerization of TGFβ receptors at sites of cellular focal adhesions in chondrocytes (61). Specifically, focal adhesions discretely organize TGFβ receptors such that TβRI is included within adhesions and TβRII is specifically excluded from these sites. Disruption of cellular tension through the use of chemical inhibitors or culturing cells on compliant substrates releases this highly structured organization and drives TβRI/TβRII heteromerization, leading to an increase in downstream effector Smad phosphorylation. Receptor multimerization thus acts as a mechanism for mechanocoupling of TGFβ receptor signaling, and possibly for other pathways (61,101). Others have shown that the solid-state presentation of ligands plays a critical role in structuring multimeric receptor clusters. For example, major histocompatibility complexes (MHC) bound to antigen presenting cells are able to structure the organization of T cell receptors (101). Likewise, ligands embedded in the ECM, such as TGFβ or collagen II, may be important for the structured organization of both TGFβ receptors and integrin α2β1 (61,102). These protein complexes may create geometric constraints that structure receptor clusters and provide focal adhesions with the capability to integrate signaling between physical and biochemical cues.

This organization and its sensitivity to cell tension have several functional implications. For example, the organized TGFβ receptors at focal adhesions would have increased access to the reservoir of tension-activated TGFβ in the ECM, especially in response to stiff substrates or mechanical loads. Furthermore, this organization might provide a mode to sequester TGFβ

receptors and prevent activation of downstream signaling until the optimum threshold of physical cues is encountered. This optimum likely acts as a gradient, such that the threshold for activation may vary not only between cell types, but also range depending on physical properties of the microenvironment, the presence or combination of biological factors, or even the stage of cell differentiation. Although preliminary findings show this observation is conserved across multiple cell types, more work is needed to determine the extent to which this receptor organization is present in and relevant to bone and other skeletal cells. It will also be interesting to study whether this spatial organization changes during cell differentiation or in disease. During disease processes ranging from vascular disorders to osteoarthritis, the TβRII multimerization partner inappropriately switches from Alk5 to Alk1 (103). Although we do not observe any organizational differences between Alk5 and Alk1 so far, it will be interesting to examine the spatial organization of TGFβ receptors in osteoarthritic chondrocytes, where the surrounding physical environment and the biological mechanisms are disrupted.

Downstream TGFβ effectors

Recent studies have revealed the ability of physical cues to regulate downstream components of the TGFβ pathway within the context of cell differentiation. Smad3 phosphorylation, localization, and transcriptional activity are regulated by physical cues during differentiation of chondrocytes on substrates of varying stiffness (24). Allen et al. demonstrated that ECM stiffness is sufficient to induce Smad3 phosphorylation and nuclear translocation, as well as Sox9 and Col2a1 expression, even in the absence of exogenous TGFβ (24). Interestingly, the combination of ECM stiffness and exogenous TGFβ leads to a synergistic induction of downstream signaling relative to either cue alone. Similar findings of tension-dependent regulation of Smad3 were

observed in during TGFb-inducible epithelial mesenchymal transition (104), as well as with Smad1 in osteoinduction of MSCs grown in spread or confined configurations (105). At a larger scale, during load-induced bone formation, mechanical load rapidly represses TGFβ signaling, leading to reduced phosphorylation and activity of downstream effectors Smad2 and Smad3 (50). This response seems to be acutely sensitive to other factors, potentially including the type or magnitude of strain. More work is needed to elucidate the effects of static and dynamic physical cues on downstream effector Smad activity in both cartilage and bone.

In addition to the canonical TGFβ effectors like Smad3, YAP and TAZ are effectors shared by TGFβ and mechanotransduction cascades. They act as nuclear relays of mechanical signals from ECM stiffness and cell shape. Nuclear translocation of YAP/TAZ is dependent on Rho activity and cellular tension (106). YAP/TAZ function is required for osteogenic differentiation of MSCs on a stiff ECM (106). Transfer of cellular tension to the nucleus is essential for activation of YAP/TAZ signaling in response to dynamic stretch (107). Even in vivo, MT1-MMP (*Mmp14*)-dependent changes in the local ECM microenvironment were required for YAP/TAZ nuclear translocation in the regulation of osteogenic differentiation (108). YAP and TAZ are also transcriptional coregulators that can direct the nuclear localization of Smad2/3 in embryonic stem cells (109). Whether YAP/TAZ nuclear localization contributes to the stiffness-sensitive translocation of Smad3 remains to be determined (24).

Molecular Model of a Physical Optimum for TGFβ signaling

These findings collectively reveal the close relationship between physical cues and TGFβ signaling, and further suggest the presence of a signaling feedback mechanism. For example, we and others have reported that the effect of substrate stiffness or cellular tension/Rho/ROCK activity on downstream TGFβ signaling is synergistic and nonlinear (24,110). We propose a model (Figure 2) by which the combination of an optimal physical environment and TGFβ best drive the induction of skeletal cell differentiation. In a sub-optimal physical environment, TGFβ receptors are sequestered from each other at sites of adhesion. Furthermore, due to lack of cell tension in this environment, integrins are unable to release TGFβ from its latent form. This results in basal levels of downstream TGFβ signaling. Addition of exogenous TGFβ to this microenvironment leads to an increase in TGFβ signaling away from sites of adhesion and an induction in downstream Smad effectors. In an environment with optimal physical cues – either static (e.g. ECM stiffness) or dynamic (e.g. mechanical loading) – TGFβ receptors are no longer sequestered from each other, allowing them to form a complex and initiate downstream signaling. Upon this more ideal substrate, integrins release activated TGFβ ligand from its latent form, and the ligand can bind to TGFβ receptors that are already in a primed position. Addition of exogenous TGFβ to this physical environment results in multimerization and activation of TGFβ receptors at and away from sites of adhesion, leading to increased levels of downstream Smad activity and an ideal situation for TGFβ-inducible differentiation. Interestingly, Allen et al. demonstrated that ECM stiffness alone can induce TGFβ1 expression, which might participate in this feedback mechanism, further driving the activation of TGFβ signaling and differentiation within the optimal physical environment (24). The physical cues that comprise this optimum environment may differ between cell and tissue types, and may vary from development to

disease. Furthermore, it is important to note that these cues most likely act through a gradient or threshold levels rather than a simple "on/off" mechanism, further adding to the complexity of this proposed mechanism.

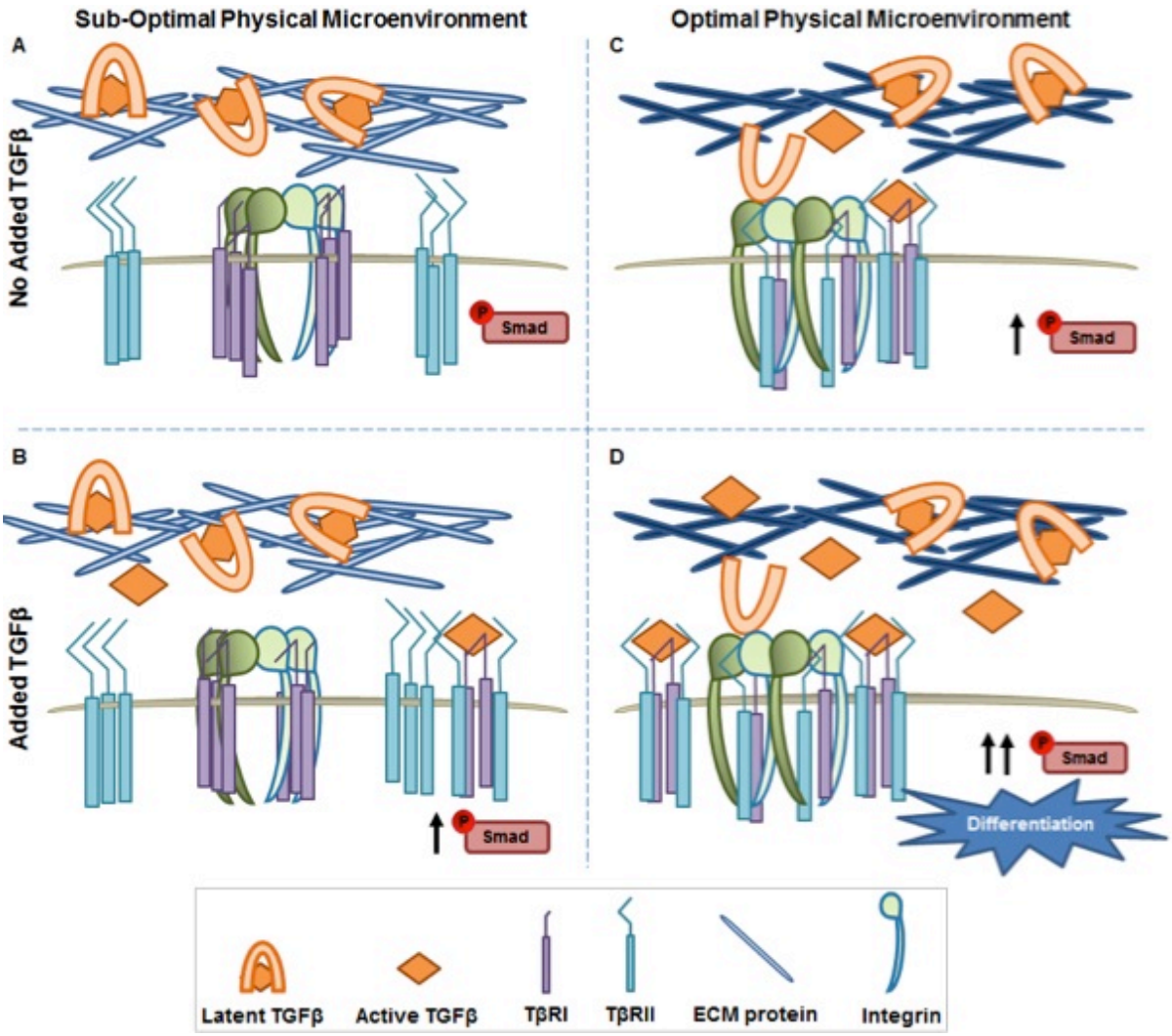

Figure 1.2. Proposed mechanism of interaction between physical cues and TGFβ in inducing skeletal cell differentiation. In a non-optimum physical microenvironment (A, B), TGFβ receptors are sequestered from each other at sites of adhesion. Due to lack of ideal cellular tension, integrins are unable to release activated TGFβ ligand from the ECM. This combination of cues leads to basal levels of downstream TGFβ signaling (A), unless exogenous TGFβ is added (B). Upon addition of TGFβ, TGFβ receptors away from sites of sequestration at adhesions are able to bind the ligand and initiate downstream signaling (B). In an optimum physical microenvironment (C, D), the sequestration of TGFβ receptors at sites of adhesion is released. The receptors are able to bind active ligand that was released by integrin interactions with LAP (C). Addition of TGFβ to the optimum physical microenvironment leads to a synergistic induction of downstream TGFβ signaling and an ideal microenvironment to induce skeletal cell differentiation (D).

Summary

In this review, we summarize the ability of static and dynamic physical cues to regulate TGFβ signaling from the ligand to the nuclear level in skeletal cells. We propose a mechanism that might enable cells to recognize an optimal physical environment and generate a coordinated response to the complex cues in the microenvironment, thus regulating TGFβ signaling and inducing cell differentiation. However, many questions remain regarding the cell's ability to distinguish between and integrate such cues in a manner that regulates both behavior at the cellular scale and properties at the tissue scale. It will be interesting to not only answer these questions, but also to investigate how these abilities and the gradients of cues shift between cell types or during differentiation, homeostasis, and disease progression. The continued elucidation of these mechanisms will provide essential insight into the roles that these integrated cues play in skeletal processes from development to disease.

Acknowledgements

This work was supported by National Science Foundation Graduate Research Fellow Program Grant No. 1144247 (J.R.), Department of Defense through the National Defense Science and Engineering Graduate Fellowship Program (D.M.), National Institute of Arthritis, Musculoskeletal and Skin Disease R21 AR067439-01 (T.A.), National Institute of Dental and Craniofacial Research R01 DE019284 (T.A.), and Department of Defense Peer-Reviewed Orthopaedic Research Program OR130191 (T.A.). Any opinions, findings, and conclusions or recommendations expressed in this material are those of the author and do not necessarily reflect the views of the National Science Foundation.

Table 1.1. Effects of physical cues on TGFβ signaling

mRNA and protein expression			
TGFβ1 mRNA	Substrate stiffness	Chondrocytes, cell	Allen et al. (24)
TGFβ1 protein	Substrate stiffness	Chondrocytes, cell	Allen et al. (24)
TGFβ mRNA	Mechanical load	Bone, tissue	Raab-Cullen et al. (82)
TGFβ1 protein	Shear stress	Bone, cell	Sakai et al. (83)
TGFβ1,3 mRNA	Cyclic compression	Chondrocytes, cell	Li et al. (84)
TGFβ1,3 protein	Cyclic compression	Chondrocytes, cell	Li et al. (84)
TGFβ1 protein	Topography	Bone, cell	Lohman et al. (85)
Ligand			
TGFβ ligand, activation	Cell tension, substrate stiffness	Myofibroblasts	Wipff et al. (13)
TGFβ ligand, activation	Shear stress	Cartilage, tissue	Albro et al. (88)
TGFβ ligand, activation	Mechanical stretch	Tendon, cell	Skutek et al. (89)
TGFβ ligand, activation	Tensile load, shear stress	Tendon, tissue and cell	Maeda et al. (90)
Receptor			
TGFβ receptor, organization	Cell tension, ROCK activity	Chondrocytes, cell	Rys et al. (61)
Effectors			
Smad3, nuclear translocation	Substrate stiffness	Cartilage, cell	Allen et al. (24)
Smad3, phosphorylation	Substrate stiffness	Cartilage, cell	Allen et al. (24)
Smad2/3, phosphorylation	Mechanical load	Bone, tissue	Nguyen et al. (50)
Smad1, nuclear translocation	Cell shape, ROCK activity	Bone, cell	Wang et al. (105)
Smad1, phosphorylation	Cell shape, ROCK activity	Bone, cell	Wang et al. (105)
YAP/TAZ, nuclear translocation	Substrate stiffness, Rho activity	Bone, cell	Dupont et al. (106)
YAP/TAZ, nuclear translocation	Dynamic stretch, strain transfer	MSC, cell	Driscoll et al. (107)
Skeletal cell differentiation			
Sox 9, Collagen II	Substrate stiffness	Cartilage, cell	Allen et al. (24)
Alkaline phosphatase	Cell density, shape, tension, RhoA activity	Bone, tissue	McBeath et al. (45)
Collagen II	Substrate stiffness	Cartilage, cell	Park et al. (49)

References

1. Alliston, T. (2014). Biological regulation of bone quality. Curr Osteoporos Rep 12, 366-375.
2. Robling, A. G., Castillo, A. B. & Turner, C. H. (2006). Biomechanical and molecular regulation of bone remodeling. Annu Rev Biomed Eng 8, 455-498.
3. Tang, S. Y. & Alliston, T. (2013). Regulation of postnatal bone homeostasis by TGFbeta. Bonekey Rep 2, 255.
4. Balooch, G., Balooch, M., Nalla, R. K., Schilling, S., Filvaroff, E. H., Marshall, G. W., Marshall, S. J., Ritchie, R. O., Derynck, R. & Alliston, T. (2005). TGF-beta regulates the mechanical properties and composition of bone matrix. Proc Natl Acad Sci U S A 102, 18813-18818.
5. Hinz, B. (2015). The extracellular matrix and transforming growth factor-beta1: Tale of a strained relationship. Matrix Biol 47, 54-65.
6. Grafe, I., Yang, T., Alexander, S., Homan, E. P., Lietman, C., Jiang, M. M., Bertin, T., Munivez, E., Chen, Y., Dawson, B., Ishikawa, Y., Weis, M. A., Sampath, T. K., Ambrose, C., Eyre, D., Bachinger, H. P. & Lee, B. (2014). Excessive transforming growth factor-beta signaling is a common mechanism in osteogenesis imperfecta. Nat Med 20, 670-675.
7. Blaney Davidson, E. N., van der Kraan, P. M. & van den Berg, W. B. (2007). TGF-beta and osteoarthritis. Osteoarthritis Cartilage 15, 597-604.
8. van de Laar, I. M., Oldenburg, R. A., Pals, G., Roos-Hesselink, J. W., de Graaf, B. M., Verhagen, J. M., Hoedemaekers, Y. M., Willemsen, R., Severijnen, L. A., Venselaar, H., Vriend, G., Pattynama, P. M., Collee, M., Majoor-Krakauer, D., Poldermans, D., Frohn-Mulder, I. M., Micha, D., Timmermans, J., Hilhorst-Hofstee, Y., Bierma-Zeinstra, S. M., Willems, P. J., Kros, J. M., Oei, E. H., Oostra, B. A., Wessels, M. W. & Bertoli-Avella, A. M. (2011). Mutations in SMAD3 cause a syndromic form of aortic aneurysms and dissections with early-onset osteoarthritis. Nat Genet 43, 121-126.
9. Schilling, S. H., Hjelmeland, A. B., Rich, J. N. & Wang, X. F. (2008). TGF-beta: A Multipotential Cytokine. In The TGF-beta Family (Derynck, R. & Miyazono, K., eds), pp. 45-77, Cold Spring Harbor Laboratory Press, Cold Spring Harbor.
10. Munger, J. S., Huang, X. Z., Kawakatsu, H., Griffiths, M. J. D., Dalton, S. L., Wu, J. F., Pittet, J. F., Kaminski, N., Garat, C., Matthay, M. A., Rifkin, D. B. & Sheppard, D. (1999). The integrin alpha v beta 6 binds and activates latent TGF beta 1: A mechanism for regulating pulmonary inflammation and fibrosis. Cell 96, 319-328.
11. Munger, J. S. & Sheppard, D. (2011). Cross talk among TGF-beta signaling pathways, integrins, and the extracellular matrix. Cold Spring Harb Perspect Biol 3, a005017.
12. Annes, J. P., Munger, J. S. & Rifkin, D. B. (2003). Making sense of latent TGF beta activation. Journal of Cell Science 116, 217-224.
13. Wipff, P.-J., Rifkin, D. B., Meister, J.-J. & Hinz, B. (2007). Myofibroblast contraction activates latent TGF-beta 1 from the extracellular matrix. Journal of Cell Biology 179, 1311-1323.
14. Oursler, M. J. (1994). Osteoclast synthesis and secretion and activation of latent transforming growth factor beta. J Bone Miner Res 9, 443-452.
15. Oh, S. P., Seki, T., Goss, K. A., Imamura, T., Yi, Y., Donahoe, P. K., Li, L., Miyazono, K., ten Dijke, P., Kim, S. & Li, E. (2000). Activin receptor-like kinase 1 modulates

transforming growth factor-beta 1 signaling in the regulation of angiogenesis. Proc Natl Acad Sci U S A 97, 2626-2631.
16. Wrana, J. L., Ozdamar, B., Le Roy, C. & Benchabane, H. (2008). Signaling Receptors of the TGF-beta Family. In The TGF-beta Family (Derynck, R. & Miyazono, K., eds), pp. 151-177, Cold Spring Harbor Laboratory Press, Cold Spring Harbor.
17. Feng, X. H. & Derynck, R. (2005). Specificity and versatility in tgf-beta signaling through Smads. Annu Rev Cell Dev Biol 21, 659-693.
18. Derynck, R. & Zhang, Y. E. (2003). Smad-dependent and Smad-independent pathways in TGF-beta family signalling. Nature 425, 577-584.
19. Massague, J. (2012). TGFbeta signalling in context. Nat Rev Mol Cell Biol 13, 616-630.
20. Furumatsu, T., Tsuda, M., Taniguchi, N., Tajima, Y. & Asahara, H. (2005). Smad3 induces chondrogenesis through the activation of SOX9 via CREB-binding protein/p300 recruitment. J Biol Chem 280, 8343-8350.
21. de Crombrugghe, B., Lefebvre, V., Behringer, R. R., Bi, W., Murakami, S. & Huang, W. (2000). Transcriptional mechanisms of chondrocyte differentiation. Matrix Biol 19, 389-394.
22. Alliston, T., Choy, L., Ducy, P., Karsenty, G. & Derynck, R. (2001). TGF-beta-induced repression of CBFA1 by Smad3 decreases cbfa1 and osteocalcin expression and inhibits osteoblast differentiation. EMBO J 20, 2254-2272.
23. Kang, J. S., Alliston, T., Delston, R. & Derynck, R. (2005). Repression of Runx2 function by TGF-beta through recruitment of class II histone deacetylases by Smad3. EMBO J 24, 2543-2555.
24. Allen, J. L., Cooke, M. E. & Alliston, T. (2012). ECM stiffness primes the TGF beta pathway to promote chondrocyte differentiation. Molecular Biology of the Cell 23, 3731-3742.
25. Edwards, D. R., Murphy, G., Reynolds, J. J., Whitham, S. E., Docherty, A. J., Angel, P. & Heath, J. K. (1987). Transforming growth factor beta modulates the expression of collagenase and metalloproteinase inhibitor. EMBO J 6, 1899-1904.
26. Sehgal, I. & Thompson, T. C. (1999). Novel regulation of type IV collagenase (matrix metalloproteinase-9 and -2) activities by transforming growth factor-beta1 in human prostate cancer cell lines. Mol Biol Cell 10, 407-416.
27. Chen, Q., Sivakumar, P., Barley, C., Peters, D. M., Gomes, R. R., Farach-Carson, M. C. & Dallas, S. L. (2007). Potential role for heparan sulfate proteoglycans in regulation of transforming growth factor-beta (TGF-beta) by modulating assembly of latent TGF-beta-binding protein-1. J Biol Chem 282, 26418-26430.
28. Bi, Y., Stuelten, C. H., Kilts, T., Wadhwa, S., Iozzo, R. V., Robey, P. G., Chen, X. D. & Young, M. F. (2005). Extracellular matrix proteoglycans control the fate of bone marrow stromal cells. J Biol Chem 280, 30481-30489.
29. Pelton, R. W., Saxena, B., Jones, M., Moses, H. L. & Gold, L. I. (1991). Immunohistochemical localization of TGF beta 1, TGF beta 2, and TGF beta 3 in the mouse embryo: expression patterns suggest multiple roles during embryonic development. J Cell Biol 115, 1091-1105.
30. Alliston, T., Piek, E. & Derynck, R. (2008). TGF-beta Family Signaling in Skeletal Development, Maintenance, and Disease. In The TGF-beta Family (Derynck, R. & Miyazono, K., eds), pp. 667-723, Cold Spring Harbor Laboratory Press, Cold Spring Harbor.

31. Akhurst, R. J. & Hata, A. (2012). Targeting the TGFbeta signalling pathway in disease. Nat Rev Drug Discov 11, 790-811.
32. Janssens, K., ten Dijke, P., Janssens, S. & Van Hul, W. (2005). Transforming growth factor-beta1 to the bone. Endocr Rev 26, 743-774.
33. Fox, S. W. & Lovibond, A. C. (2005). Current insights into the role of transforming growth factor-beta in bone resorption. Mol Cell Endocrinol 243, 19-26.
34. Sugiyama, T., Price, J. S. & Lanyon, L. E. (2010). Functional adaptation to mechanical loading in both cortical and cancellous bone is controlled locally and is confined to the loaded bones. Bone 46, 314-321.
35. Schaffler, M. B., Cheung, W. Y., Majeska, R. & Kennedy, O. (2014). Osteocytes: master orchestrators of bone. Calcif Tissue Int 94, 5-24.
36. Chang, J. L., Brauer, D. S., Johnson, J., Chen, C. G., Akil, O., Balooch, G., Humphrey, M. B., Chin, E. N., Porter, A. E., Butcher, K., Ritchie, R. O., Schneider, R. A., Lalwani, A., Derynck, R., Marshall, G. W., Marshall, S. J., Lustig, L. & Alliston, T. (2010). Tissue-specific calibration of extracellular matrix material properties by transforming growth factor-beta and Runx2 in bone is required for hearing. EMBO Rep 11, 765-771.
37. Mohammad, K. S., Chen, C. G., Balooch, G., Stebbins, E., McKenna, C. R., Davis, H., Niewolna, M., Peng, X. H., Nguyen, D. H., Ionova-Martin, S. S., Bracey, J. W., Hogue, W. R., Wong, D. H., Ritchie, R. O., Suva, L. J., Derynck, R., Guise, T. A. & Alliston, T. (2009). Pharmacologic inhibition of the TGF-beta type I receptor kinase has anabolic and anti-catabolic effects on bone. PLoS One 4, e5275.
38. Edwards, J. R., Nyman, J. S., Lwin, S. T., Moore, M. M., Esparza, J., O'Quinn, E. C., Hart, A. J., Biswas, S., Patil, C. A., Lonning, S., Mahadevan-Jansen, A. & Mundy, G. R. (2010). Inhibition of TGF-beta signaling by 1D11 antibody treatment increases bone mass and quality in vivo. J Bone Miner Res 25, 2419-2426.
39. Morita, Y., Watanabe, S., Ju, Y. & Xu, B. (2013). Determination of optimal cyclic uniaxial stretches for stem cell-to-tenocyte differentiation under a wide range of mechanical stretch conditions by evaluating gene expression and protein synthesis levels. Acta Bioeng Biomech 15, 71-79.
40. Hytonen, V. P. & Vogel, V. (2008). How force might activate talin's vinculin binding sites: SMD reveals a structural mechanism. PLoS Comput Biol 4, e24.
41. Hoffman, B. D., Grashoff, C. & Schwartz, M. A. (2011). Dynamic molecular processes mediate cellular mechanotransduction. Nature 475, 316-323.
42. DuFort, C. C., Paszek, M. J. & Weaver, V. M. (2011). Balancing forces: architectural control of mechanotransduction. Nature Reviews Molecular Cell Biology 12, 308-319.
43. Engler, A. J., Sen, S., Sweeney, H. L. & Discher, D. E. (2006). Matrix elasticity directs stem cell lineage specification. Cell 126, 677-689.
44. Wen, J. H., Vincent, L. G., Fuhrmann, A., Choi, Y. S., Hribar, K. C., Taylor-Weiner, H., Chen, S. & Engler, A. J. (2014). Interplay of matrix stiffness and protein tethering in stem cell differentiation. Nat Mater 13, 979-987.
45. McBeath, R., Pirone, D. M., Nelson, C. M., Bhadriraju, K. & Chen, C. S. (2004). Cell shape, cytoskeletal tension, and RhoA regulate stem cell lineage commitment. Dev Cell 6, 483-495.
46. Masaki, C., Schneider, G. B., Zaharias, R., Seabold, D. & Stanford, C. (2005). Effects of implant surface microtopography on osteoblast gene expression. Clin Oral Implants Res 16, 650-656.

47. Dalby, M. J., Gadegaard, N., Tare, R., Andar, A., Riehle, M. O., Herzyk, P., Wilkinson, C. D. & Oreffo, R. O. (2007). The control of human mesenchymal cell differentiation using nanoscale symmetry and disorder. Nat Mater 6, 997-1003.
48. Joergensen, N. L., Le, D. Q., Andersen, O. Z., Foss, M., Danielsen, C. C., Foldager, C. B., Lind, M. & Lysdahl, H. (2015). Topography-Guided Proliferation: Distinct Surface Microtopography Increases Proliferation of Chondrocytes In Vitro. Tissue Eng Part A
49. Park, J. S., Chu, J. S., Tsou, A. D., Diop, R., Tang, Z., Wang, A. & Li, S. (2011). The effect of matrix stiffness on the differentiation of mesenchymal stem cells in response to TGF-beta. Biomaterials 32, 3921-3930.
50. Nguyen, J., Tang, S. Y., Nguyen, D. & Alliston, T. (2013). Load regulates bone formation and Sclerostin expression through a TGFbeta-dependent mechanism. PLoS One 8, e53813.
51. Robling, A. G., Niziolek, P. J., Baldridge, L. A., Condon, K. W., Allen, M. R., Alam, I., Mantila, S. M., Gluhak-Heinrich, J., Bellido, T. M., Harris, S. E. & Turner, C. H. (2008). Mechanical stimulation of bone in vivo reduces osteocyte expression of Sost/sclerostin. J Biol Chem 283, 5866-5875.
52. Donnelly, E. (2011). Methods for assessing bone quality: a review. Clin Orthop Relat Res 469, 2128-2138.
53. Sanchez-Adams, J., Leddy, H. A., McNulty, A. L., O'Conor, C. J. & Guilak, F. (2014). The mechanobiology of articular cartilage: bearing the burden of osteoarthritis. Curr Rheumatol Rep 16, 451.
54. Smith, R. L., Rusk, S. F., Ellison, B. E., Wessells, P., Tsuchiya, K., Carter, D. R., Caler, W. E., Sandell, L. J. & Schurman, D. J. (1996). In vitro stimulation of articular chondrocyte mRNA and extracellular matrix synthesis by hydrostatic pressure. J Orthop Res 14, 53-60.
55. Smith, R. L., Lin, J., Trindade, M. C., Shida, J., Kajiyama, G., Vu, T., Hoffman, A. R., van der Meulen, M. C., Goodman, S. B., Schurman, D. J. & Carter, D. R. (2000). Time-dependent effects of intermittent hydrostatic pressure on articular chondrocyte type II collagen and aggrecan mRNA expression. J Rehabil Res Dev 37, 153-161.
56. Guilak, F., Erickson, G. R. & Ting-Beall, H. P. (2002). The effects of osmotic stress on the viscoelastic and physical properties of articular chondrocytes. Biophys J 82, 720-727.
57. Phan, M. N., Leddy, H. A., Votta, B. J., Kumar, S., Levy, D. S., Lipshutz, D. B., Lee, S. H., Liedtke, W. & Guilak, F. (2009). Functional characterization of TRPV4 as an osmotically sensitive ion channel in porcine articular chondrocytes. Arthritis Rheum 60, 3028-3037.
58. Millward-Sadler, S. J. & Salter, D. M. (2004). Integrin-dependent signal cascades in chondrocyte mechanotransduction. Ann Biomed Eng 32, 435-446.
59. Wann, A. K., Zuo, N., Haycraft, C. J., Jensen, C. G., Poole, C. A., McGlashan, S. R. & Knight, M. M. (2012). Primary cilia mediate mechanotransduction through control of ATP-induced Ca2+ signaling in compressed chondrocytes. FASEB J 26, 1663-1671.
60. O'Conor, C. J., Leddy, H. A., Benefield, H. C., Liedtke, W. B. & Guilak, F. (2014). TRPV4-mediated mechanotransduction regulates the metabolic response of chondrocytes to dynamic loading. Proc Natl Acad Sci U S A 111, 1316-1321.
61. Rys, J., DuFort, C. C., Monteiro, D. A., Baird, M. A., Oses-Prieto, J. A., Chand, S., Burlingame, A., Davidson, M. W. & Alliston, T. (2015). Discrete spatial organization of TGF-beta receptors couples receptor multimerization and signaling to cellular tension. eLife (Accepted)

62. Chang, C. F., Ramaswamy, G. & Serra, R. (2012). Depletion of primary cilia in articular chondrocytes results in reduced Gli3 repressor to activator ratio, increased Hedgehog signaling, and symptoms of early osteoarthritis. Osteoarthritis Cartilage 20, 152-161.
63. Alman, B. A. (2015). The role of hedgehog signalling in skeletal health and disease. Nat Rev Rheumatol 11, 552-560.
64. Knecht, S., Vanwanseele, B. & Stussi, E. (2006). A review on the mechanical quality of articular cartilage - implications for the diagnosis of osteoarthritis. Clin Biomech (Bristol, Avon) 21, 999-1012.
65. Wang, J. H., Guo, Q. & Li, B. (2011). Tendon biomechanics and mechanobiology--a minireview of basic concepts and recent advancements. J Hand Ther 25, 133-140; quiz 141.
66. Langberg, H., Rosendal, L. & Kjaer, M. (2001). Training-induced changes in peritendinous type I collagen turnover determined by microdialysis in humans. J Physiol 534, 297-302.
67. Szczodry, M., Zhang, J., Lim, C., Davitt, H. L., Yeager, T., Fu, F. H. & Wang, J. H. (2009). Treadmill running exercise results in the presence of numerous myofibroblasts in mouse patellar tendons. J Orthop Res 27, 1373-1378.
68. Rooney, S. I., Tobias, J. W., Bhatt, P. R., Kuntz, A. F. & Soslowsky, L. J. (2015). Genetic Response of Rat Supraspinatus Tendon and Muscle to Exercise. PLoS One 10, e0139880.
69. Nakatani, T., Marui, T., Hitora, T., Doita, M., Nishida, K. & Kurosaka, M. (2002). Mechanical stretching force promotes collagen synthesis by cultured cells from human ligamentum flavum via transforming growth factor-beta1. J Orthop Res 20, 1380-1386.
70. Hering, S., Jost, C., Schulz, H., Hellmich, B., Schatz, H. & Pfeiffer, H. (2002). Circulating transforming growth factor beta1 (TGFbeta1) is elevated by extensive exercise. Eur J Appl Physiol 86, 406-410.
71. Heinemeier, K. M., Olesen, J. L., Haddad, F., Langberg, H., Kjaer, M., Baldwin, K. M. & Schjerling, P. (2007). Expression of collagen and related growth factors in rat tendon and skeletal muscle in response to specific contraction types. J Physiol 582, 1303-1316.
72. Pryce, B. A., Watson, S. S., Murchison, N. D., Staverosky, J. A., Dunker, N. & Schweitzer, R. (2009). Recruitment and maintenance of tendon progenitors by TGFbeta signaling are essential for tendon formation. Development 136, 1351-1361.
73. Zelzer, E., Blitz, E., Killian, M. L. & Thomopoulos, S. (2014). Tendon-to-bone attachment: from development to maturity. Birth Defects Res C Embryo Today 102, 101-112.
74. Lorda-Diez, C. I., Montero, J. A., Martinez-Cue, C., Garcia-Porrero, J. A. & Hurle, J. M. (2009). Transforming growth factors beta coordinate cartilage and tendon differentiation in the developing limb mesenchyme. J Biol Chem 284, 29988-29996.
75. Berthet, E., Chen, C., Butcher, K., Schneider, R. A., Alliston, T. & Amirtharajah, M. (2013). Smad3 binds Scleraxis and Mohawk and regulates tendon matrix organization. J Orthop Res 31, 1475-1483.
76. Blitz, E., Viukov, S., Sharir, A., Shwartz, Y., Galloway, J. L., Pryce, B. A., Johnson, R. L., Tabin, C. J., Schweitzer, R. & Zelzer, E. (2009). Bone ridge patterning during musculoskeletal assembly is mediated through SCX regulation of Bmp4 at the tendon-skeleton junction. Dev Cell 17, 861-873.
77. Nowlan, N. C., Murphy, P. & Prendergast, P. J. (2007). Mechanobiology of embryonic limb development. Ann N Y Acad Sci 1101, 389-411.

78. Nowlan, N. C., Sharpe, J., Roddy, K. A., Prendergast, P. J. & Murphy, P. (2010). Mechanobiology of embryonic skeletal development: Insights from animal models. Birth Defects Res C Embryo Today 90, 203-213.
79. Shefelbine, S. J., Tardieu, C. & Carter, D. R. (2002). Development of the femoral bicondylar angle in hominid bipedalism. Bone 30, 765-770.
80. Bonassar, L. J., Grodzinsky, A. J., Frank, E. H., Davila, S. G., Bhaktav, N. R. & Trippel, S. B. (2001). The effect of dynamic compression on the response of articular cartilage to insulin-like growth factor-I. J Orthop Res 19, 11-17.
81. Elder, B. D. & Athanasiou, K. A. (2008). Synergistic and additive effects of hydrostatic pressure and growth factors on tissue formation. PLoS One 3, e2341.
82. Raab-Cullen, D. M., Thiede, M. A., Petersen, D. N., Kimmel, D. B. & Recker, R. R. (1994). Mechanical loading stimulates rapid changes in periosteal gene expression. Calcif Tissue Int 55, 473-478.
83. Sakai, K., Mohtai, M. & Iwamoto, Y. (1998). Fluid shear stress increases transforming growth factor beta 1 expression in human osteoblast-like cells: modulation by cation channel blockades. Calcif Tissue Int 63, 515-520.
84. Li, Z., Kupcsik, L., Yao, S. J., Alini, M. & Stoddart, M. J. (2010). Mechanical load modulates chondrogenesis of human mesenchymal stem cells through the TGF-beta pathway. J Cell Mol Med 14, 1338-1346.
85. Lohmann, C. H., Tandy, E. M., Sylvia, V. L., Hell-Vocke, A. K., Cochran, D. L., Dean, D. D., Boyan, B. D. & Schwartz, Z. (2002). Response of normal female human osteoblasts (NHOst) to 17beta-estradiol is modulated by implant surface morphology. J Biomed Mater Res 62, 204-213.
86. Wipff, P.-J. & Hinz, B. (2008). Integrins and the activation of latent transforming growth factor beta 1 - An intimate relationship. European Journal of Cell Biology 87, 601-615.
87. Horiguchi, M., Ota, M. & Rifkin, D. B. (2012). Matrix control of transforming growth factor-beta function. J Biochem 152, 321-329.
88. Albro, M. B., Cigan, A. D., Nims, R. J., Yeroushalmi, K. J., Oungoulian, S. R., Hung, C. T. & Ateshian, G. A. (2012). Shearing of synovial fluid activates latent TGF-beta. Osteoarthritis Cartilage 20, 1374-1382.
89. Skutek, M., van Griensven, M., Zeichen, J., Brauer, N. & Bosch, U. (2001). Cyclic mechanical stretching modulates secretion pattern of growth factors in human tendon fibroblasts. Eur J Appl Physiol 86, 48-52.
90. Maeda, T., Sakabe, T., Sunaga, A., Sakai, K., Rivera, A. L., Keene, D. R., Sasaki, T., Stavnezer, E., Iannotti, J., Schweitzer, R., Ilic, D., Baskaran, H. & Sakai, T. (2011). Conversion of mechanical force into TGF-beta-mediated biochemical signals. Curr Biol 21, 933-941.
91. Kinoshita, A., Saito, T., Tomita, H., Makita, Y., Yoshida, K., Ghadami, M., Yamada, K., Kondo, S., Ikegawa, S., Nishimura, G., Fukushima, Y., Nakagomi, T., Saito, H., Sugimoto, T., Kamegaya, M., Hisa, K., Murray, J. C., Taniguchi, N., Niikawa, N. & Yoshiura, K. (2000). Domain-specific mutations in TGFB1 result in Camurati-Engelmann disease. Nat Genet 26, 19-20.
92. Saito, T., Kinoshita, A., Yoshiura, K., Makita, Y., Wakui, K., Honke, K., Niikawa, N. & Taniguchi, N. (2001). Domain-specific mutations of a transforming growth factor (TGF)-beta 1 latency-associated peptide cause Camurati-Engelmann disease because of the formation of a constitutively active form of TGF-beta 1. J Biol Chem 276, 11469-11472.

93. Janssens, K., ten Dijke, P., Ralston, S. H., Bergmann, C. & Van Hul, W. (2003). Transforming growth factor-beta 1 mutations in Camurati-Engelmann disease lead to increased signaling by altering either activation or secretion of the mutant protein. J Biol Chem 278, 7718-7724.
94. Tang, Y., Wu, X., Lei, W., Pang, L., Wan, C., Shi, Z., Zhao, L., Nagy, T. R., Peng, X., Hu, J., Feng, X., Van Hul, W., Wan, M. & Cao, X. (2009). TGF-beta1-induced migration of bone mesenchymal stem cells couples bone resorption with formation. Nat Med 15, 757-765.
95. Bethani, I., Skanland, S. S., Dikic, I. & Acker-Palmer, A. (2010). Spatial organization of transmembrane receptor signalling. Embo Journal 29, 2677-2688.
96. Di Guglielmo, G. M., Le Roy, C., Goodfellow, A. F. & Wrana, J. L. (2003). Distinct endocytic pathways regulate TGF-beta receptor signalling and turnover. Nature Cell Biology 5, 410-421.
97. Groves, J. T. & Kuriyan, J. (2010). Molecular mechanisms in signal transduction at the membrane. Nature Structural & Molecular Biology 17, 659-665.
98. Salaita, K., Nair, P. M., Petit, R. S., Neve, R. M., Das, D., Gray, J. W. & Groves, J. T. (2010). Restriction of Receptor Movement Alters Cellular Response: Physical Force Sensing by EphA2. Science 327, 1380-1385.
99. Le Roy, C. & Wrana, J. L. (2005). Clathrin- and non-clathrin-mediated endocytic regulation of cell signalling. Nat Rev Mol Cell Biol 6, 112-126.
100. Garamszegi, N., Garamszegi, S. P., Samavarchi-Tehrani, P., Walford, E., Schneiderbauer, M. M., Wrana, J. L. & Scully, S. P. (2010). Extracellular matrix-induced transforming growth factor-beta receptor signaling dynamics. Oncogene 29, 2368-2380.
101. Hartman, N. C. & Groves, J. T. (2011). Signaling clusters in the cell membrane. Curr Opin Cell Biol 23, 370-376.
102. Zhu, Y., Oganesian, A., Keene, D. R. & Sandell, L. J. (1999). Type IIA procollagen containing the cysteine-rich amino propeptide is deposited in the extracellular matrix of prechondrogenic tissue and binds to TGF-beta1 and BMP-2. J Cell Biol 144, 1069-1080.
103. Blaney Davidson, E. N., Remst, D. F., Vitters, E. L., van Beuningen, H. M., Blom, A. B., Goumans, M. J., van den Berg, W. B. & van der Kraan, P. M. (2009). Increase in ALK1/ALK5 ratio as a cause for elevated MMP-13 expression in osteoarthritis in humans and mice. J Immunol 182, 7937-7945.
104. Leight, J. L., Wozniak, M. A., Chen, S., Lynch, M. L. & Chen, C. S. (2012). Matrix rigidity regulates a switch between TGF-beta1-induced apoptosis and epithelial-mesenchymal transition. Mol Biol Cell 23, 781-791.
105. Wang, Y. K., Yu, X., Cohen, D. M., Wozniak, M. A., Yang, M. T., Gao, L., Eyckmans, J. & Chen, C. S. (2012). Bone morphogenetic protein-2-induced signaling and osteogenesis is regulated by cell shape, RhoA/ROCK, and cytoskeletal tension. Stem Cells Dev 21, 1176-1186.
106. Dupont, S., Morsut, L., Aragona, M., Enzo, E., Giulitti, S., Cordenonsi, M., Zanconato, F., Le Digabel, J., Forcato, M., Bicciato, S., Elvassore, N. & Piccolo, S. (2011). Role of YAP/TAZ in mechanotransduction. Nature 474, 179-U212.
107. Driscoll, T. P., Cosgrove, B. D., Heo, S. J., Shurden, Z. E. & Mauck, R. L. (2015). Cytoskeletal to Nuclear Strain Transfer Regulates YAP Signaling in Mesenchymal Stem Cells. Biophys J 108, 2783-2793.

108. Tang, Y., Rowe, R. G., Botvinick, E. L., Kurup, A., Putnam, A. J., Seiki, M., Weaver, V. M., Keller, E. T., Goldstein, S., Dai, J., Begun, D., Saunders, T. & Weiss, S. J. (2013). MT1-MMP-dependent control of skeletal stem cell commitment via a beta1-integrin/YAP/TAZ signaling axis. Dev Cell 25, 402-416.
109. Varelas, X., Sakuma, R., Samavarchi-Tehrani, P., Peerani, R., Rao, B. M., Dembowy, J., Yaffe, M. B., Zandstra, P. W. & Wrana, J. L. (2008). TAZ controls Smad nucleocytoplasmic shuttling and regulates human embryonic stem-cell self-renewal. Nat Cell Biol 10, 837-848.
110. Rape, A. D., Zibinsky, M., Murthy, N. & Kumar, S. (2015). A synthetic hydrogel for the high-throughput study of cell-ECM interactions. Nat Commun 6, 8129.

Chapter 2

Materials and methods

Plasmids

The plasmids pRK5 TGFβ type I receptor Flag and pRK5 TGFβ type II receptor Flag were gifts from Rik Derynck (Addgene plasmids 14831, 31719). The plasmid pRK5 TGFβ type I receptor Myc was also a gift from Rik Derynck.

All fluorescent protein expression vectors are available in the Michael Davidson Fluorescent Protein Collection on Addgene.

All fluorescent protein expression vectors were constructed using C1 or N1 (Clontech-style) cloning vectors and initially characterized using the advanced EGFP variant mEmerald to verify proper localization of the fusions. To construct the N-terminal (with respect to the fluorescent protein) human integrin alpha2 (NM_002203.3) fusions, the following primers were used to amplify the integrin alpha 2, and create the 18-amino acid linker (GSAGGSGVPRARDPPVAT):

XhoI forward: CTC CGT CTC GAG ACC GCC ATG GGG CCA GAA CGG ACA GGG GCC

KpnI reverse: CGG AAC GGT ACC CCG CTT CCG CCT GCG CTG CCG CTA CTG AGC TCT GTG GTC TCA TCA ATC TCA TCT GGA TTT TTG GTC

Following digestion and gel purification, the PCR product was ligated into a similarly digested mEmerald-N1 cloning vector to produce mEmerald-Integrin alpha2-N-18. The resulting fusion, along with mCherry-N1 cloning vector, was sequentially digested with AgeI and NotI to yield mCherry-Integrin alpha2-N-18.

To generate the N-terminal human integrin alpha V (NM_002210.4) fusions, the following primers were used to amplify the protein and create the 25-amino acid linker (PGSRAQASNSAVDGTAGPGSPPVAT)

AgeI forward: CCC GGG ATC CAC CGG TCG CCA CCA TGG CTT TTC CGC CGC GGC GAC GGC TGC GCC TCG GTC

HindIII reverse: AAT TGA AGC TTG AGC TCG AGA TCC CGG AAG TTT CTG AGT TTC CTT CAC CAT TTT CAT GAG GTT GAA GCT GCT CCC TTT CTT GTT CTT CTT GAG

The PCR product was digested, gel purified, and ligated into a similarly treated mEmerald-N1 or mCherry-N1 cloning vector to yield the mEmerald-Integrin alphaV-25 or mCherry-Integrin-alphaV-25 fusions.

To construct the N-terminal tagged human vinculin (NM_003373.3) plasmids, the following primers were used to PCR-amplify and create a 21-amino acid linker (SGGSGILQSTVPRARDPPVAT):

NheI forward: GTC AGA TCC GCT AGC ACC GCC ACC ATG CCA GTG TTT CAT ACG CGC ACG ATC GAG AGC

EcoR1 reverse: CGA CTG CAG AAT TCC GCT GCC ACC GGA CTG GTA CCA GGG AGT CTT TCT AAC CCA GCG CAG

The PCR product was digested and ligated into a similarly cut mEmerald-N1 or mCherry-N1 cloning vector to yield mEmerald-Vinculin-N-21 or mCherry-Vinculin-N-21 expression vectors.

To construct the C-terminal human TBR2 (NM_001024847.2) fusion plasmids, the following primers were used to amplify the TBR2 and generate an 18-amino acid linker (SGLRSRESGSGGSSGSGS):

XhoI forward: GAC GAG CTC GAG AGA GTG GCT CTG GTG GGT CGA GTG GAA GTG GCA GCG GTC GGG GGC TGC TCA GGG GCC TG

BamHI reverse: CGT CTA GGA TCC CTA TTT GGT AGT GTT TAG GGA GCC GTC TTC AGG AAT CTT CTC C

Following digestion and gel purification, the PCR product was ligated into a similarly digested mEmerald-C1 cloning vector, to produce mEmerald-TBRII-C-18. The fusion, along with mCherry-C1 and mEos2-C1 cloning vectors, was sequentially digested with AgeI and BamHI and ligated to yield mCherry-TBRII-C-18 and mEos2-TBRII-C-18.

To generate the N-terminal human TBRII plamids and create an 18-amino acid linker (SSGGASAASGSADPPVAT), the following primers were used:

NheI forward: CGA TCC GCT AGC GCC ACC ATG GGT CGG GGG CTG CTC AGG GGC

BamHI reverse: CCT GTA CGG ATC CGC GCT ACC ACT GGC TGC GCT TGC TCC ACC GCT GCT TTT GGT AGT GTT TAG GGA GCC GTC TTC AGG AAT CTT CTC C

The PCR fragment was digested, gel purified, and ligated with a similarly treated mEmerald-N1 cloning vector to produce mEmerald-TBRII-N-18. The resulting fusion, along with mCherry-N1 and mEos2-N1, was double digested with BamHI and NotI to yield mCherry-TBRII-N-18 and mEos2-TBRII-N-18 respectively.

To construct the N-terminal human Alk1 (NM_000020.2) expression vectors, the following primers were used to amplify the plasmid, and create a 13-amino acid linker (GSAGGSGDPPVAT):

EcoRI forward: GCG TTG AAT TCA CCG CCA TGA CCT TGG GCT CCC CCA GGA AAG GCC

BamHI reverse: CGG AAC GGA TCC CCG CTT CCG CCT GCG CTG CCT TGA ATC ACT TTA GGC TTC TCT GGA CTG TTG CTA ATT TTT TGT AGT GTC TTC TTG ATC

Following amplification, the PCR fragment was digested, purified, and ligated to a similarly treated mEmerald-N1 cloning vector to yield mEmerald-Alk1-N-13. Upon sequence verification, the resulting fusion, along with mCherry-N1, was digested with BamH1 and NotI and ligated to yield mCherry-Alk1-N-13.

To generate the C-terminal human Alk5 (NM_004612.2) expression vectors, the following primers were used to amplify the plasmid, and create an 18-amino acid linker (SGLRSGSSAGSASGGSGS):

BglII forward: GAC TCG AGA TCT GGC TCC AGC GCA GGC AGC GCA TCC GGC GGA AGC GGA AGC GAG GCG GCG GTC GCT GCT CCG CGT C

HindIII reverse: CGG TCA AAG CTT TTA CAT TTT GAT GCC TTC CTG TTG ACT GAG TTG CGA TAA TGT TTT CTT AAT CCG C

Following amplification, the PCR fragment was digested, purified, and ligated to a similarly treated mEmerald-C1 cloning vector to yield mEmerald-Alk5-C-18. The resulting fusion, along

with mCherry-C1 and mEos2-C1, was double digested with BglII and NheI to yield mCherry-Alk5-C-18 and mEos2-Alk5-C-18.

To construct the N-terminally labeled Alk5 fusions, the following primers were used to amplify the Alk5 and generate a 13-amino acid linker (GSGGAGGGGPVAT):

BglII forward: GTC TGT AGA TCT GCC ACC ATG GAG GCG GCG GTC GCT GCT CCG

AgeI reverse: CGG TCA ACC GGT CCT CCG CCG CCC GCA CCC CCG GAA CCC ATT TTG ATG CCT TCC TGT TGA CTG AGT TGC GAT AAT GTT TTC TTA ATC CGC

Following amplification, the resulting fragment was digested, purified, and ligated to a similarly treated mEmerald-N1 cloning vector, resulting in mEmerald-Alk5-N-13. Following sequence verification, the plasmid, along with mCherry-N1 and mEos2-N1 cloning vectors, was sequentially digested with AgeI and NotI and ligated to produce mCherry-Alk5-N-13 and mEos2-Alk5-N-13 fusions.

All DNA for transfection was prepared using the Plasmid Maxi kit (QIAGEN, Valencia, CA) and characterized by transfection in HeLa cells (CCL2 line; ATCC, Manassas, VA) using Effectene (QIAGEN) followed by observation under widefield fluorescence illumination to ensure proper localization. The sequences for all vectors were confirmed using Big Dye technology (The Florida State University Bioanalytical and Molecular Cloning DNA Sequencing Laboratory Tallahassee, FL).

Cell Culture and Transfection

Studies were performed using ATDC5 murine chondroprogenitor cells (RCB0565, RIKEN), NIH3T3 fibroblasts, MCF10A human mammary epithelial cells, and Human Embryonic Kidney

(HEK) 293 cells. Cells were treated as indicated with TGFβ1 (5 ng/ml, HumanZyme), Y27632 (10 μM, Sigma-Aldrich), and blebbistatin (10 μM, Cayman Chemical).

For imaging experiments, glass-bottom imaging wells (In Vitro Scientific) were coated with collagen II (1mg/ml in acetic acid diluted 1:100 in PBS), fibronectin (1mg/ml diluted 1:100 in PBS), or poly-l-lysine (0.1 mg/ml). ATDC5, NIH3T3, and MCF10A cells were transfected using Nucleofection (Lonza) or Effectene (Qiagen), and then plated on to the imaging wells. For biochemical assays, 293 cells were plated in 100 mm cell-culture dishes and transfected using Effectene (Qiagen) at 80% confluency.

Antibodies, Co-immunoprecipitation, Immunoblotting, and Immunofluorescence

For co-immunprecipitation experiments, 293 cells were transfected with integrin αV-mCherry, cofilin-mEmerald, TβRI-Flag, TβRII-Flag, and/or TβRI-Myc. 24 hours after transfection, cells were treated with TGFβ or Y27632 for 15 minutes. Cells were lysed (50 mM Tris pH 7.5, 150 mM NaCl, 2 mM EDTA, 0.5% Igepal, 0.25% sodium deoxycholate, supplemented with protease and phosphatase inhibitor tablets) and immunoprecipitated with anti-Flag M2 beads (Sigma-Aldrich) overnight prior to Western analysis (2). For immunoblotting experiments of downstream endogenous proteins, 293 cells were cultured on plastic or fibronectin-coated gel substrates (Advanced BioMatrix), treated with TGFβ as indicated for 30 minutes and then lysed. Blots were probed with anti-Flag (F3165, Sigma-Aldrich), anti-CD51, integrin αV (611013, BD Bioscience), anti-cofilin (ACFL02, Cytoskeleton), anti-pSmad3 (gift from E. Leof), anti-β-actin (ab8226, Abcam) and anti-TβRI (sc-398, Santa Cruz), and anti-mouse anti-rabbit secondary antibodies that were conjugated to 680 or 800CW IRDye fluorophores for detection using a LI-COR infrared imaging system (LI-COR Biosciences). Blots shown are representative of multiple

technical replicates of at least three independent experiments for each condition (N≥3). Where indicated, quantitative analysis was performed using ImageJ. Band intensity for proteins of interest was normalized to band intensity of controls (Flag for co-IP and β-actin for whole cell extract). Fold change in band intensity was calculated relative to plastic control samples. ANOVA followed by Bonferroni correction and student's *t* test were used to evaluate statistical significance.

For immunofluorescence studies, ATDC5 cells were cultured on collagen II-coated glass substrates in 8 well Lab-Tek chamber slides (Nunc). Cells were fixed (4% paraformaldehyde) and permeabilized (0.5% Triton X-100 in PBS). Primary antibodies included anti-TβRII (sc-1700, sc-400, Santa Cruz) and anti-TβRI (sc-398, sc-9048, Santa Cruz). Cells were imaged as described below.

Affinity purification and reversed-phase liquid chromatography-electrospray tandem mass spectrometry (LC-MS/MS)

Cells expressing TβRII-Flag or TβRI-Flag and integrin αV-mCherry in 10 cm cell culture dishes were lysed as above and affinity-purified with M2-Flag magnetic beads (Sigma-Aldrich), followed by on-bead trypsin digestion and mass spectrometry approaches to study associated proteins as described (N=3) (3). Peptides recovered were analyzed by reversed-phase liquid chromatography-electrospray tandem mass spectrometry (LC-MS/MS) as described (4). Briefly, peptides were separated by nano-flow chromatography in a C18 column, and the eluate was coupled to a hybrid linear ion trap-Orbitrap mass spectrometer (LTQ-OrbitrapVelos, ThermoScientific, San Jose, CA) equipped with a nanoelectrospray ion source. Following LC-MS/MS analysis, peak lists generated from spectra were searched against the human subset of

the SwissProt database using in-house ProteinProspector (5). For analysis, peptide counts of each protein were normalized by the total protein content in the sample and the molecular weight of the respective protein. This provided an abundance index for each protein that served as a comparison between pulldowns. The ratio between abundance indices for TβR pulldowns to untransfected control (mock) pulldowns was used to screen candidate proteins.

Image Acquisition and Analysis

ATDC5, NIH3T3, and MCF10A cells were transiently transfected with fluorescently labeled expression plasmids and plated on collagen II, fibronectin or poly-l-lysine-coated glass-bottom imaging wells. Cells were imaged 24 hours after transfection, and treated with Y27632, blebbistatin, or TGFβ as indicated. Confocal images were obtained on a motorized Yokogawa CSU-X1 spinning disk confocal unit on an inverted microscope system (Ti-E Perfect Focus System, Nikon), with either a 100X/NA 1.49 oil-immersion objective (CFI Apo TIRF, Nikon) or a 40X/NA 1.15 water-immersion objective (CFI Apo LWD, Nikon), on a front illuminated CMOS camera (Zyla sCMOS, Andor). For TIRF and sptPALM, imaging was performed on a motorized objective-type TIRF inverted microscope system (Ti-E Perfect Focus System, Nikon) with activation and excitation lasers of 405 nm, 488 nm, and 561 nm, and an electron-multiplying charged-coupled device camera (QuantEM 512, Photometrics), a 100X/NA 1.49 oil-immersion objective (CFI Apo TIRF, Nikon), a stage top incubator (Okolab), and controlled by NIS-Elements software (Nikon). Cells expressing mEos2-tagged constructs were simultaneously activated with a 405 nm laser and excited with a 561 nm laser. Laser intensities were adjusted to maintain a constant sparse population of activated molecules that were spaced well enough for accurate localization and tracking. Prior to each sptPALM imaging sequence and photoconversion of mEos2, the mEmerald signal from mEmerald fusions of vinculin was imaged

to localize focal adhesions. NIS-Elements software (Nikon) was used for the acquisition of images at 10 fps. Individual receptors were localized and tracked using a previously described algorithm (6) written in MosaicSuite for ImageJ and available at (www.mosaic.mpi-cbg.de). All images were processed using ImageJ with a 0.6 gaussian blur filter to remove noise. Images shown are representative of multiple cells (N≥5) for at least three independent experiments for each condition.

Colocalization quantification

TIRF mode imaging was used to obtain intensity profiles of two distinct molecules over adhesion-rich regions of interest (for example, regions shown in Fig. 4.3A-C). The similarity of the two profiles was quantified to provide a measure of colocalization, specifically by comparing pixel intensities (8-bit grayscale) at each point across the two profiles. For each pixel, an ordered pair containing the intensities at that particular coordinate from both images was plotted. Values closer to the line y=x refer to coordinates that have very similar intensities in both profiles. Values further from y=x are coordinates that have a mismatch in intensities. By reflecting all points in the top half of this graph across y=x, a distribution of points is created between y=x and the x-axis, but the distance of individual points from y=x is preserved. The magnitude of the slope of the regression line through these points can be used as a quantitative metric of colocalization. The greater this slope, the higher the degree of colocalization. Plots are representative of multiple cells (N≥3) and multiple regions of interest (N=5). ANOVA followed by Bonferroni correction was used to evaluate statistical significance.

Single-Molecule Tracking

Each sptPALM imaging sequence generates tens of thousands of molecule trajectories per cell (N=6 cells for each TβR). From these, only trajectories lasting between 0.5 seconds and 2 seconds (5 to 20 frames at 10 fps) were selected for analysis. Tracks that were not confined to either inside or outside focal adhesions were not considered in the quantitative analysis. For each individual track, a series of parameters were calculated to quantify receptor dynamics. These parameters include mean squared displacement (MSD), diffusion coefficient (D), and radius of confinement (r_{conf}). MSD was computed as per equation 1 (7):

Equation 1: $MSD(\tau = n \cdot \Delta t) = \frac{\sum_{i=1}^{N-n}(x_{i+n}-x_i)^2+(y_{i+n}-y_i)^2}{N-n}$.

Where x_i and y_i are the coordinates of the molecule at time $i * \Delta t$ and N is the number of frames for which the trajectory persisted. The radius of confinement (r_{conf}) of a track is defined to be the magnitude of the radius of the smallest circle that encloses all points in that track. D is defined as one-fourth of the slope of the regression line fitted to the first four values of the MSD as per equation 2:

Equation 2: $MSD(\tau) = 4D\tau$.

Using these variables, trajectories were pooled into three fractions: immobile, confined, and freely diffusive. Immobile molecules were defined as being restricted to a radius of confinement equal to one pixel ($r_{conf} < 0.166$ μm). Confined molecules were defined as non-immobile tracks with a diffusion coefficient D of less than 0.2 $\mu m^2/s$, and the remaining tracks were considered freely diffusive. Custom routines written for Python were used for track quantification, analysis, and visualization. To account for variability in these large data sets consisting of tens of

thousands of tracks, we report mean and standard error of the mean (SEM). ANOVA followed by Bonferroni correction and student's *t* test were used to evaluate statistical significance.

To quantify the diffusive behavior of TβRI and TβRII around focal adhesions, we calculated an enrichment ratio to compare track densities in several (N≥5) focal adhesion-rich regions (where vinculin covered more than 25% of total area) across at least three cells. The enrichment ratio was defined as the ratio of the track density (tracks/μm^2) inside adhesions to the track density outside adhesions within a given area. Student's *t* test was used to evaluate statistical significance.

Statistical Analysis

For colocalization quantification (Fig. 4.3 and Fig. 4.6) and enrichment ratio (Fig. 4.4C), we report mean and standard deviation (SD). There are three circumstances in which it was more statistically appropriate to report the standard error of the mean (SEM). Specifically, to account for variability in large sptPALM data sets (consisting of tens of thousands of tracks), we report mean and SEM (Fig. 4.2E,F and Fig. 4.4I). Significance was calculated with ANOVA followed by Bonferroni correction and student's *t* test, with significance defined as $p < 0.01$.

--

2D Gel Substrate Preparation

Elastic modulus of polyacrylamide gels was modulated by varying the concentration of the crosslinker, piperazine diacrylamide (PDA) (Bio-Rad, 161-0202), from 1% to 3% (w/v), while maintain a constant concentration of the monomer, acrylamide (Bio-Rad, 161, 0140), at 30%. Polymerization of substrates was initiated with 10% (w/v) ammonium persulfate (APS) added at

a 1:200 dilution and enhanced by TEMED added at a 1:2000 dilution. Gels were vortexed thoroughly then polymerized in a 1 mm thick vertical glass mold for hand casting gels.

Preparing Polyacrylamide Gels for Cell Attachment

Polyacrylamide gels were conjugated with collagen II to facilitate cell attachment as previously described (8). A 1.8% (w/v) solution of acrylic acid n-hydroxysuccinimide ester (N2, Sigma, A8060) in 50% ethanol was diluted 1:6 into a solution containing 0.01% (w/v) bisacrylamide (Bio-Rad, 161-0142), 0.17% (w/v) Irgacure 2959 (BASF, 55047962), and 0.05 M Hepes NaOH (pH 6) (8). Polyacrylamide gel slabs were removed from the hand casting molds and cut into 3 cm diameter cylinders using a stainless steel biscuit cutter. The gel cylinders were covered with 200 µl of N2 solution and sandwiched horizontally between two large sterile glass slides prior to exposure from a handheld UV lamp (306 nm) for 10 minutes. Collagen II was dissolved in 0.1 M acetic acid at a concentration of 1 mg/ml and then diluted 1:100 in 1 M Hepes buffer (pH 8). The gels were incubated with 2 ml of collagen II solution overnight at 4C in ultra-low attachment 6 well plates on an orbital shaker. Gels were rinsed with PBS and then allowed to equilibrate in cell culture media for one hour prior to cell seeding. Plastic or glass controls were coated with 1 mg/ml collagen II in acetic acid, diluted 1:100 in sterile PBS for one hour at 37C. The solution was then removed and the plates were rinsed with PBS before seeding cells.

QPCR

RNA was isolated from hMSCs using RNeasy column purification (Qiagen). The lysis buffer was added to both plastic and gel conditions and RNA was isolated according to the manufacturer's instructions, including on column DNase treatment. The concentration and purity of RNA was determined using a Nanodrop ND-1000 Spectrophotometer. 1 ug of RNA was

converted to cDNA in a reverse transcription (RT) reaction using the iScript cDNA Synthesis Kit (Bio-Rad). Quantitative PCR analysis of each sample was performed in a C1000 Thermal Cycler with CFX96 Real-Time System (Bio-Rad). Forward and reverse intro-spanning primers and iQ SYBR-Green Supermix (Bio-Rad) were used to amplify each cDNA of interest. Each sample was run in duplicate and all results were standardized to the housekeeping gene 18S. Fold changes in gene expression were calculated using the delta-delta Ct method (1). Figures display the mean and standard deviation for a representative experiment.

Immunofluorescence

Cells were cultured as indicated on collagen II-coated gel or glass substrates in 8 well Lab-Tek chamber slides (Nunc), with and without TGFβ for 45 minutes prior to analysis. Cells were washed in PBS twice and then fixed in 4% paraformaldehyde in PBS for 20 minutes at room temperature. After three PBS washes, cells were permeabilized in PBS with 0.5% Triton X-100 for 5 minutes, and then washed again (3x PBS). Cells were blocked for 1 hour (PBS, 10% goat serum, and 0.5% Triton X-100) prior to overnight incubation at 4C with primary antibodies diluted in PBS, 2% goat serum, and 3% Triton X-100. Primary antibodies included Smad2/3 (Santa Cruz), JNK (Cell Signaling), YAP (Santa Cruz), TβRII (Santa Cruz), and integrin β1 (R&D Systems). For cell surface receptor experiments (TβRII and integrin β1), cells were not permeabilized and Triton X-100 was not included in the protocol. Cells were washed three times with PBS and then incubated with secondary antibodies (goat anti-rabbit Alexa Fluor 488)) diluted in PBS with 2% goat serum and 1.5% Triton X-100 for 1 hour at room temperature. Cells were washed three times with PBS and then stained with rhodamine phalloidin (Invitrogen) diluted 1:800 in PBS for 20 minutes at room temperature. Cells were washed again three times with PBS and the well walls were removed. For cells cultured on glass, the gasket was also

removed for adding Slowfade Gold mounting medium with DAPI (Invitrogen) and covering with a coverslip. For cells cultured on gels, the gasket was left attached and mounting medium was added to each gel before applying the coverslip. Cells were imaged using an Olympus IX Widefield Microscope. Images were processed in ImageJ as previously described.

References

1. Livak KJ, Schmittgen TD. Analysis of relative gene expression data using real-time quantitative PCR and the 2(T)(-Delta Delta C) method. Methods. 2001 Dec;25(4):402-8.
2. Alliston T, Choy L, Ducy P, Karsenty G, Derynck R. TGF-beta-induced repression of CBFA1 by Smad3 decreases cbfa1 and osteocalcin expression and inhibits osteoblast differentiation. EMBO J. 2001 May 1;20(9):2254-72.
3. Kean MJ, Couzens AL, Gingras A-C. Mass spectrometry approaches to study mammalian kinase and phosphatase associated proteins. Methods. 2012 Aug;57(4):400-8.
4. Duong BH, Onizawa M, Oses-Prieto JA, Advincula R, Burlingame A, Malynn BA, et al. A20 Restricts Ubiquitination of Pro-Interleukin-1 beta Protein Complexes and Suppresses NLRP3 Inflammasome Activity. Immunity. 2015 Jan 20;42(1):55-67.
5. Clauser KR, Baker P, Burlingame AL. Role of accurate mass measurement (+/- 10 ppm) in protein identification strategies employing MS or MS MS and database searching. Analytical Chemistry. 1999 Jul 15;71(14):2871-82.
6. Sbalzarini IF, Koumoutsakos P. Feature point tracking and trajectory analysis for video imaging in cell biology. Journal of Structural Biology. 2005 Aug;151(2):182-95.
7. Rossier O, Octeau V, Sibarita JB, Leduc C, Tessier B, Nair D, et al. Integrins beta(1) and beta(3) exhibit distinct dynamic nanoscale organizations inside focal adhesions. Nature Cell Biology. 2012 Oct;14(10):1057-+.
8. Allen JL, Cooke ME, Alliston T. ECM stiffness primes the TGF beta pathway to promote chondrocyte differentiation. Molecular Biology of the Cell. 2012 Sep;23(18):3731-42.

Chapter 3

The use and optimization of novel high resolution imaging techniques

Introduction

Physical and biochemical cues in the cellular microenvironment play essential roles in the regulation of cell behavior. The initial interaction of these cues in the microenvironment and the cell's first response to these combinations begins at the cell surface receptor level. Studying these interactions at such a level that would reveal the mechanisms by which receptors integrate these cues to generate a coordinated response has been technically challenging. This chapter details the imaging approaches utilized and optimized to investigate the interactions between TGFβ receptors and integrins at the cell surface.

Conventional approaches

Biochemical approaches are commonly utilized to study the interaction and localization of proteins of interest, despite their inability to capture and provide spatial information at high resolution. We started by employing such an approach, utilizing immunofluorescence to examine the localization of TGFβ receptor type II and integrins on the cell surface. This approach allows for the detection and visualization of endogenous levels of proteins. However, there are two major drawbacks of this approach that limit the study of these interactions: 1) the need to fix cells prior to labeling resulting in the inability to study live cellular and protein dynamics and 2) the non-specific labeling issues with antibodies, especially for TGFβ receptors. As shown in Figure 3.1, the labeling for TβRII using this approach appears diffuse and punctate throughout the whole cell.

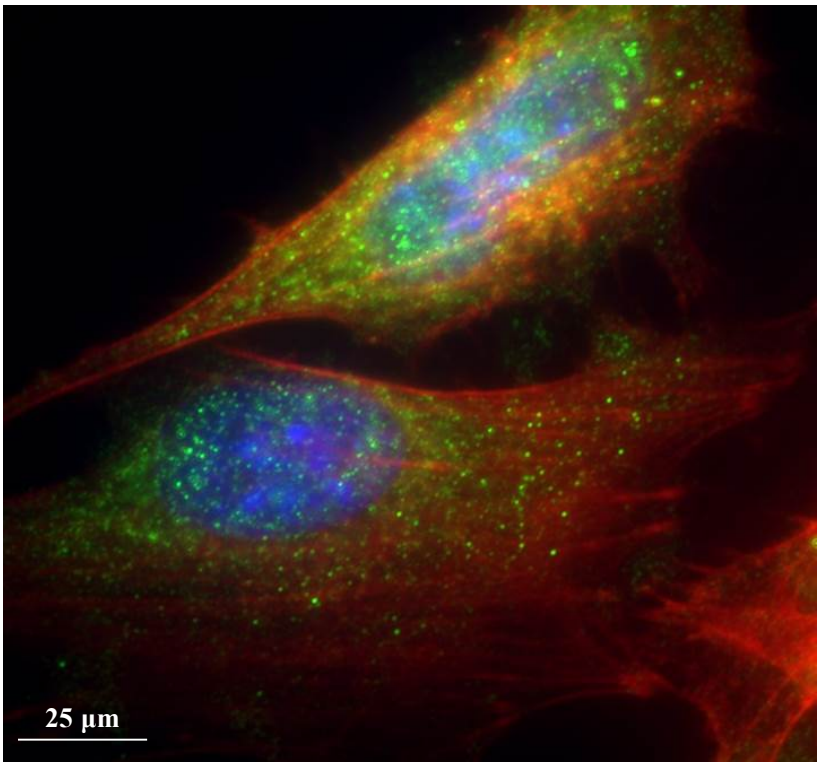

Figure 3.1. Staining of endogenous TβRII shows punctate organization. Immunofluorescence of ATDC5 cells imaged at 100x using widefield imaging provides limited insight into the structure and organization of TGFβ receptors. (green, TβRII; red, phalloidin; blue, dapi)

Furthermore, the localization and extent of diffusivity of staining was inconsistent between biological replications. The addition of exogenous factors such as TGFβ or ROCK inhibitor did not affect the localization or relative amount of labeling (not shown). However, this result is not surprising given the lack of consistency and the overall non-specificity of the antibodies for TβRII. Therefore, we wanted to investigate this question from a different approach, in order to ensure we were able to properly visualize the proteins on the cell surface.

Expression constructs

Fluorescently tagged expression constructs resolve the two shortcomings of using antibody-labeling approaches – they allow for live cell imaging and are inherently specific to the protein of interest. They do present an issue in that you are no longer studying endogenous protein activity, but rather that of an artificially overexpressed protein. However, the ability of expression constructs to overcome the aforementioned issues makes them the most suitable for this system, until a more perfect technique is developed in the future. Several constructs expressing focal adhesion proteins – vinculin, paxillin, integrins – were generated to facilitate the study of TGFβ receptor behavior at the cell surface and at sites of adhesion. These constructs were also useful for validation of the model system, as their localization to focal adhesions indicated normal cell phenotypic behavior (Figures 3.2 and 3.3).

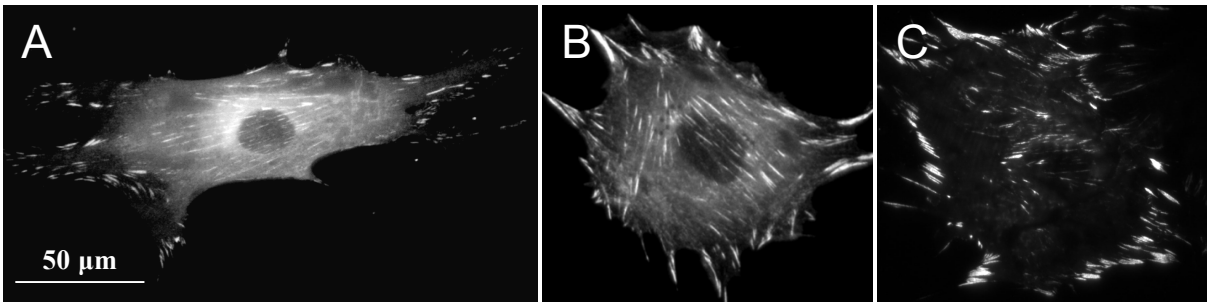

Figure 3.2. Vinculin and FAK expression constructs localize to adhesions. Fluorescently labeled expression constructs for vinculin (A,B) and FAK (C) localize to focal adhesions in hMSCs (A) and ATDC5 cells (B,C).

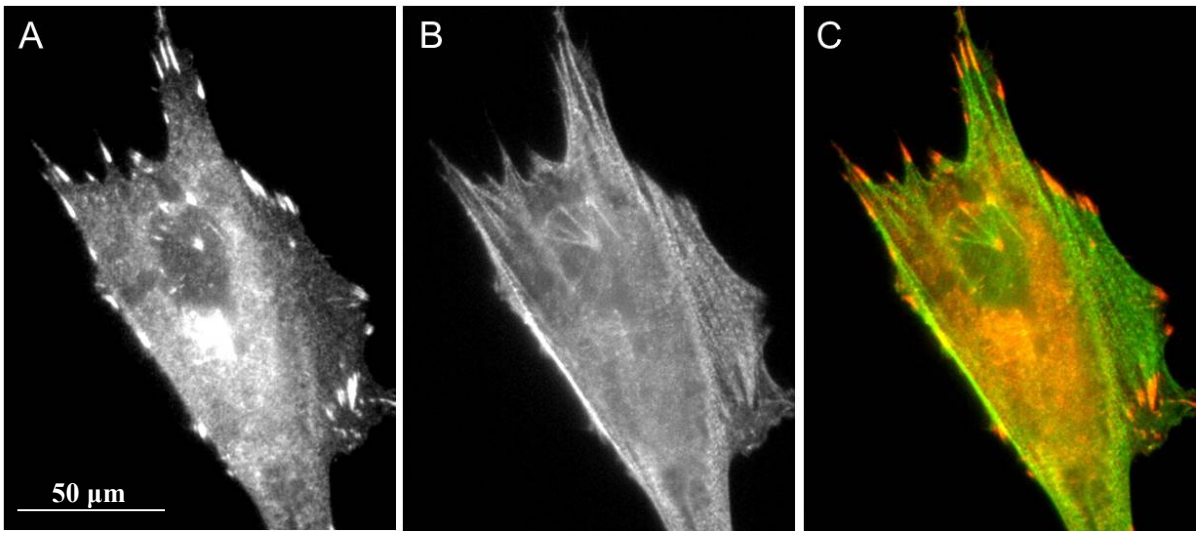

Figure 3.3. Co-transfection of expression constructs allows for simultaneous visualization of two proteins. The co-transfection of fluorescently labeled vinculin (A) and filamin (B) constructs reveals co-localization (C) at sites of cellular adhesion.

Fluorescently tagged constructs expressing TGFβ receptors were also generated for these studies (Appendix). This allowed for the visualization of TGFβ receptors and focal adhesion markers in the same cell.

Total Internal Reflection Fluorescence Microscopy

The mode of microscopy was also optimized for imaging the localization and behavior of TGFβ receptors at sites of adhesion. Figures 3.5 and 3.6 shows ATDC5 cells expressing mEmerald-tagged TGFβ receptor type II, imaged by spinning disc confocal microscopy at 40x and widefield microscopy at 100x.

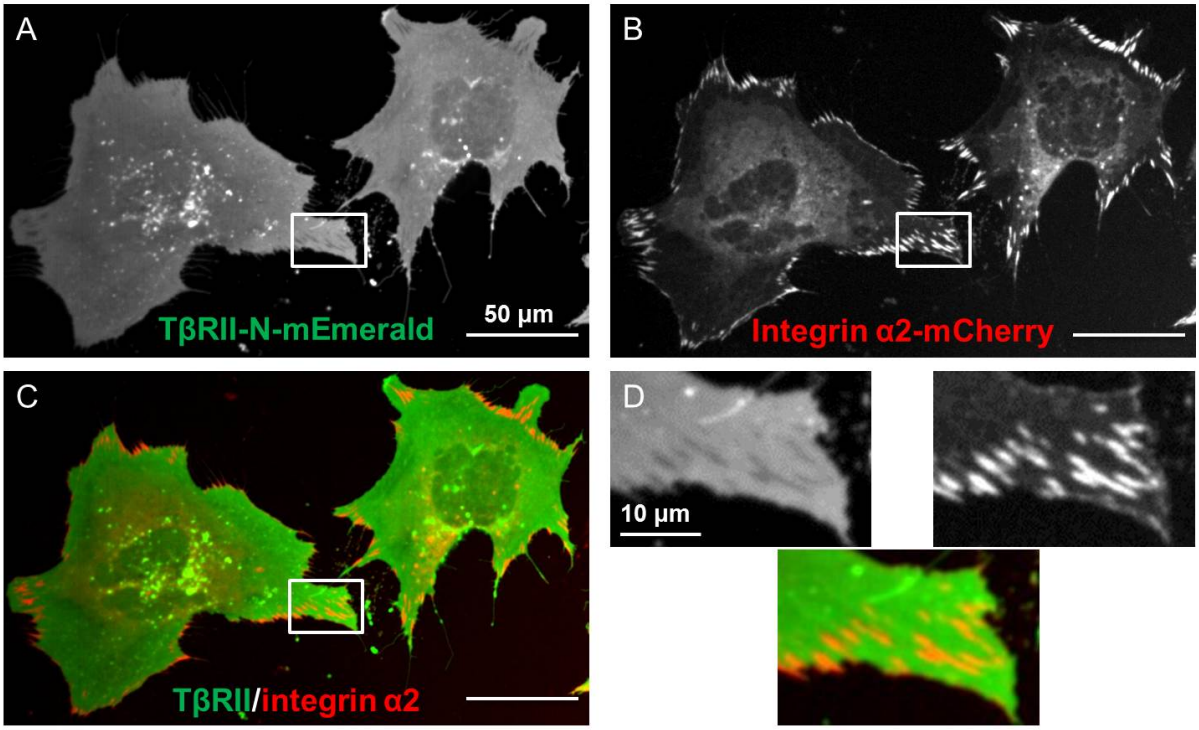

Figure 3.4. TβRII is absent from sites of adhesion. Spinning disc confocal imaging at 40x of ATDC5 cells co-transfected with TβRII-mEmerald (A) and integrin α2-mCherry (B) reveals shadowed regions of TβRII (A) and discrete localization patterns (C, D).

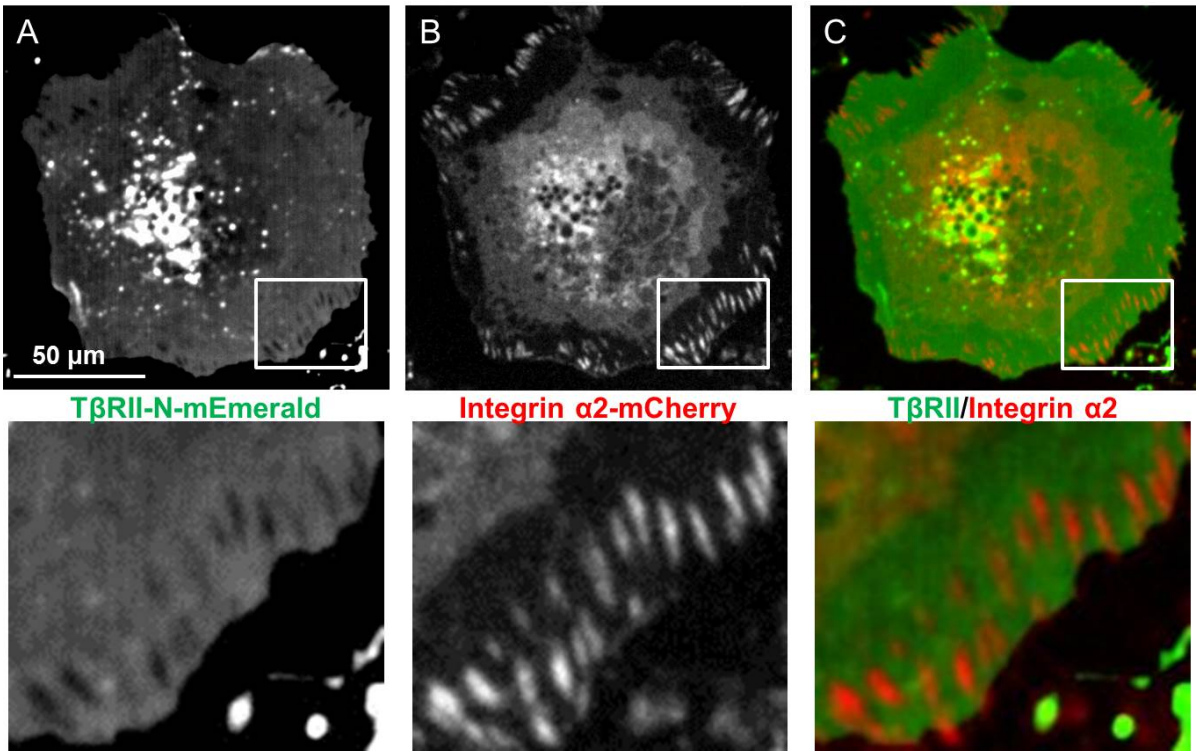

Figure 3.5. Depleted regions of TβRII correspond to integrin α2 localization. Widefield imaging at 100x of ATDC5 cells co-transfected with TβRII-mEmerald (A) and integrin α2-mCherry (B) reveals shadowed regions of TβRII and distinct localization patterns (C).

Using these imaging techniques, we observed shadowed regions of TβR within protrusions near the cell edges indicating the absence or depletion of TβR in these areas. Also noticeable, is the level of fluorescent cytoplasmic background throughout the cell. In order to gain a better understanding of the organization at cell edges and near the cell surface, we needed to utilize an imaging approach called Total Internal Reflection Fluorescence (TIRF) microscopy at 100x magnification. TIRF microscopy is a high signal-to-noise ratio technique used to image a thin section of the sample and reduce background noise (1). TIRF utilizes an incident light that approaches the specimen from an angle, creating an evanescent field when the beam strikes an interface between two media. This evanescent wave at the coverslip-sample interface is typically less than 100 nm, ensuring that only fluorophores within that region, at the cell membrane, are

excited and captured during imaging. The effect of transitioning from out of TIRF mode to in TIRF mode can be seen in Figure 3.6.

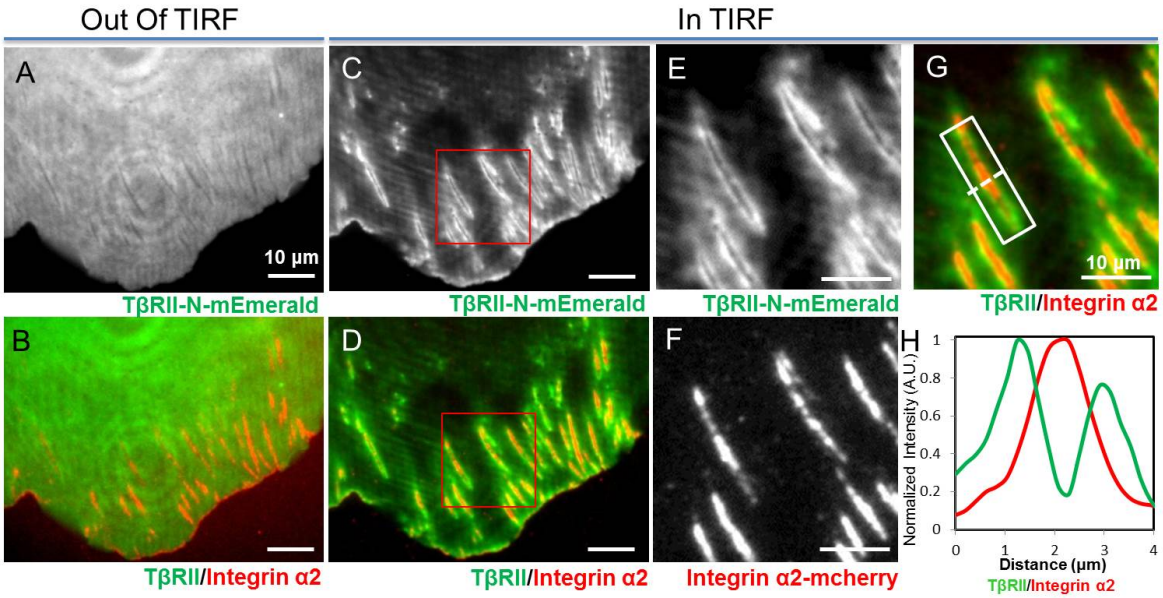

Figure 3.6. TβRII is specifically excluded from sites of adhesion. A and B show the expression patterns of TβR2 and integrin α2 using out of TIRF, widefield imaging. Switching to TIRF mode (C,D) reveals a striking spatial organization where TβRII is not only excluded from focal adhesions, but it actually forms a peripheral ring around integrin α2 and other focal adhesion proteins. Regions of interest at sites of adhesion (E-G) provide a better appreciation of this distinct spatial organization of surrounding of TβRII around integrin α2. A quantitative representation (H) of a profile plot of intensity demonstrates a central peak of integrin α2 expression surrounded by two peaks of TβRII expression.

Reducing the cytoplasmic background and focusing on the cell membrane reveals an unprecedented view of TGFβ receptors at the cell surface near sites of adhesion, as marked by integrin expression. This mode of imaging unveiled a discrete spatial organization of TβRII within these areas of focal adhesions that could not be visualized using conventional microscopy approaches. Although this approach yields high resolution and specific insight into the localization, organization, and structure of TGFβ receptors at sites of adhesion, it is limited by the inability to spatially and temporally distinguish individual receptor molecules (Figure 3.7).

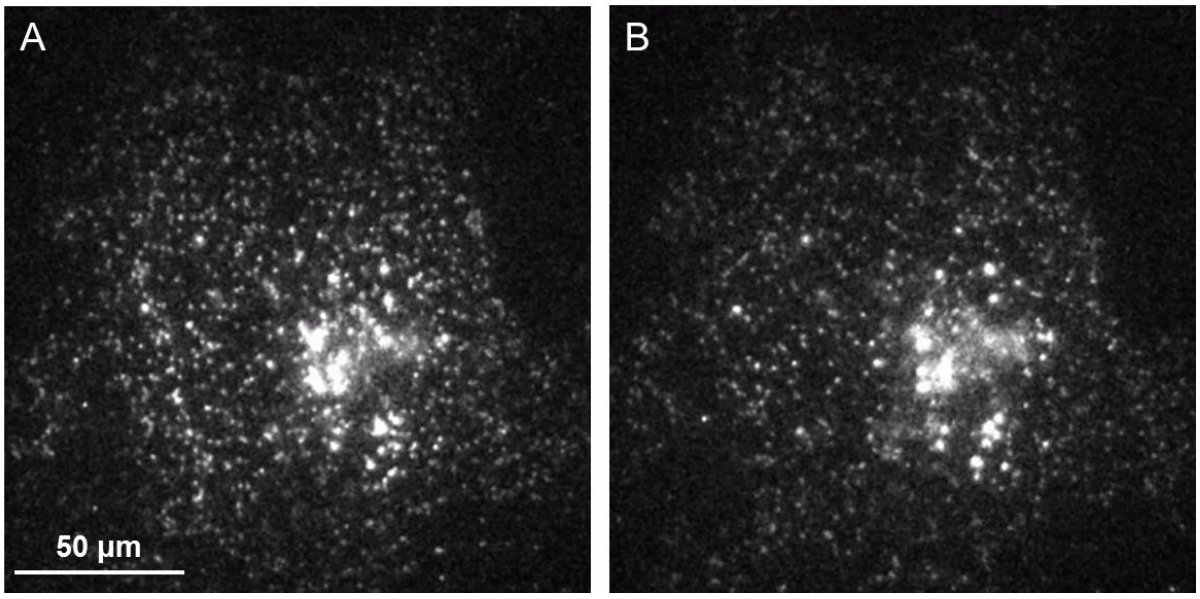

Figure 3.7. Conventional labeling presents density and photobleaching issues. Imaging GFP-labeled TGFβ receptors is limited by an inability to control labeling density and distinguish individual receptor molecules spatially temporally (A). Conventional labels also photobleach within seconds (B), presenting difficulties with dynamic imaging.

Furthermore, conventional labels present additional challenges with fluorophore bleaching and a limited control of labeling density. In this way, it might require 10-100 cells with an average of 10 tracks per cell to achieve meaningful results. Understanding the dynamics of single receptors, and specifically examining the organization and dynamics at the boundary of this spatial organization is critical for providing a mechanistic basis for how individual proteins facilitate cell function.

Single particle tracking photoactivated localization microscopy

Single particle tracking photoactivated localization microscopy (sptPALM) is a novel technique that combines single particle tracking with super resolution imaging. By performing this approach, we can observe the heterogeneities in the movements of individual proteins even in a crowded membrane environment, providing insights into cellular function. The use of

photoactivatable markers provides the ability to examine subdiffraction localization and dynamics of individual molecules. Specifically, subsets of mEos2-labeled proteins are continuously and stochastically activated to intermittently photoswitch individual photoactivatable molecules to a bright state, which are then imaged and bleached. This continuous process allows us to spatially and temporally resolve individual receptor molecules that would otherwise be indistinguishable (Figure 3.8) (2).

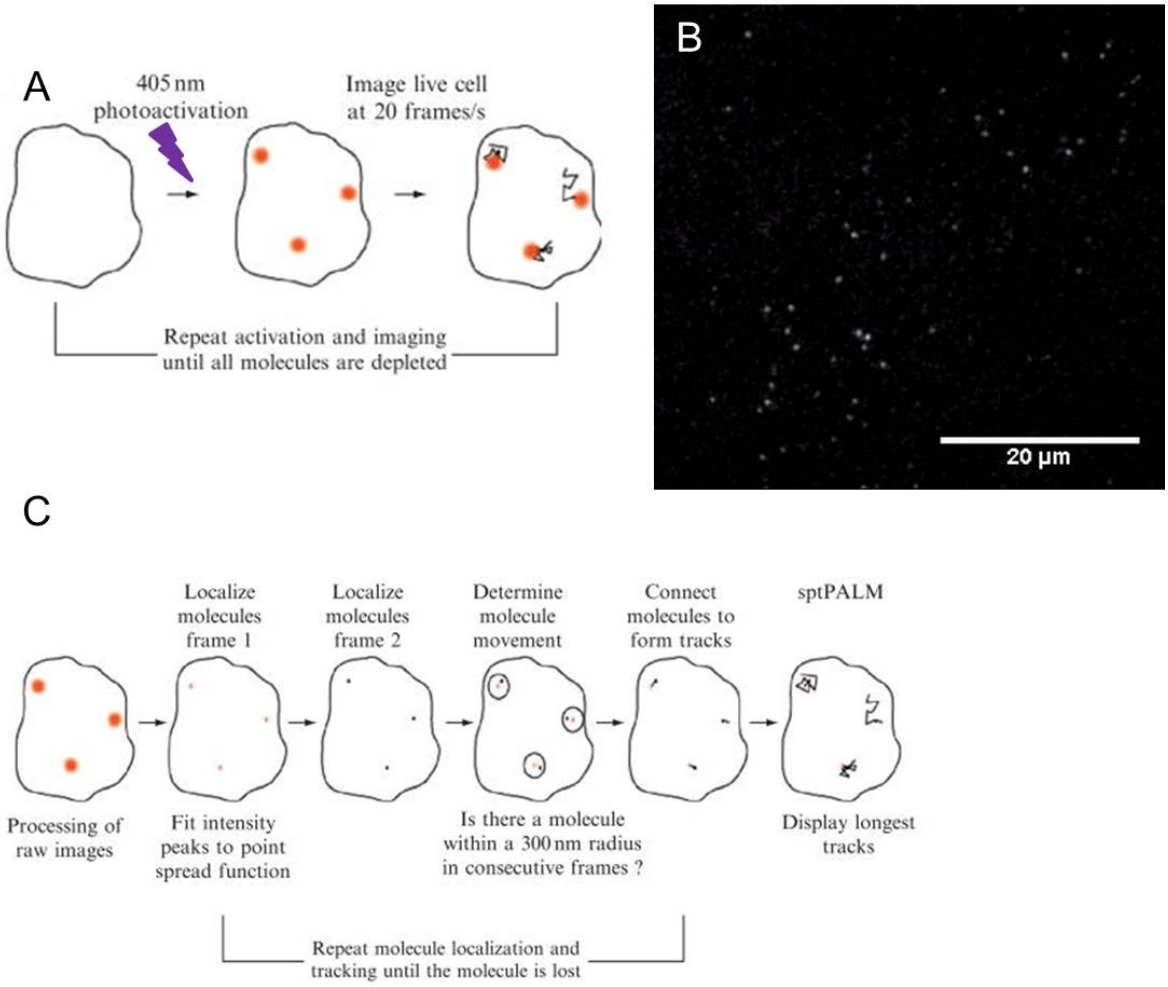

Figure 3.8. sptPALM Imaging. In PALM imaging, fluorophores are continuously activated, imaging, and photobleached (A) so that only a subset of fluorophores (B) is activated at any given time. This allows for the ability to spatially and temporally resolve individual receptor molecules. Single particle tracking entails localizing and tracking an individual molecule in consecutive frames to map its trajectory (C). Diagram modified from Manley et al. 2008.

This unique strategy overcomes the diffraction barrier present in traditional forms of fluorescence microscopy, in which a resolution limit is imposed by the diffraction of light. In sptPALM, single molecules are identified and tracked such that trajectories of individual molecules can be reconstructed by connecting the positions of fluorophores in consecutive imaging frames. We wrote custom Python scripts that provided qualitative and quantitative information at the individual molecule and at the whole cell level. We then overlaid these maps of trajectories on to a binary mask of the adhesion marker vinculin in order to observe changes in receptor localization and dynamics at these sites. These analyses were an essential contribution to our findings, as given the novelty of sptPALM imaging, few publicly available methods for tracking individual particles existed. In fact, this is the first documented report of using sptPALM to track individual TGFβ receptor molecules. These findings shed new light on the organization and dynamics of TGFβ receptors, providing essential insight into this growth factor signaling pathway and its interplay with physical cues and mechanotransduction pathways.

Discussion

Overall, the use and optimization of these novel imaging techniques – TIRF and sptPALM – allowed for unprecedented insight into the spatiotemporal organization and dynamics of TGFβ receptors at sites of adhesion. We revealed novel structural information on TGFβ receptors that was previously concealed by conventional immunofluorescence and imaging approaches. These findings provide fundamental insight into the mechanisms by which growth factor signaling and mechanotransduction pathways interact, which has implications from cell and tissue development to disease progression.

References

1. Axelrod D. Total internal reflection fluorescence microscopy in cell biology. Traffic. 2001 Nov;2(11):764-74.
2. Manley S, Gillette JM, Patterson GH, Shroff H, Hess HF, Betzig E, et al. High-density mapping of single-molecule trajectories with photoactivated localization microscopy. Nature Methods. 2008 Feb;5(2):155-7.

Chapter 4

Discrete spatial organization of TGFβ receptors couples receptor multimerization and signaling to cellular tension

Joanna P. Rys*[a,b], Christopher C. DuFort*[b], David A. Monteiro[a,b], Michelle A. Baird[c], Juan A. Oses-Prieto[d], Shreya Chand[d], Al Burlingame[d], Michael W. Davidson[c] and Tamara Alliston[a,b,e,1].

[a]University of California, Berkeley–University of California, San Francisco Graduate Program in Bioengineering, University of California, Berkeley, CA 94720

[b]Department of Orthopaedic Surgery, University of California, San Francisco, CA 94143

[c]National High Magnetic Field Laboratory and Department of Biological Science, Florida State University, Tallahassee, FL 32310

[d]Mass Spectrometry Facility, Department of Pharmaceutical Chemistry, University of California, San Francisco, CA 94143

[e]Department of Bioengineering and Therapeutic Sciences, Department of Otolaryngology–Head and Neck Surgery, and Eli and Edythe Broad Center of Regeneration Medicine and Stem Cell Research, University of California, San Francisco, CA 94143

*These authors contributed equally to this work.
[1]To whom correspondence should be addressed. Email: tamara.alliston@ucsf.edu

Author contributions: J.P.R., C.C.D., and T.A. designed research; J.P.R., C.C.D., D.A.M., J.A.O, and S.C. performed research, D.A.M., M.A.B., and M.W.D. contributed new analytical tools and reagents; J.P.R., C.C.D., D.A.M., J.A.O., S.C. A.B. and T.A. analyzed data; and all authors contributed to writing the manuscript.

The authors declare no conflict of interest.

Abstract

Cell surface receptors are central to the cell's ability to generate coordinated responses to the multitude of biochemical and physical cues in the microenvironment. However, the mechanisms by which receptors enable this concerted cellular response remain unclear. To investigate the effect of cellular tension on cell surface receptors, we combined novel high-resolution imaging and single particle tracking with established biochemical assays to examine TGFβ signaling. We find that TGFβ receptors are discretely organized to segregated spatial domains at the cell surface. Integrin-rich focal adhesions organize TβRII around TβRI, limiting the integration of TβRII while sequestering TβRI at these sites. Disruption of cellular tension leads to a collapse of this spatial organization and drives formation of heteromeric TβRI/TβRII complexes and Smad activation. This work details a novel mechanism by which cellular tension regulates TGFβ receptor organization, multimerization, and function, providing new insight into the mechanisms that integrate biochemical and physical cues.

Introduction

The diversity and specificity of cellular responses rely on the precise integration of biochemical and physical cues from the microenvironment. Cells generate a coordinated response through interactions among signaling pathways – from ligands and receptors to intracellular effectors. Receptors are a particularly versatile locus of control since they undergo regulated microdomain clustering, internalization and homo/hetero-meric multimerization. Because these mechanisms affect ligand binding, enzymatic activity and effector recruitment, receptors play a crucial role in defining signal intensity, duration, location, and quality (1-4). However, many questions remain about the mechanisms by which receptors participate in the concerted cellular response to a multitude of concurrent cues.

The TGFβ signaling pathway exemplifies the importance of regulated receptor multimerization. TGFβ signals through a heterotetrameric complex of transmembrane receptor kinases. Once the TGFβ ligand is activated from its latent form, it binds directly to a dimer of type II receptors (TβRII) (5-8). The ligand-bound TβRII complex recruits and phosphorylates two type I receptors (TβRI) – either Alk5 or Alk1 (9). TβRI, in turn, phosphorylates and activates canonical Smad proteins and multiple non-canonical effectors, such as RhoA, TAK1 and Akt (10, 11). Specifically, recruitment of Alk5 to the TβRII complex stimulates phosphorylation of Smad2/3, whereas Alk1 recruitment drives activation of Smad1/5/8 (12). The inappropriate shift of TβRII multimerization partner from Alk5 to Alk1 underlies disease processes ranging from vascular disorders to osteoarthritis (13, 14). Not only do TGFβ receptors associate with one another, but also with a number of other receptor families, notably integrins (15, 16). Garamszegi et al. revealed a physical interaction between integrin α2β1 and TGFβ receptors involved in collagen-induced Smad phosphorylation (16). TGFβ receptor interactions alter ligand specificity and

effector selection, offering a regulatory mechanism to calibrate TGFβ signaling based on the cellular microenvironment.

Integrins, another class of multimeric receptors, are central to cellular mechanotransduction. Upon integrin binding to the extracellular matrix, the formation of focal adhesions stimulates actomyosin contractility to generate cellular tension (17-19). Through this Rho/ROCK-dependent mechanism, cells establish tensional homeostasis with the physical features of the extracellular environment (17). Cellular tension can amplify, alter, or suppress cellular responses to growth factor signaling (20-22). The functional state of many intracellular effectors, including β-catenin, YAP/TAZ, and MAPK, is modulated by cellular tension (23-25). In the case of TGFβ signaling, we and others have identified several mechanosensitive responses (20, 22, 26). The activation of latent TGFβ ligand, as well as the phosphorylation, nuclear translocation and transactivation of Smads is regulated by cellular tension in a Rho/ROCK-dependent manner (20, 27). However, the mechanisms by which changes in cellular tension modulate effector activity remain unclear.

The effect of cellular tension on the multimerization of receptors other than integrins is largely unexplored. In spite of the established tension-sensitive regulation of downstream signaling effectors, the effect of physical cues on growth factor receptor interactions is unknown. This gap in understanding is partly due to the fact that until recently, studies of cell surface receptor colocalization and physical interactions have mostly utilized biochemical, biophysical, or fluorescence imaging approaches. While invaluable, these approaches are limited by their inability to discriminate spatially discrete molecular interactions that occur in specific cellular domains. Novel super-resolution imaging approaches provide the capability to visualize receptor responses to biochemical and physical cues at the single molecule level with spatial and temporal

specificity (28-32). To elucidate mechanisms by which physical cues regulate growth factor signaling, we utilize high-resolution imaging, single particle tracking, mass spectrometry and biochemical assays to test the hypothesis that cellular tension regulates TGFβ receptor multimerization. We find that cellular tension controls the spatial organization, multimerization and activity of a discrete population of TGFβ receptors at integrin-rich focal adhesions, suggesting a novel mechanism by which physical cues calibrate the activity of the TGFβ signaling pathway.

Results

Discrete localization of TβRI and TβRII to segregated spatial domains

To investigate the spatiotemporal control of TGFβ receptors, we evaluated the localization of endogenous and fluorescently tagged TβRII and TβRI in ATDC5 chondroprogenitor cells and NIH3T3 fibroblasts. Immunofluorescence of TβRII in both wildtype and transfected ATDC5 cells yielded similar results, revealing specific punctate staining that did not provide structural information (Fig. 4.1A, Fig. 4.1 – figure supplement 1). Proceeding with fluorescently tagged TβRII allowed for visualization of fine structural features in static and dynamic conditions. Spinning disc confocal microscopy of TβRII-mEmerald allowed visualization of its spatial organization, revealing shadowed regions where TβRII expression is completely absent (indicated by arrows, Fig. 4.1B-D). Total internal reflection fluorescence (TIRF) microscopy improves visualization of transmembrane proteins by examining a thin section of the sample at the adherent cell surface. Switching from widefield microscopy (Fig. 4.1E) to TIRF on the same cell vividly revealed segregated domains of TβRII (Fig. 4.1F) and TβRI (Fig. 4.1G,H). The sequestration of TβRII from TβRI was present with either the canonical (Alk5) or non-canonical (Alk1) type I TGFβ receptors (Fig. 4.1G,H). Indeed, when co-expressed in the same cell, TβRII is enriched at the boundary of discrete TβRI domains, demonstrating a novel spatial segregation of these signaling partners (Fig. 4.1I-L).

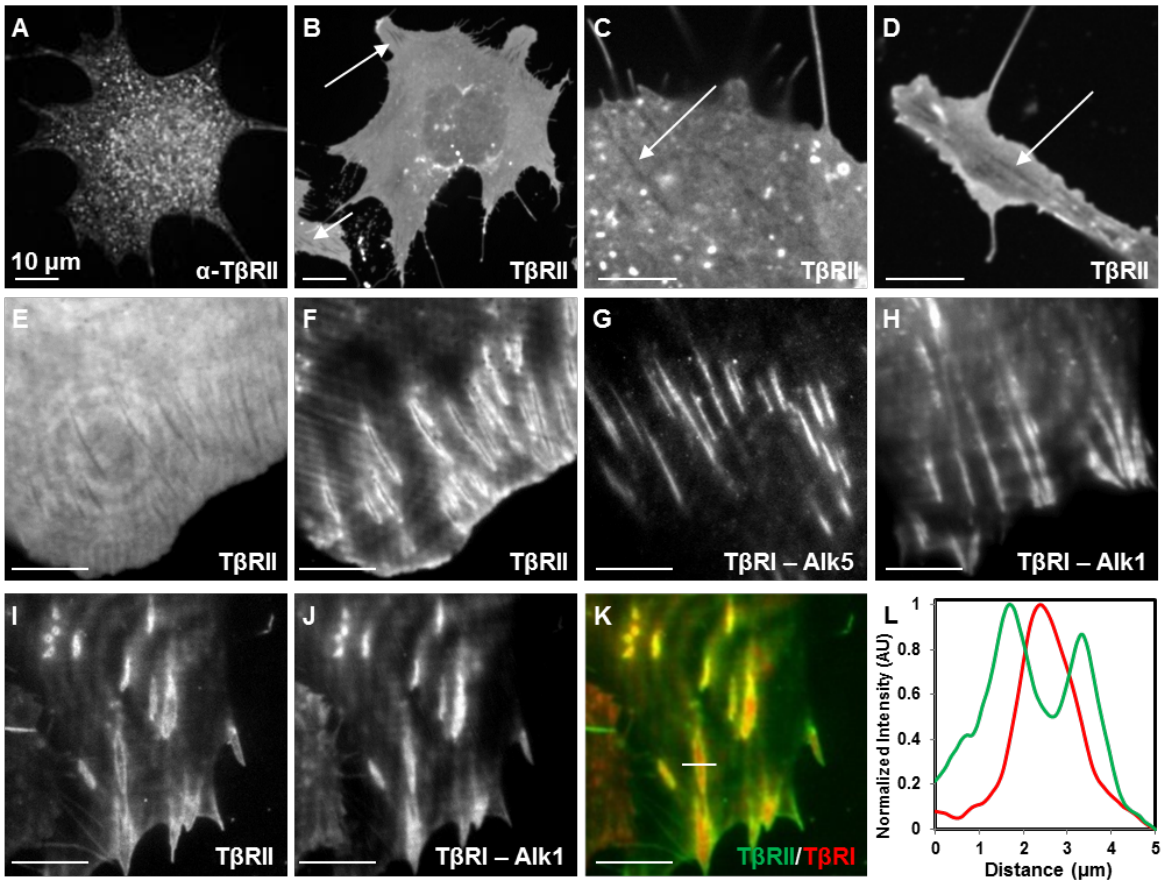

Figure 4.1. Spatial segregation of TβRII from TβRI. Spinning disc confocal imaging of endogenous TβRII (A, Fig. 1 – figure supplement 1) demonstrates punctate staining. Imaging of mEmerald-labeled TβRII (B) reveals TβRII-absent domains in ATDC5 (B,C) and NIH3T3 (D) cells expressing mEmerald-TβRII. Switching from widefield (E) to TIRF mode imaging (F) on the same cell unveils a specific spatial organization of TβRII, which is discrete from that of TβRI (Alk5 and Alk1) (G,H). ATDC5 cells co-expressing mEmerald-TβRII and mCherry-TβRI (Alk1) reveal that TβRII surrounds specific domains of TβRI (I-L). Quantitative profile plot of expression intensity demonstrates separate and distinct localization patterns of TβRI and TβRII (L).

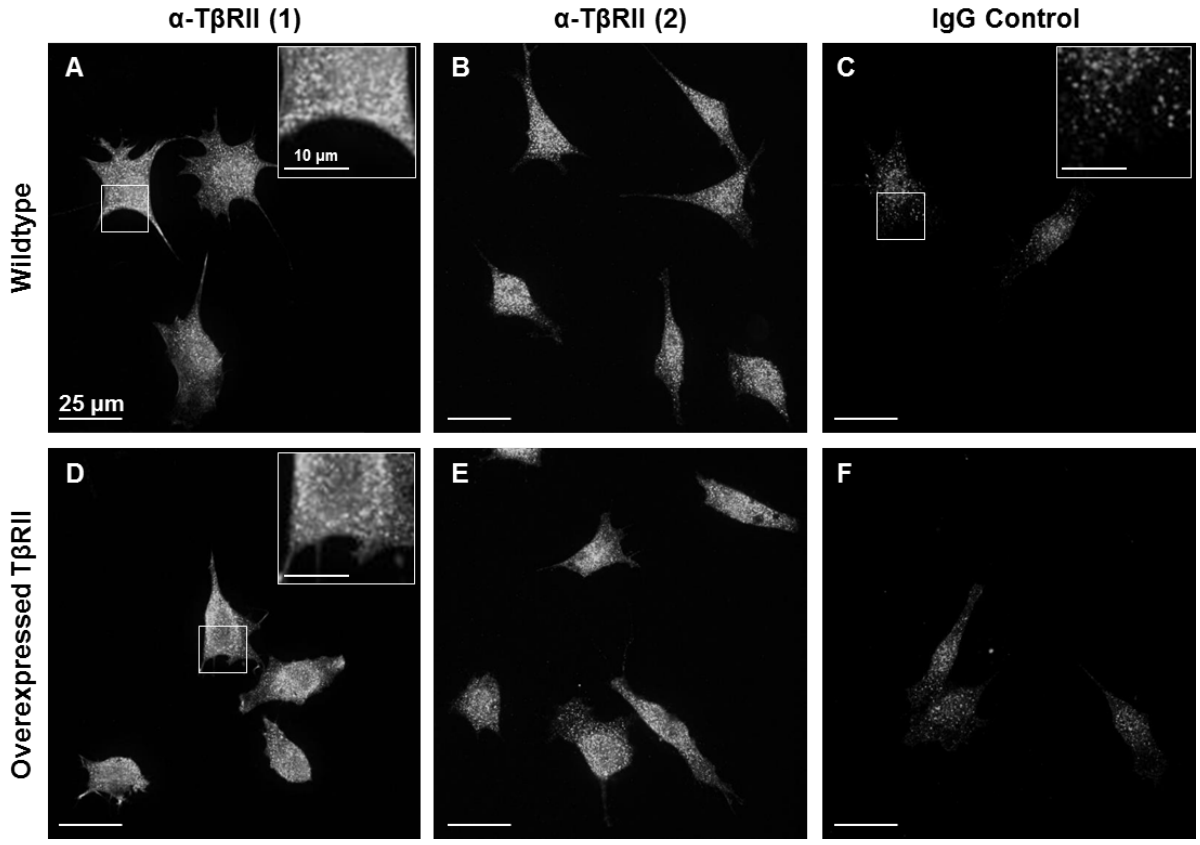

Figure 4.1 – figure supplement 1. Endogenous staining of TβRII insufficient for spatial organization visualization. Wildtype ATDC5 cells (A-C) and ATDC5 cells expressing TβRII-mCherry were stained with two different anti-TβRII (A,D and B,E) antibodies and an IgG control (C,F). Staining of TβRII between wildtype and transfected cells differs only in intensity and not structurally, indicating that the observed spatial organization is not due to expression constructs alone. Although TβRII antibodies showed specificity relative to IgG staining, this bright punctate staining is insufficient for visualizing fine structural organization.

Single molecule trajectories reveal specific regulation of TGFβ receptor dynamics

Since dynamic recruitment of TβRI to TGFβ-bound TβRII complexes stimulates downstream effectors, we sought to determine if spatial segregation of TGFβ receptors affects receptor mobility. Single-particle tracking photoactivated localization microscopy (sptPALM) resolves the dynamics of individual molecules in live single cells. Using sptPALM, we captured

thousands of trajectories of individual TβRI (Alk5) and TβRII proteins labeled with photoswitchable mEos2 (Fig. 4.2A,B) (33). The large number of long duration molecular trajectories (Fig. 4.2C) allowed us to visualize single molecule track behavior and describe molecular environments within individual cells. For both TβRI and TβRII, individual receptors showed a range of mobility, resulting in groups of immobile, confined, or freely diffusive receptors (representative tracks, Fig. 4.2D). Mobility of each group of TβRI did not differ significantly from TβRII (Fig. 4.2E), but the diffusion coefficient of TβRI was slightly higher (Fig. 4.2F), perhaps because of its lower molecular weight (TβRI/Alk5 56 kDa vs. TβRII 65 kDa). Relative to whole cell TGFβ receptor dynamics, TβRI and TβRII are significantly less mobile in cellular domains enriched with clusters of spatially organized receptors (Fig. 4.2F). Thus, this spatially organized population of TGFβ receptors is slower and more confined, possibly due to interactions with other proteins.

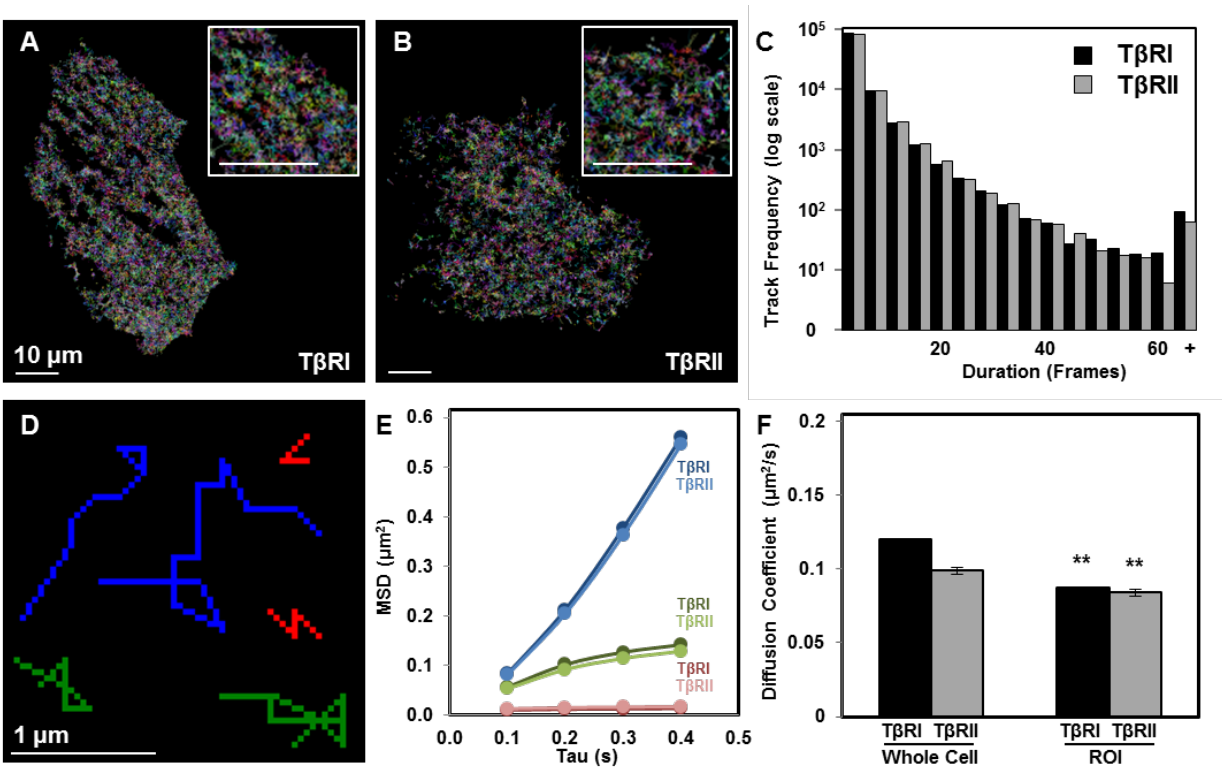

Figure 4.2. Limited TβRI (Alk5) and TβRII mobility in areas of receptor spatial organization. All mEos2-tagged TβRI and TβRII sptPALM single molecule trajectories with durations of at least 5 frames (500 ms) are plotted for representative ATDC5 cells, in which each color represents a different track (A,B). Cellular domains outside the imaging plane appear black. The histogram represents the distribution within a single cell of trajectory durations for individual TβRI and TβRII molecules (C). Representative individual TβRI sptPALM single molecule trajectories exhibiting immobile (red), confined (green), and freely diffusive (blue) movement are plotted in (D), with calculated mean squared displacement (MSD) plots for each population of TβRI and TβRII shown in E (mean ± SEM). Comparison of diffusion coefficients for TβRI and TβRII (F, mean ± SEM) in whole cells relative to areas of segregated TβRI/TβRII identify a less mobile population of TGFβ receptors in these regions of interest (ROI).

Focal adhesions organize TβRII around a segregated pool of TβRI

The distinct localization of TGFβ receptors could result from physical interactions with any number of known TGFβ receptor-associated proteins. Among these, integrins bind to TβRI and TβRII and functionally interact with the TGFβ pathway at multiple levels (9, 15). The primary

integrins in chondrocytes are integrins α2 and αV, which bind collagen and vitronectin/fibronectin (34). Both integrins interact with the TGFβ pathway (15, 16). TIRF imaging of mCherry-labelled integrin α2 revealed the presence of focal adhesions at these TβR-rich sites. Specifically, TβRII is absent from sites of adhesions and forms a peripheral ring surrounding integrin α2, resulting in distinct patterns of spatial localization (Fig. 4.3A). Interestingly, this spatial organization is absent in cells grown on poly-l-lysine-coated substrates that facilitate integrin-independent cell adhesion (Fig. 4.3 – figure supplement 1). Therefore, TβRII organization at sites of adhesion is dependent upon integrin activity. Profile plots of intensity and a custom analysis (Fig. 4.3Ai,Bi,Ci) were utilized to quantify colocalization between TβRs and integrin α2 across multiple cells. The slope of the regression line can be used as a metric, in which the higher values indicate increased colocalization of two proteins. TβRI (Alk5 and Alk1) is precisely colocalized with integrin α2 within focal adhesions, such that adhesions appear yellow (Fig. 4.3B,C) and regression line slopes (Fig. 4.3Bi,Ci) are higher relative to TβRII (Fig. 4.3A,Ai). This analysis reveals that integrin α2 colocalizes significantly more with Alk5 and Alk1 than with TβRII (Fig. 4.3D). The specific localization of TβRII near focal adhesions is apparent in cells of both mesenchymal (ATDC5, Fig. 4.3A-C, E; Saos-2, Fig. 4.3F) and epithelial (MCF10A, Fig. 4.3G) origin and is observed whether integrin α2 or integrin αV is tagged with a fluorescent protein (Fig. 4.3E,G). Furthermore, this observation still holds if the fluorescent labels for TβRII and integrin α2 are switched, as well as if TβRII is expressed and imaged alone (Fig. 4.3E,H). The overall spatial organization of TGFβ receptors at sites of adhesion is not affected upon stimulation with exogenous TGFβ (Fig. 4.3I), suggesting that this spatiotemporal organization is regulated through mechanisms independent from TGFβ ligand addition. Given the critical role of integrins in mechanotransduction and the known sensitivity of

TGFβ signaling to cellular tension (20), the unique pattern of TGFβ receptor and integrin localization could prime TGFβ receptors for regulation by elements of the mechanotransduction pathway.

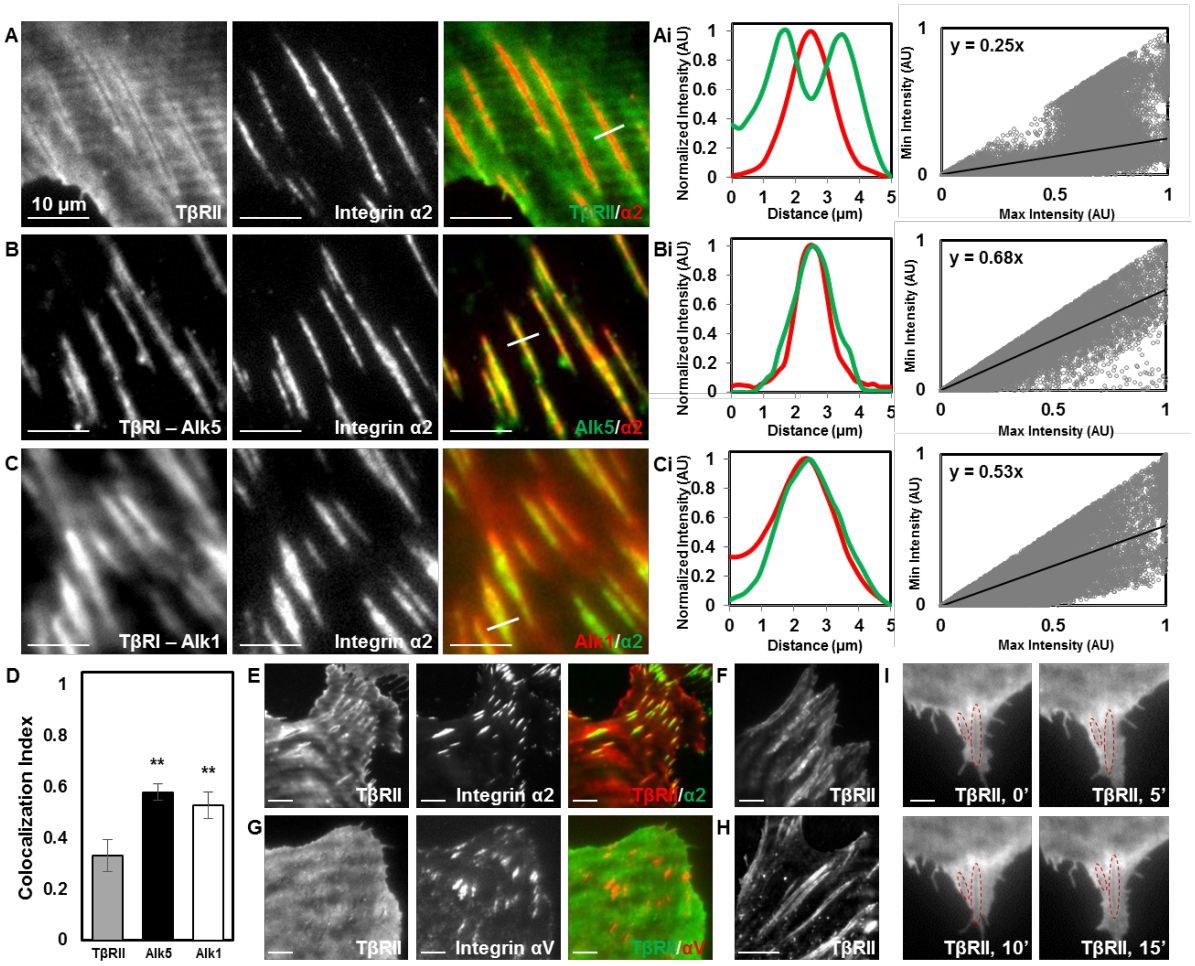

Figure 4.3. Focal adhesions sequester TβRI from TβRII. TIRF mode imaging and a custom colocalization analysis were used to evaluate localization of TβRII (A), Alk5 (B), or Alk1 (C) with integrin α2 in ATDC5 cells. TβRII surrounds integrin α2 (A), whereas both subtypes of TβRI, Alk5 (B) and Alk1 (C), are included within integrin-rich focal adhesions, as reflected by profile plots and the slope values of the regression lines (Ai,Bi,Ci). Quantification of colocalization reveals that Alk5 and Alk1 are significantly more colocalized with integrin α2 relative to TβRII (**, $p < 0.001$, mean ± SD, D). This organization is also present in ATDC5 cells when the fluorescent labels for TβRII and integrin α2 have been switched (E), in osteosarcoma Saos-2 cells (F), or in epithelial MCF10A cells (G), when labeling focal adhesions with integrin αV (G), and when TβRII is expressed and imaged alone (H). TβRII spatial organization is unaffected by addition of TGFβ, indicated by red outlines in the same cellular region following 15 minutes of TGFβ treatment (I).

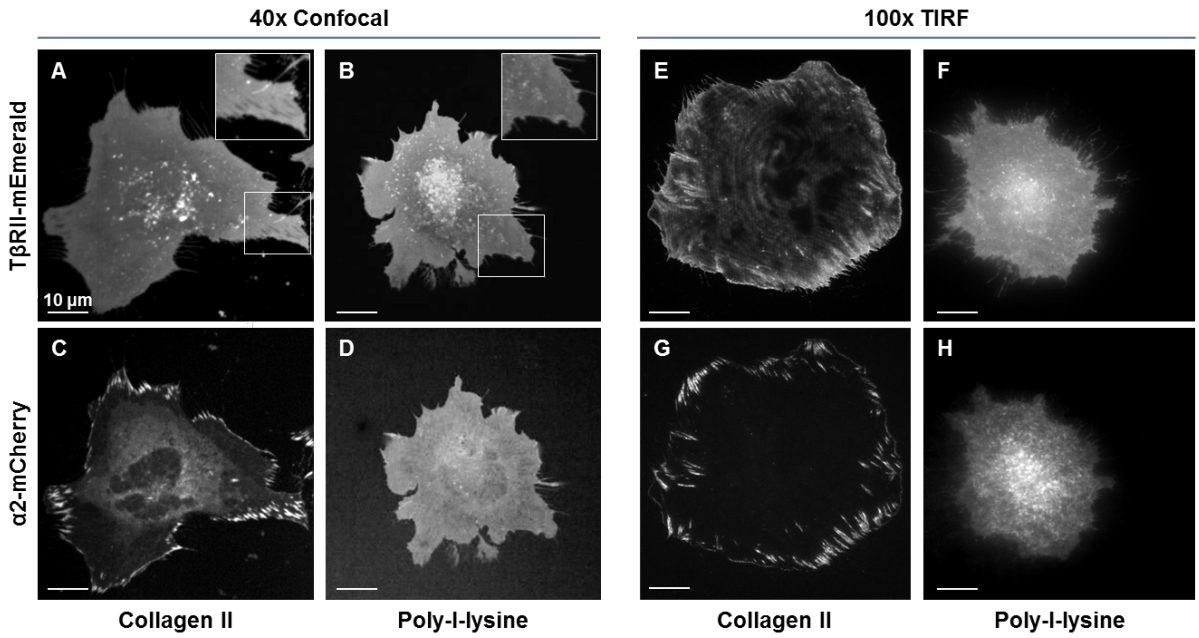

Figure 4.3 – figure supplement 1. Focal adhesion formation and TβRII spatial organization are dependent on integrin activity. TβRII spatial organization (A,B,E,F) and focal adhesion formation (C,D,G,H) are absent on poly-l-lysine (B,D,F,H) coated glass substrates relative to collagen II (A,C,E,G). Spinning disc confocal microscopy at 40x (A-D) and TIRF microscopy at 100x (E-H) of ATDC5 cells expressing TβRII-mEmerald and integrin α2-mCherry demonstrate a loss of TβRII depleted regions (A,B), TβRII peripheral ring formations (E,F), and integrin α2 developed adhesions (C,D,G,H) on poly-l-lysine relative to collagen II-coated substrates.

Focal adhesions immobilize TβRI and limit the integration of TβRII

To investigate the effect of focal adhesions on TβRI (Alk5) and TβRII dynamics, we used sptPALM to visualize TGFβ receptor trajectories near or within these vinculin-rich domains (Fig. 4.4A,B). SptPALM shows, both qualitatively and quantitatively, that TβRI is preferentially enriched and TβRII is preferentially excluded at sites of adhesion (Fig. 4.4A-C). Analysis of individual TβRII trajectories showed that TβRII 'bounces' around the edges of individual focal adhesions (Fig. 4.4E) but is rarely incorporated within the focal adhesion, as was common for TβRI (Fig. 4.4D, i-ii). To determine if focal adhesions shifted the fractions of freely diffusive,

confined, or immobile receptors, TβRI and TβRII trajectories near sites of adhesion were mapped based on receptor mobility. Trajectory maps reveal that TβRII mobility is confined near focal adhesions, which sequester and immobilize TβRI (Fig. 4.4F,G). Indeed, a higher fraction of immobilized TβRI is present inside adhesions relative to outside (Fig. 4.4H). Accordingly, the diffusion coefficient for TβRI decreases for tracks inside adhesions compared to those outside, demonstrating that this spatial organization specifically limits TβRI mobility (Fig. 4.4I). The differential localization and dynamics of TβRI and TβRII in adhesion-rich domains, relative to one another and to the whole cell TGFβ receptor population, indicates that this spatial control has functional implications for TGFβ signaling and for mechanotransduction.

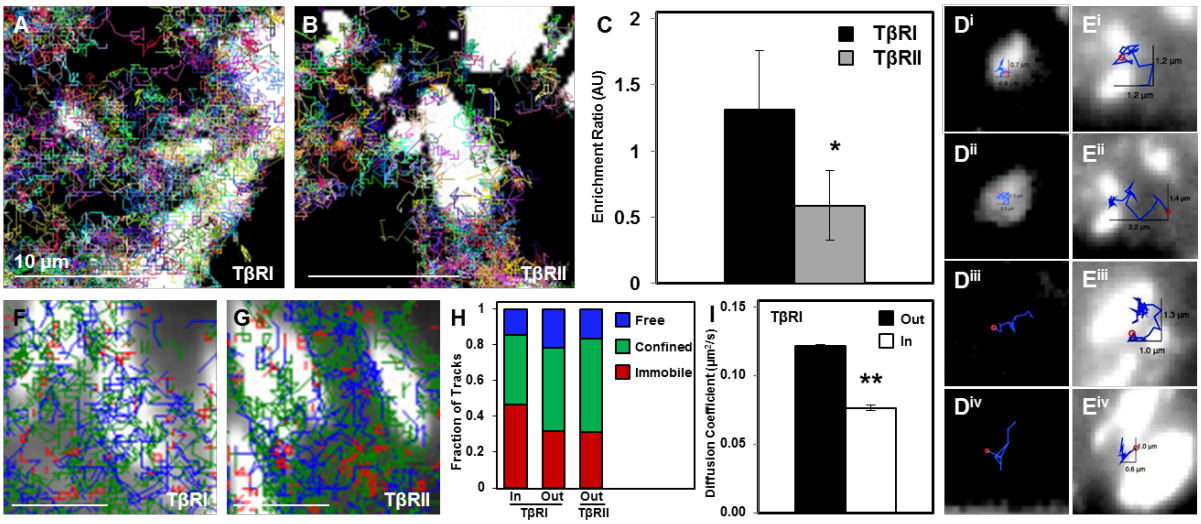

Figure 4.4. Dynamic interaction of TβRs with integrins facilitate spatial organization. Representative trajectories for TβRI (Alk5) overlaid with the tagged focal adhesion marker vinculin are consistent with TIRF results showing a colocalization and interaction between integrin-based adhesions and TβRI (A) but not TβRII (B). Quantification of these regions shows that TβRI is preferentially enriched inside adhesions relative to outside, and that TβRII is preferentially excluded at these same sites (*, $p < 0.01$, mean ± SD, C). Representative single molecule trajectories show sequestration of TβRI in focal adhesions (D, i-ii) and free diffusion outside adhesions (D, iii-iv), whereas TβRII bounces around the edges of focal adhesions in a freely diffusive (E, i-ii) or confined (E, iii-iv) manner. Analyzing TβR trajectories at focal adhesions based on diffusion (Red: Immobile, Green: Confined, Blue: Freely Diffusive) shows a higher density of tracks inside adhesions for TβRI (F) compared to TβRII (G), and demonstrates a higher fraction of immobile TβRI tracks inside relative to outside adhesions (H). The diffusion coefficient of TβRI trajectories decreases inside adhesions (mean ± SD, I).

TGFβ receptors form complexes with integrin αV and the actin-binding protein cofilin

To determine whether these changes in receptor mobility at sites of adhesion are due to direct or indirect physical interactions with other proteins, we performed mass spectrometry and co-immunoprecipitation experiments. Mass spectrometric analysis of proteins that precipitate with Flag-tagged TβRI (Alk5) and TβRII revealed hundreds of proteins, several of which were specifically enriched compared with precipitates of untransfected (mock) cells. The analysis identified proteins already known to interact with TβRs, such as PRMT5 and PRMT1 (35). TβRs

also precipitated several adhesion-related proteins, including integrin αV and endogenous cofilin, as shown in the annotated spectra (Fig. 4.5A,B). The peptide counts (graph insets) indicate that integrin αV associates with both TβRI and TβRII, and that cofilin preferentially associates with TβRII (Fig. 4.5A,B). Cofilin is an actin-binding protein that severs ADP-actin filaments at the leading edge of migratory cells (36). Previous reports implicate cofilin as a target of TGFβ-activated RhoA, which promotes actin reorganization through ROCK, LIMK and cofilin (37, 38). However, this is the first report, to our knowledge, of a complex between TGFβ receptors and cofilin. To confirm these mass spectrometry findings, we performed co-immunoprecipitation on cells expressing Flag-tagged TβRI/II and tagged integrin αV or cofilin (Fig. 4.5C,D). Consistent with the mass spectrometry peptide counts, integrin αV forms a complex with both TβRI and TβRII, whereas cofilin primarily interacts with TβRII. Although the novel finding of a complex formation, either through direct or indirect interactions, between TβRII and cofilin remains to be further explored, it suggests a potential mechanism underlying the discrete spatial organization of TβRII at focal adhesions.

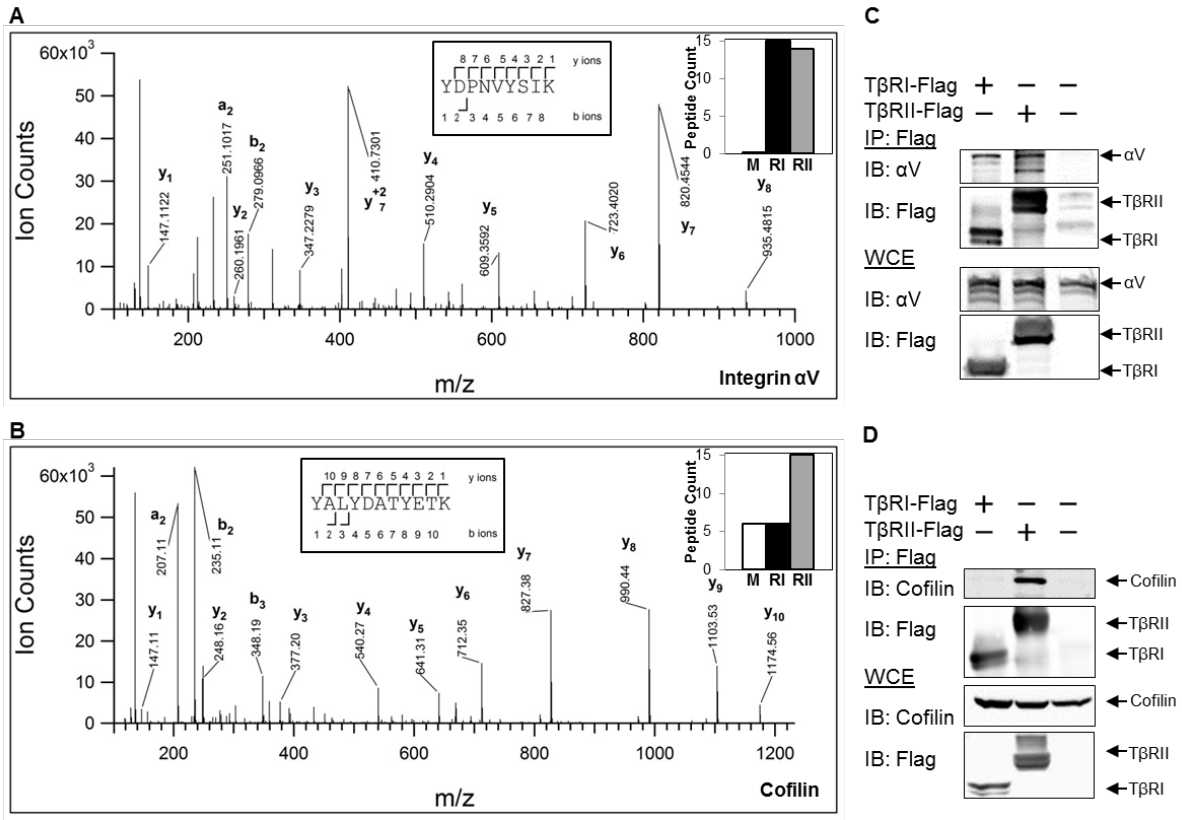

Figure 4.5. TβRs form complexes with integrin αV and cofilin. High-energy collision dissociation–tandem mass spectra obtained from precursor ions with mass 549.7775+2 (A) and 669.3185+2 (B) found in tryptic digests of immunoaffinity pulldowns of TβRI/II, corresponding to peptides spanning residues Y153-K165 of human integrin αV (A) and Y82-K92 of human cofilin (B). b- and y- type ion series are labeled in the figure. Insets show the sequences of the peptides as well as representative peptide counts for integrin αV (A) and cofilin (B) for mock (M), TβRI (RI, Alk5), and TβRII (RII) pulldowns. Co-immunoprecipitation of Flag-tagged TβRI and TβRII demonstrate the presence of integrin αV and cofilin in these complexes (C, D).

Cellular tension regulates TGFβ receptor organization at focal adhesions

Integrins transmit changes in the physical microenvironment across the plasma membrane to modulate cellular tension and signaling. The presence of a focal adhesion-associated TGFβ-receptor population suggests a novel mechanism by which cellular tension may regulate TGFβ

signaling. To test the hypothesis that TGFβ receptor organization at focal adhesions is sensitive to cellular tension, we treated ATDC5 cells with the ROCK inhibitor Y27632 or the myosin II inhibitor blebbistatin. Within 15 minutes of adding Y27632 (Fig. 4.6A,B) or blebbistatin (Fig. 4.6C,D), the peripheral ring of TβRII completely collapses. The segregation of TβRII from TβRI and integrin α2 at sites of adhesion is dynamically released, such that TβRII converges and colocalizes with integrin α2. Quantitative analysis demonstrates that TβRII is significantly more colocalized with integrin α2 after addition of Y27632 and blebbistatin (Fig. 4.6E).

To assess the effect of cellular tension on physical associations among TβRI, TβRII and integrins, we performed co-immunoprecipitation experiments. We find that cellular tension not only regulates the spatial organization of integrins and TGFβ receptors, but also affects their physical associations with each other; though these interactions may be direct or indirect. Specifically, while disruption of tension with the ROCK inhibitor enhanced integrin αV association with TβRI, it almost completely blocked the association between integrin αV and TβRII (Fig. 4.6F).

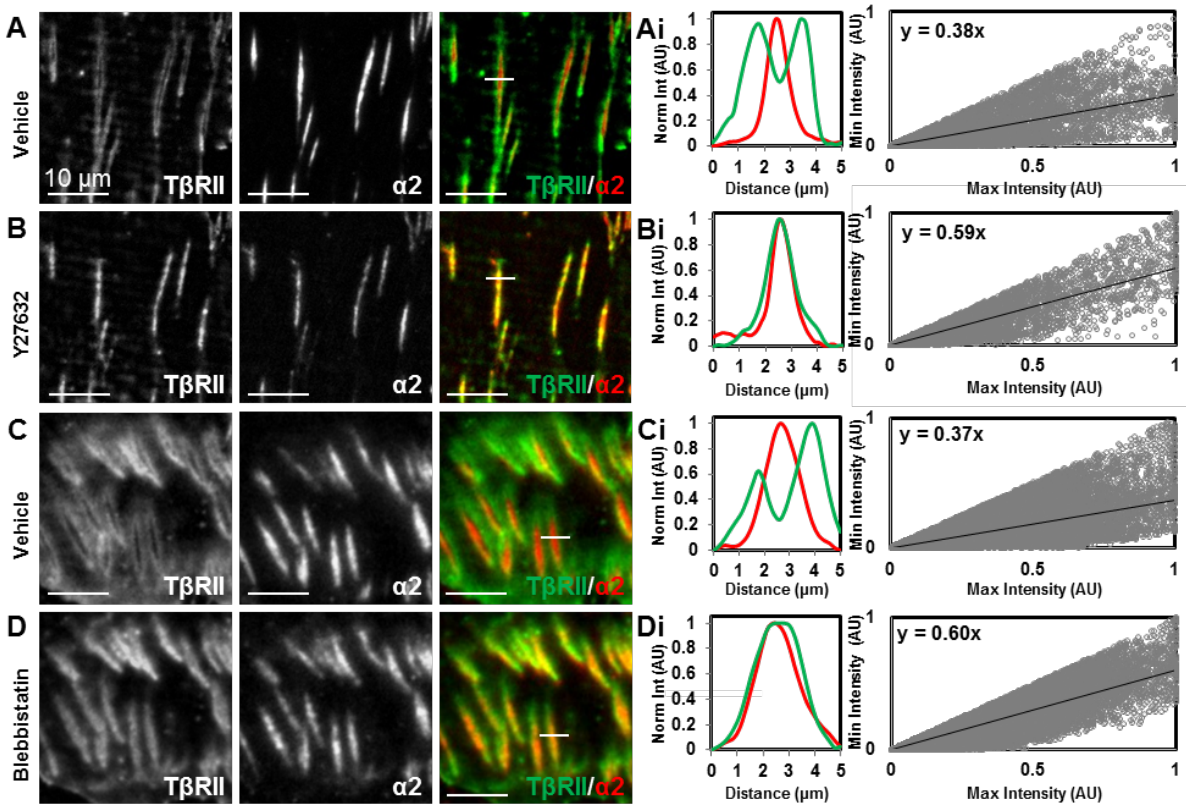

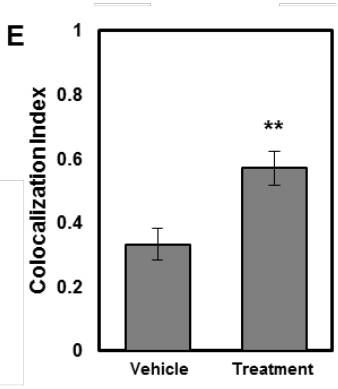

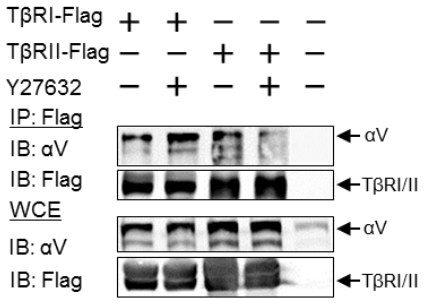

Figure 4.6. Tension-sensitive regulation of TβR spatial organization. Within 15 minutes of disrupting cellular tension by adding the ROCK inhibitor Y27632 (A,B) or the myosin II inhibitor blebbistatin (C,D), the peripheral ring of TβRII-mEmerald around focal adhesions (A,C) completely collapses (B,D). Colocalization quantification (Ai,Bi,Ci) demonstrates that TβRII is significantly more colocalized with integrin α2 post-treatment (Y27632, blebbistatin) relative to pre-treatment (**, $p < 0.001$, mean ± SD, E). Disruption of tension with Y27632 enhances integrin αV association with TβRI but reduces its association with TβRII (F).

Tension-sensitive regulation of TGFβ receptor heteromerization and signaling

Since a reduction in cellular tension drives colocalization of TβRI and TβRII, we sought to determine if this change in spatial organization had functional consequences for TGFβ signaling. We first evaluated the effect of reduced cellular tension on TβRI/TβRII heteromerization using co-immunoprecipitation. Release of this discrete spatial segregation of TGFβ receptors at focal adhesions allows the receptor subunits to interact such that ROCK-inhibition stimulates formation of heteromeric TβRI/TβRII complexes (Fig. 4.7A). To examine the effect of manipulating cellular tension under physiological conditions, we cultured cells on substrates of varying stiffness. A reduction in cellular tension through culture on compliant substrates significantly drives TβRI/TβRII complex formation (Fig. 4.7B). Therefore, a reduction in cellular tension, due to pharmacologic ROCK inhibition or changes to the stiffness of the microenvironment, drives formation of a multimeric TβRI/TβRII complex that is required for the activation of downstream TGFβ effectors.

To determine the effect of tension-sensitive TβR localization and heteromerization on downstream TGFβ effectors, we evaluated the phosphorylation of Smad3. Culturing cells on compliant substrates leads to significantly increased endogenous Smad3 phosphorylation (Fig. 4.7C). Interestingly, the effect of TGFβ on Smad3 phosphorylation is substrate-dependent, such that TGFβ induces Smad3 phosphorylation on 0.5 kPa substrates but not on 16 kPa substrates (Fig. 4.7C). This is consistent with the established non-linear response of TGFβ signaling and other cellular behaviors to cellular tension (20, 39). Thus the spatial organization of TβRI and TβRII by integrins at focal adhesions affords tension-sensitive control of TβRI and TβRII

multimerization and activation of Smad3, providing a mechanosensitive mechanism by which cells calibrate their response to TGFβ.

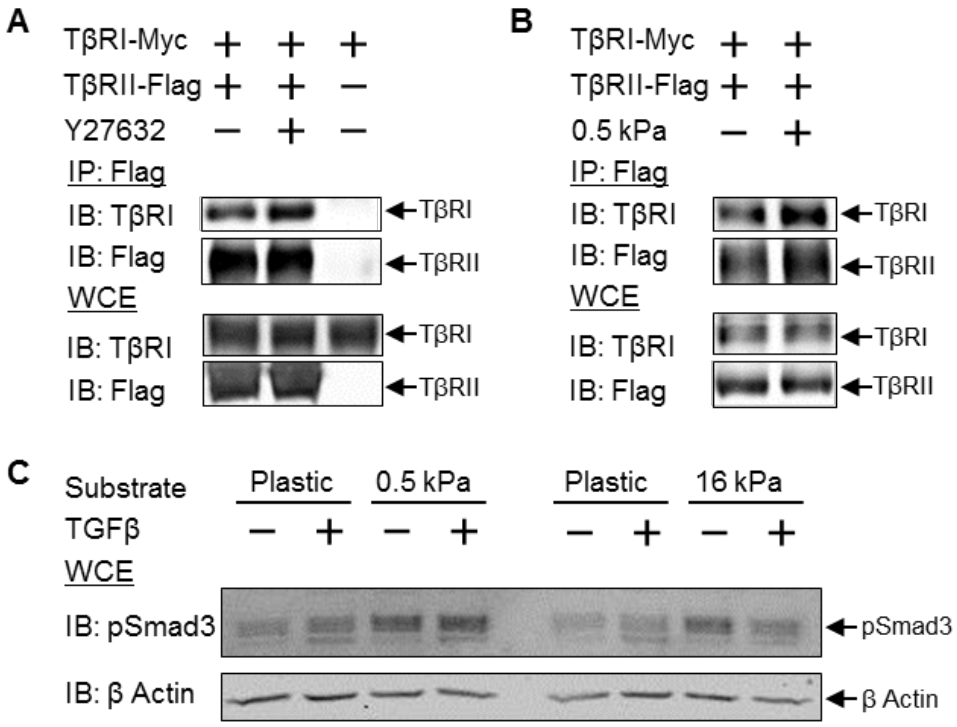

Figure 4.7. Disruption of tension-sensitive TβR segregation increases TβRI/TβRII multimerization and phosphorylation of Smad3. ROCK inhibition releases the discrete spatial organization of TβRs at focal adhesions and drives the formation of heteromeric TβRI/TβRII complexes within 15 minutes of Y27632 exposure (A), as shown by Flag co-immunoprecipitation (IP) and immunoblotting (IB). Likewise, manipulation of cellular tension through culturing cells on collagen II-coated glass or 0.5 kPa polyacrylamide substrates increases co-immunoprecipitation of TβRI with Flag-tagged TβRII (B). In cells grown on collagen II-coated compliant (0.5 kPa) or stiff (16 kPa) polyacrylamide substrates, endogenous Smad3 phosphorylation is increased (C). The effect of TGFβ on Smad3 phosphorylation is substrate-dependent, such that maximal TGFβ-inducibility is observed on 0.5 kPa substrates, consistent with a tension-sensitive calibration of TβR localization and activity (C).

Discussion

Here we show that cellular tension regulates TGFβ receptor spatial organization and interactions at focal adhesions, providing a novel mechanism for the cellular integration of signaling by physical and biochemical cues. We observe a novel spatiotemporal regulation of the TGFβ pathway such that TβRII is segregated from TβRI and integrins at sites of adhesions. Single particle tracking reveals the dynamics of individual TGFβ receptor molecules, and identifies populations of TGFβ receptors with distinct behaviors and mobility near and far from sites of focal adhesions. The confined population of TGFβ receptors at focal adhesions has lower mobility than the freely diffusive receptor population far from sites of adhesion. TGFβ receptors associate with several adhesion-related proteins, including the actin-binding protein cofilin, which preferentially associates with TβRII relative to TβRI. This novel spatial organization of TβRI and TβRII at sites of adhesion provides mechanosensitive control of TGFβ receptor multimerization and function independently of TGFβ ligand stimulation. Overall, this reveals the potential of two differentially regulated populations of TGFβ receptors – one that is TGFβ-sensitive and one that is tension-sensitive – a finding that may contribute to the context-dependent signaling outcomes of this pathway.

This tension-dependent mechanism for the regulation of TGFβ receptors has a number of interesting functional implications. At the level of the TGFβ ligand, integrins activate TGFβ from its latent form through cellular tension generated by actomyosin contraction (7, 8, 40, 41). The observed recruitment of TGFβ receptors to focal adhesions would enrich their access to this reservoir of integrin-activated TGFβ. At the receptor level, focal adhesions may sequester TβRI from TβRII to limit their activity in the presence of ligand. The extent to which this sequestration is cofilin-dependent requires further investigation. This sequestration of TβRI may contribute to

its slow internalization, relative to TβRII, following TGFβ stimulation (42, 43). Alternatively, focal adhesions may create structured TβRI and TβRII boundaries that prime a robust response when cells encounter the correct combination of physical and biochemical cues. We demonstrate tension-sensitive regulation of endogenous downstream Smad3 phosphorylation by cellular tension and TGFβ. In addition, chondrocytes grown in TGFβ on 0.5 MPa substrates induce differentiation markers far beyond levels induced by either cue alone (20). We and others have reported that the effect of substrate stiffness or cellular tension/Rho/ROCK activity on downstream TGFβ signaling is synergistic and nonlinear (20, 22, 26). Therefore, it is possible that lower cell tension in one cell type may have a differential effect on Smad phosphorylation, nuclear localization, and transactivation than in another cell type. It would be interesting to examine this effect utilizing a substrate system that provides independent and continuous gradients of ligand density and substrate stiffness (39). The mechanisms responsible for such synergy have been unclear, but this newly described regulation of TGFβ receptor multimerization and downstream signaling may couple the mechanosensitive activity of the TGFβ pathway to physical cues. Fully understanding the functional implications of this spatially-distinct TGFβ receptor population will require the development of new imaging tools, such as those that can dynamically visualize TGFβ effector activity locally at focal adhesions.

The current study of TGFβ receptors opens the possibility that tension-sensitive receptor multimerization may underlie mechanosensitive signaling by other pathways. Cellular tension impacts the activation, translocation, and function of intracellular effectors including small GTP-ases, kinases and transcriptional regulators such as Smads and YAP/TAZ (20, 22, 24, 26). However, known mechanisms are insufficient to explain the ability of physical cues to modulate cell-type specific responses to BMP, EGF and other growth factors (22, 44). Several receptor

families share features with TGFβ receptors that may contribute to their mechanosensitivity, such as their association with integrin-rich focal adhesions and their potential for the formation of stable receptor clusters by geometric constraints (1, 4, 45). Previous studies have established important physical and functional links between focal adhesion components and growth factor receptors. EGF receptor binds actin and colocalizes with integrin α2β1 (46), while the receptor CD44 interacts with several components of the focal adhesion complex, such that hyaluronan-bound CD44 activates c-Src and Rac1 (47). Aside from TGFβ, shown herein, the extent to which these physical associations contribute to mechanosensitive control of receptor multimerization or downstream signaling remains to be determined. Nonetheless, others have postulated receptor multimerization as a mechanism for mechanocoupling of TGFβ, ephrin and T cell receptor signaling (45, 48). In each case, the solid state presentation of the ligand is thought to play a critical role in structuring multimeric receptor clusters. In T cell receptor and ephrin signaling, the solid state is provided by ligands on the neighboring cell, which create geometric constraints that mechanically trap receptors to induce clustering (1, 4, 45). For growth factors like TGFβ, BMP and EGF, the ECM serves as the solid state (48). ECM proteins such as collagen II bind both TGFβ and integrin α2β1 (49), imposing geometric constraints that may structure receptor clusters. Therefore, growth factor receptor multimerization at focal adhesions, controlled by receptor interactions with integrins and with solid state growth factors, provide focal adhesions with the capability to integrate signaling between physical and biochemical cues.

Understanding the mechanosensitive regulation of TGFβ signaling has significant biological implications. We find that focal adhesions segregate TβRI from TβRII in both epithelial and mesenchymal cell lineages, opening the possibility that this is a general cellular mechanism for the control of TGFβ signaling. It will be interesting to determine if TGFβ receptor

multimerization at focal adhesions responds to physical cues that aberrantly promote TGFβ-induced epithelial-mesenchymal transition (EMT) in cancer or the loss of chondrocyte homeostasis in osteoarthritis. On stiff substrates, TGFβ preferentially activates PI3K to induce EMT instead of apoptosis (26). In osteoarthritis, the material properties of the cartilage ECM deteriorate as chondrocytes inappropriately shift the balance from canonical (Alk5/Smad2/3) to non-canonical (Alk1/Smad1/5/8) TβRI signaling (13). In each case, the extent to which changing the physical environment alters TGFβ effector selection through differential TGFβ receptor multimerization remains to be determined. Applied physical cues, such as compression or shear flow, also regulate TGFβ signaling in cartilage, vasculature and other tissues (50-52). Whether similar mechanisms operate in response to exogenous physical cues remains to be elucidated.

In conclusion, we utilized novel high-resolution imaging and single particle tracking microscopy coupled with biochemical assays to explore the spatial organization of TGFβ signaling at the receptor level. At focal adhesions, TβRII is uniquely segregated from its TβRI counterpart. Cellular tension modulates the spatial organization, multimerization and downstream signaling of TGFβ receptors at sites of adhesion, suggesting the existence of a functionally distinct subpopulation of TGFβ receptors. Overall, this finding provides a new mechanism by which cellular tension and physical cues exert control of growth factor signaling at the cellular membrane.

Acknowledgements

The authors wish to thank V. Weaver, J. Lakins, and the Weaver lab members for their important intellectual discussions and contributions, K. Thorn and D. Larsen from the Nikon Imaging Center for sharing their expertise and assisting with microscopy studies, and E. Leof for the phospho-Smad3 antibody. Mass spectrometry analysis was provided by the Bio-Organic Biomedical Mass Spectrometry Resource at UCSF (A.L. Burlingame, Director) supported by funding from the Biomedical Technology Research Centers program of the NIH National Institute of General Medical Sciences, NIH NIGMS 8P41GM103481, and Howard Hughes Medical Institute. This work was supported by National Science Foundation Graduate Research Fellow Program Grant No. 1144247 (J.R.), Department of Defense through the National Defense Science and Engineering Graduate Fellowship Program (D.M.), National Institute of Arthritis, Musculoskeletal and Skin Disease R21 AR067439-01 (T.A.), and National Institute of Dental and Craniofacial Research R01 DE019284 (T.A.). Any opinions, findings, and conclusions or recommendations expressed in this material are those of the author and do not necessarily reflect the views of the National Science Foundation.

References

1. Bethani I, Skanland SS, Dikic I, Acker-Palmer A. Spatial organization of transmembrane receptor signalling. Embo Journal. 2010 Aug 18;29(16):2677-88.
2. Di Guglielmo GM, Le Roy C, Goodfellow AF, Wrana JL. Distinct endocytic pathways regulate TGF-beta receptor signalling and turnover. Nature Cell Biology. 2003 May;5(5):410-21.
3. Groves JT, Kuriyan J. Molecular mechanisms in signal transduction at the membrane. Nature Structural & Molecular Biology. 2010 Jun;17(6):659-65.
4. Salaita K, Nair PM, Petit RS, Neve RM, Das D, Gray JW, et al. Restriction of Receptor Movement Alters Cellular Response: Physical Force Sensing by EphA2. Science. 2010 Mar 12;327(5971):1380-5.
5. Annes JP, Munger JS, Rifkin DB. Making sense of latent TGF beta activation. Journal of Cell Science. 2003 Jan 15;116(2):217-24.
6. Munger JS, Huang XZ, Kawakatsu H, Griffiths MJD, Dalton SL, Wu JF, et al. The integrin alpha v beta 6 binds and activates latent TGF beta 1: A mechanism for regulating pulmonary inflammation and fibrosis. Cell. 1999 Feb 5;96(3):319-28.
7. Wipff P-J, Rifkin DB, Meister J-J, Hinz B. Myofibroblast contraction activates latent TGF-beta 1 from the extracellular matrix. Journal of Cell Biology. 2007 Dec 17;179(6):1311-23.
8. Munger JS, Sheppard D. Cross talk among TGF-beta signaling pathways, integrins, and the extracellular matrix. Cold Spring Harb Perspect Biol. 2011 Nov;3(11):a005017.
9. Wrana JL, Ozadamar B, Le Roy C, Benchabane H. Signaling Receptors of the TGF beta Family. The TGF beta Family. 2008.
10. Massague J. TGF-beta signal transduction. Annual Review of Biochemistry. 1998 1998;67:753-91.
11. Feng XH, Derynck R. Specificity and versatility in tgf-beta signaling through Smads. Annu Rev Cell Dev Biol. 2005;21:659-93.
12. Lin X, Chen Y-G, Feng X-H. Transcriptional Control via Smads. The TGF beta Family. 2008.
13. Davidson ENB, Remst DFG, Vitters EL, van Beuningen HM, Blom AB, Goumans M-J, et al. Increase in ALK1/ALK5 Ratio as a Cause for Elevated MMP-13 Expression in Osteoarthritis in Humans and Mice. Journal of Immunology. 2009 Jun 15;182(12):7937-45.
14. Goumans MJ, Valdimarsdottir G, Itoh S, Rosendahl A, Sideras P, ten Dijke P. Balancing the activation state of the endothelium via two distinct TGF-beta type I receptors. Embo Journal. 2002 Apr 2;21(7):1743-53.
15. Scaffidi AK, Petrovic N, Moodley YP, Fogel-Petrovic M, Kroeger KM, Seeber RM, et al. alpha(v)beta(3) Integrin interacts with the transforming growth factor beta (TGF beta) type II receptor to potentiate the proliferative effects of TGF beta 1 in living human lung fibroblasts. Journal of Biological Chemistry. 2004 Sep 3;279(36):37726-33.
16. Garamszegi N, Garamszegi SP, Samavarchi-Tehrani P, Walford E, Schneiderbauer MM, Wrana JL, et al. Extracellular matrix-induced transforming growth factor-beta receptor signaling dynamics. Oncogene. 2010 Apr;29(16):2368-80.
17. DuFort CC, Paszek MJ, Weaver VM. Balancing forces: architectural control of mechanotransduction. Nature Reviews Molecular Cell Biology. 2011 May;12(5):308-19.
18. Giancotti FG, Ruoslahti E. Transduction - Integrin signaling. Science. 1999 Aug 13;285(5430):1028-32.
19. Ingber DE. Tensegrity: The architectural basis of cellular mechanotransduction. Annual Review of Physiology. 1997 1997;59:575-99.
20. Allen JL, Cooke ME, Alliston T. ECM stiffness primes the TGF beta pathway to promote chondrocyte differentiation. Molecular Biology of the Cell. 2012 Sep;23(18):3731-42.
21. McBeath R, Pirone DM, Nelson CM, Bhadriraju K, Chen CS. Cell shape, cytoskeletal tension, and RhoA regulate stem cell lineage commitment. Developmental Cell. 2004 Apr;6(4):483-95.

22. Wang Y-K, Yu X, Cohen DM, Wozniak MA, Yang MT, Gao L, et al. Bone Morphogenetic Protein-2-Induced Signaling and Osteogenesis Is Regulated by Cell Shape, RhoA/ROCK, and Cytoskeletal Tension. Stem Cells and Development. 2012 May 1;21(7):1176-86.
23. Samuel MS, Lopez JI, McGhee EJ, Croft DR, Strachan D, Timpson P, et al. Actomyosin-Mediated Cellular Tension Drives Increased Tissue Stiffness and beta-Catenin Activation to Induce Epidermal Hyperplasia and Tumor Growth. Cancer Cell. 2011 Jun 14;19(6):776-91.
24. Dupont S, Morsut L, Aragona M, Enzo E, Giulitti S, Cordenonsi M, et al. Role of YAP/TAZ in mechanotransduction. Nature. 2011 Jun 9;474(7350):179-U212.
25. Wang F, Weaver VM, Petersen OW, Larabell CA, Dedhar S, Briand P, et al. Reciprocal interactions between beta 1-integrin and epidermal growth factor receptor in three-dimensional basement membrane breast cultures: A different perspective in epithelial biology. Proceedings of the National Academy of Sciences of the United States of America. 1998 Dec 8;95(25):14821-6.
26. Leight JL, Wozniak MA, Chen S, Lynch ML, Chen CS. Matrix rigidity regulates a switch between TGF-beta 1-induced apoptosis and epithelial-mesenchymal transition. Molecular Biology of the Cell. 2012 Mar 1;23(5):781-91.
27. Wipff P-J, Hinz B. Integrins and the activation of latent transforming growth factor beta 1 - An intimate relationship. European Journal of Cell Biology. 2008 Sep;87(8-9):601-15.
28. Coelho M, Maghelli N, Tolic-Norrelykke IM. Single-molecule imaging in vivo: the dancing building blocks of the cell. Integr Biol (Camb). 2013 May;5(5):748-58.
29. Manley S, Gillette JM, Patterson GH, Shroff H, Hess HF, Betzig E, et al. High-density mapping of single-molecule trajectories with photoactivated localization microscopy. Nature Methods. 2008 Feb;5(2):155-7.
30. Rossier O, Octeau V, Sibarita JB, Leduc C, Tessier B, Nair D, et al. Integrins beta(1) and beta(3) exhibit distinct dynamic nanoscale organizations inside focal adhesions. Nature Cell Biology. 2012 Oct;14(10):1057-+.
31. Calebiro D, Rieken F, Wagner J, Sungkaworn T, Zabel U, Borzi A, et al. Single-molecule analysis of fluorescently labeled G-protein-coupled receptors reveals complexes with distinct dynamics and organization. Proceedings of the National Academy of Sciences of the United States of America. 2013 Jan 8;110(2):743-8.
32. Xia T, Li N, Fang X. Single-molecule fluorescence imaging in living cells. Annu Rev Phys Chem. 2013;64:459-80.
33. McKinney SA, Murphy CS, Hazelwood KL, Davidson MW, Looger LL. A bright and photostable photoconvertible fluorescent protein. Nature Methods. 2009 Feb;6(2):131-3.
34. Loeser RF. Chondrocyte integrin expression and function. Biorheology. 2000 2000;37(1-2):109-16.
35. Xu J, Wang AH, Oses-Prieto J, Makhijani K, Katsuno Y, Pei M, et al. Arginine Methylation Initiates BMP-Induced Smad Signaling. Molecular Cell. Jul 11;51(1):5-19.
36. Pollard TD, Borisy GG. Cellular motility driven by assembly and disassembly of actin filaments. Cell. 2003 Feb 21;112(4):453-65.
37. Vardouli L, Moustakas A, Stournaras C. LIM-kinase 2 and cofilin phosphorylation mediate actin cytoskeleton reorganization induced by transforming growth factor-beta. Journal of Biological Chemistry. 2005 Mar 25;280(12):11448-57.
38. Lamouille S, Xu J, Derynck R. Molecular mechanisms of epithelial-mesenchymal transition. Nature Reviews Molecular Cell Biology. 2014 Mar;15(3):178-96.
39. Rape AD, Zibinsky M, Murthy N, Kumar S. A synthetic hydrogel for the high-throughput study of cell-ECM interactions. Nature Communications. 2015 2015 Sep;6:8129-.
40. Wells RG, Discher DE. Matrix Elasticity, Cytoskeletal Tension, and TGF-beta: The Insoluble and Soluble Meet. Science Signaling. 2008 Mar 11;1(10).
41. Giacomini MM, Travis MA, Kudo M, Sheppard D. Epithelial cells utilize cortical actin/myosin to activate latent TGF-beta through integrin alpha(v)beta(6)-dependent physical force. Experimental Cell Research. 2012 Apr 1;318(6):716-22.

42. Vizan P, Miller DS, Gori I, Das D, Schmierer B, Hill CS. Controlling long-term signaling: receptor dynamics determine attenuation and refractory behavior of the TGF-beta pathway. Sci Signal. 2013 Dec 10;6(305):ra106.
43. Ma X, Wang Q, Jiang Y, Xiao Z, Fang X, Chen Y-G. Lateral diffusion of TGF-beta type I receptor studied by single-molecule imaging. Biochemical and Biophysical Research Communications. 2007 Apr 27;356(1):67-71.
44. Paszek MJ, Zahir N, Johnson KR, Lakins JN, Rozenberg GI, Gefen A, et al. Tensional homeostasis and the malignant phenotype. Cancer Cell. 2005 Sep;8(3):241-54.
45. Hartman NC, Groves JT. Signaling clusters in the cell membrane. Curr Opin Cell Biol. 2011 Aug;23(4):370-6.
46. Alam N, Goel HL, Zarif MJ, Butterfield JE, Perkins HM, Sansoucy BG, et al. The integrin - Growth factor receptor duet. Journal of Cellular Physiology. 2007 Dec;213(3):649-53.
47. Turley EA, Noble PW, Bourguignon LYW. Signaling properties of hyaluronan receptors. Journal of Biological Chemistry. 2002 Feb 15;277(7):4589-92.
48. Hynes RO. The extracellular matrix: not just pretty fibrils. Science. 2009 Nov 27;326(5957):1216-9.
49. Zhu Y, Oganesian A, Keene DR, Sandell LJ. Type IIA procollagen containing the cysteine-rich amino propeptide is deposited in the extracellular matrix of prechondrogenic tissue and binds to TGF-beta1 and BMP-2. J Cell Biol. 1999 Mar 8;144(5):1069-80.
50. Li Z, Kupcsik L, Yao S-J, Alini M, Stoddart MJ. Mechanical load modulates chondrogenesis of human mesenchymal stem cells through the TGF-beta pathway. Journal of Cellular and Molecular Medicine. 2010 Jun;14(6):1338-46.
51. Sakai K, Mohtai M, Iwamoto Y. Fluid shear stress increases transforming growth factor beta 1 expression in human osteoblast-like cells: Modulation by cation channel blockades. Calcified Tissue International. 1998 Dec;63(6):515-20.
52. Streuli CH, Schmidhauser C, Kobrin M, Bissell MJ, Derynck R. Extracellular-Matrix Regulates Expression of the TGF-beta-1 Gene. Journal of Cell Biology. 1993 Jan;120(1):253-60.
53. Feng XH, Derynck R. Ligand-independent activation of transforming growth factor (TGF) beta signaling pathways by heteromeric cytoplasmic domains of TGF-beta receptors. J Biol Chem. 1996 May 31;271(22):13123-9.
54. Alliston T, Choy L, Ducy P, Karsenty G, Derynck R. TGF-beta-induced repression of CBFA1 by Smad3 decreases cbfa1 and osteocalcin expression and inhibits osteoblast differentiation. EMBO J. 2001 May 1;20(9):2254-72.
55. Kean MJ, Couzens AL, Gingras A-C. Mass spectrometry approaches to study mammalian kinase and phosphatase associated proteins. Methods. 2012 Aug;57(4):400-8.
56. Duong BH, Onizawa M, Oses-Prieto JA, Advincula R, Burlingame A, Malynn BA, et al. A20 Restricts Ubiquitination of Pro-Interleukin-1 beta Protein Complexes and Suppresses NLRP3 Inflammasome Activity. Immunity. 2015 Jan 20;42(1):55-67.
57. Clauser KR, Baker P, Burlingame AL. Role of accurate mass measurement (+/- 10 ppm) in protein identification strategies employing MS or MS MS and database searching. Analytical Chemistry. 1999 Jul 15;71(14):2871-82.
58. Sbalzarini IF, Koumoutsakos P. Feature point tracking and trajectory analysis for video imaging in cell biology. Journal of Structural Biology. 2005 Aug;151(2):182-95.

Chapter 5

ECM stiffness regulates the TGFβ pathway to induce chondrocyte lineage selection of hMSCs

Introduction

The extracellular microenvironment is rich in physical and biochemical cues that are powerful regulators of cell behavior. Physical cues such as ECM stiffness, cell shape, and cytoskeletal tension direct cell lineage selection and function. The importance of ECM stiffness in cell lineage selection is apparent in mesenchymal stem cells. Engler et al. found that MSCs cultured on 2D substrates with otherwise identical media conditions express specific lineage markers on substrates of varying stiffness. Specifically, MSCs select a neural lineage on a compliant substrate, but select myogenic and osteogenic fates when cultured on increasingly stiff substrates (1). ECM stiffness is also often disrupted in disease and can exacerbate disease progression, as in cancer. Paszek et al. demonstrated the effect on ECM stiffness on mammary epithelial cell (MEC) colonies in 3D gels. Increasing matrix stiffness progressively increased EGF-dependent ERK activation and colony size, disrupted localization of integrin β4, and led to progressive filling of the lumen (2). Physical cues can also dramatically alter the cellular response to biochemical cues, such as growth factor TGFβ (3, 4). The growth factor TGFβ is an important biochemical cue that induces chondrocyte lineage selection and cartilage matrix synthesis while inhibiting terminal chondrocyte differentiation and hypertrophy. Previous work by Allen et al. demonstrated that chondrocyte differentiation of mature chondrocytes is highly sensitive to substrate stiffness (Figure 5.1). Chondrocytes express higher levels of chondrogenic genes and deposit more proteoglycan content on 2D substrates of a specific stiffness (5).

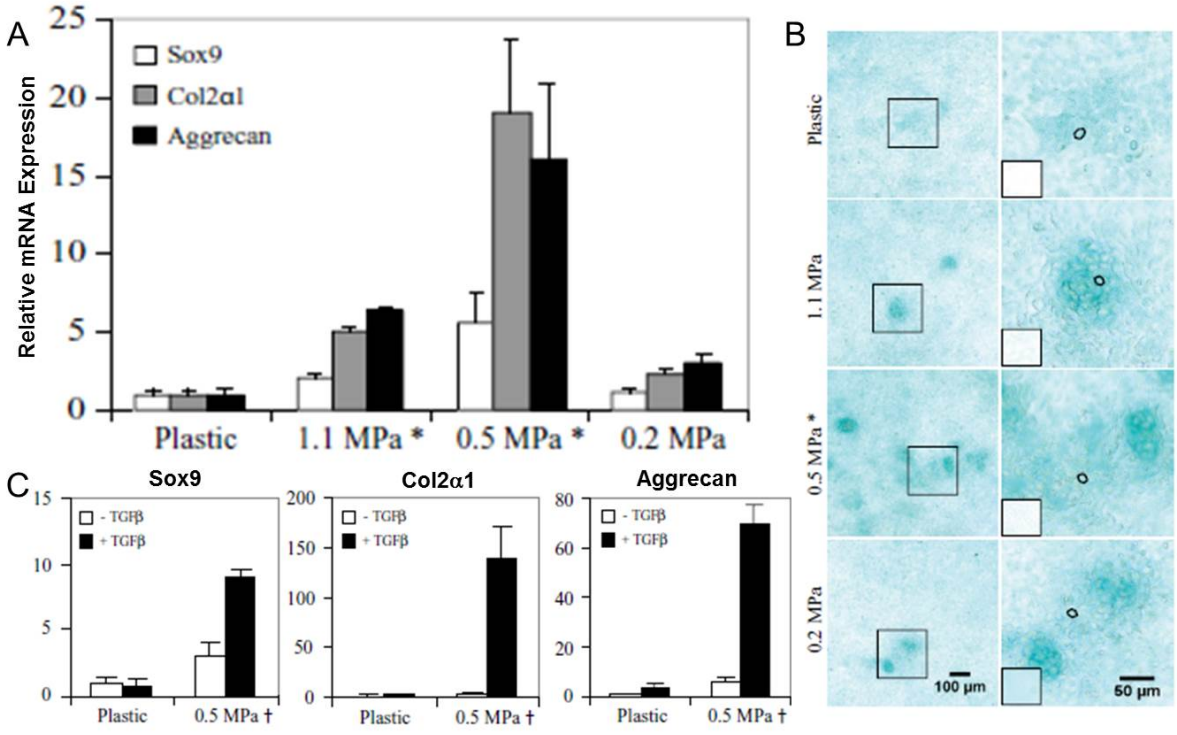

Figure 5.1. ECM stiffness primes ATDC5s for a synergistic response to TGFβ. Chondrogenic gene expression (A) and proteoglycan content deposition (B) is sensitive to substrate stiffness in mature chondrocytes. The combination of ECM stiffness and TGFβ leads to a synergistic induction of gene expression (C). Figure adapted from Allen et al. 2012.

Furthermore, ECM stiffness primes these cells for a synergistic response to the addition of TGFβ, such that the combination of these cues leads to a more robust response for chondrogenic gene expression than either cue alone (5). Therefore, in response to substrate stiffness, chondrocytes modulate TGFβ pathway activity at the ligand, effector, and receptor level. However, the mechanisms by which cells integrate physical and biochemical cues remain unclear. Cartilage provides an ideal system for investigating these mechanisms, as physical and biochemical cues intersect from development to disease, such as in osteoarthritis. Understanding how cells integrate cues from the cellular microenvironment may elucidate fundamental mechanisms involved in cell behavior and disease. We hypothesize that, as for chondrocytes (5),

substrate stiffness primes hMSCs for a synergistic response to the chondroinductive growth factor TGFβ. This interaction, between ECM stiffness and the TGFβ pathway, could occur at multiple levels as shown in Figure 5.2 – through the TGFβ ligand, TGFβ receptors, or TGFβ downstream effectors.

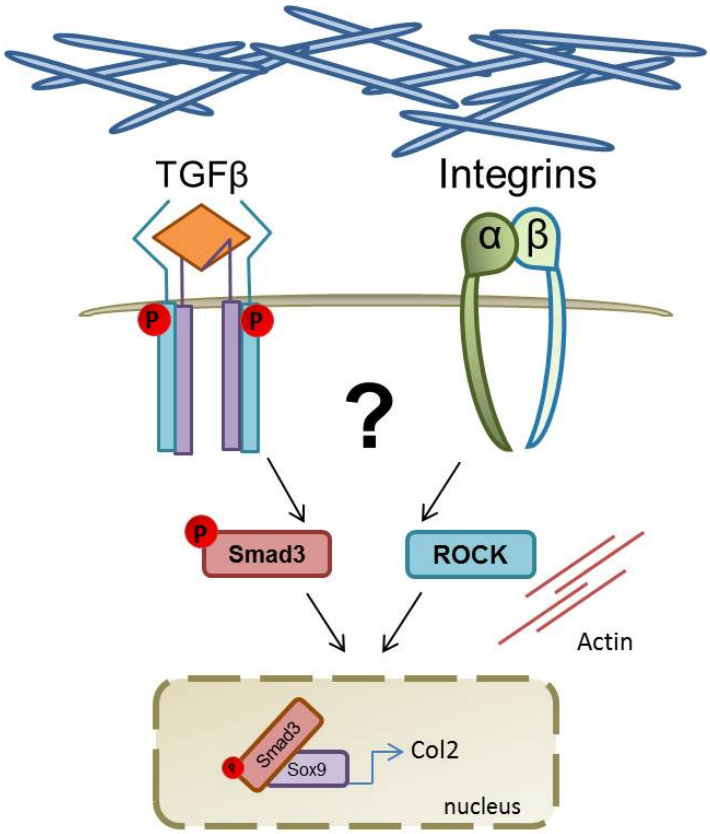

Figure 5.2. TGFβ pathway and mechanotransduction crosstalk. The interaction between the TGFβ pathway and mechanotransduction or stiffness-sensing pathway could occur through the ligand, receptor, effector, and/or nuclear levels.

The goal of this study is to use an established 2D model system, in which polyacrylamide gels span the stiffness range of healthy articular cartilage, in order to probe levels of the TGFβ pathway and elucidate molecular mechanisms involved in the integrated cellular response to ECM stiffness and TGFβ.

Results

hMSC chondroinduction, shape, and actin stress fiber formation are stiffness-sensitive

Typically, hMSCs require 3D pellet culture and TGFβ to undergo chondrocyte differentiation. However, we found that even on a compliant 2D substrate, hMSCs initiate chondrogenesis, as indicated by a 6-fold induction of Sox9 on the 2D 0.5 MPa substrate, relative to plastic. Meanwhile, the expression of Collagen I, a marker for chondrocyte dedifferentiation, is decreased in the same conditions. The stiffness-sensitive effect on chondrocyte marker genes (Sox9) in hMSCs is lost upon treatment with a chemical ROCK inhibitor (Y27632), suggesting cytoskeletal involvement. hMSC shape and actin stress fiber formation are also sensitive to substrate stiffness, consistent with previous reports (1, 6). hMSCs exhibit a more rounded morphology and less prominent stress fibers on a 0.5 MPa substrate, relative to a 0.2 MPa substrate and especially relative to plastic.

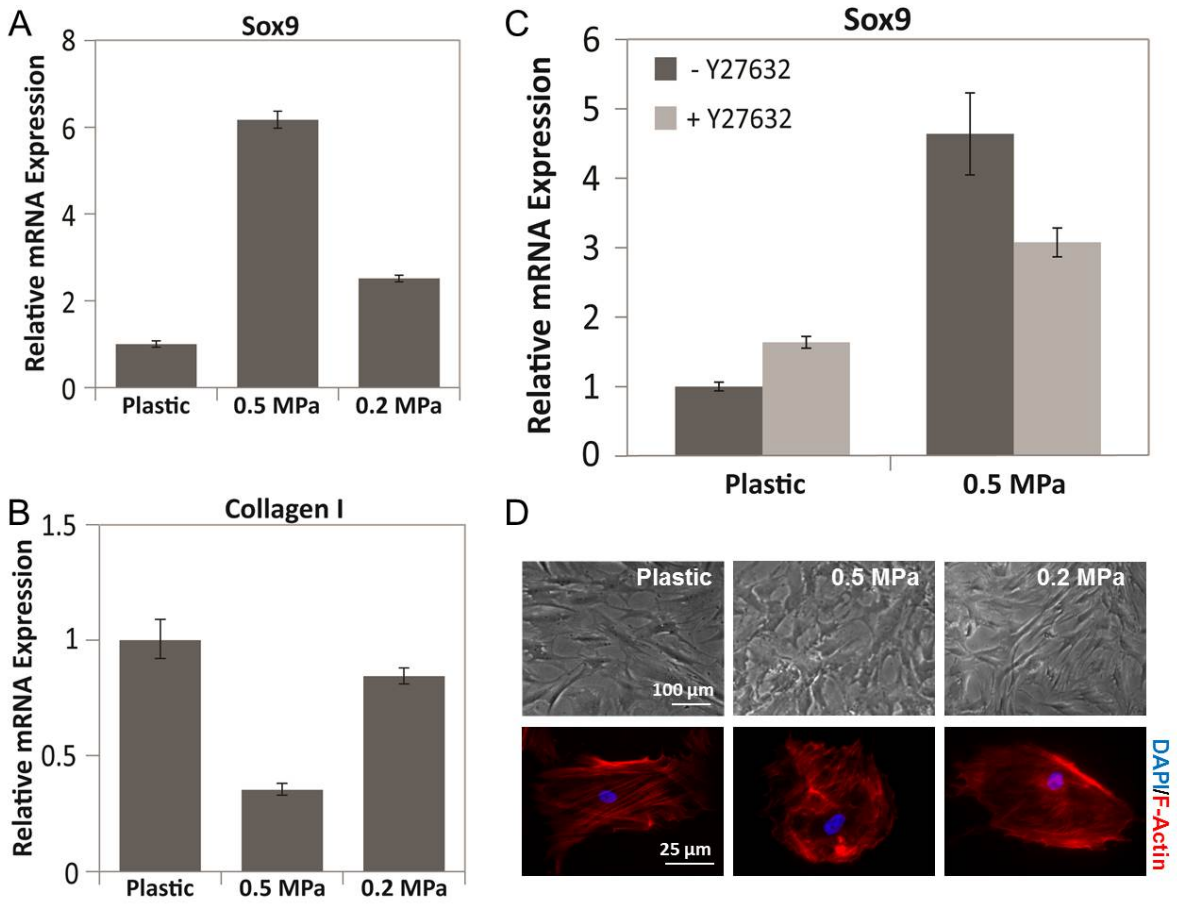

Figure 5.3. ECM stiffness and cellular tension modulate hMSC chondroinduction and stress fiber formation. hMSCs initiate chondrogenesis on a compliant substrate, upregulating Sox9 expression (A) and downregulating Collagen I expression (B). Inhibition of ROCK disrupts this stiffness-specific effect on chondrogenic gene expression (C). hMSC shape and stress fiber formation is also sensitive to substrate stiffness (D).

ECM stiffness primes hMSCs for a specific and synergistic induction of Sox9 by TGFβ

Physical cues can alter the cellular response to biochemical cues. Therefore, we went on to evaluate the effect of substrate stiffness on chondrocyte differentiation in the presence or absence of TGFβ. TGFβ further enhances Sox9 expression in hMSCs on the 0.5 MPa substrate, demonstrating that the chondroinductive synergy between ECM stiffness and TGFβ observed in mature chondrocytes also occurs in hMSCs. This effect is specific for chondrogenic genes such

as Sox9, since PAI1, the classical TGFβ response gene, is not synergistically increased in hMSCs grown on 0.5 MPa substrates.

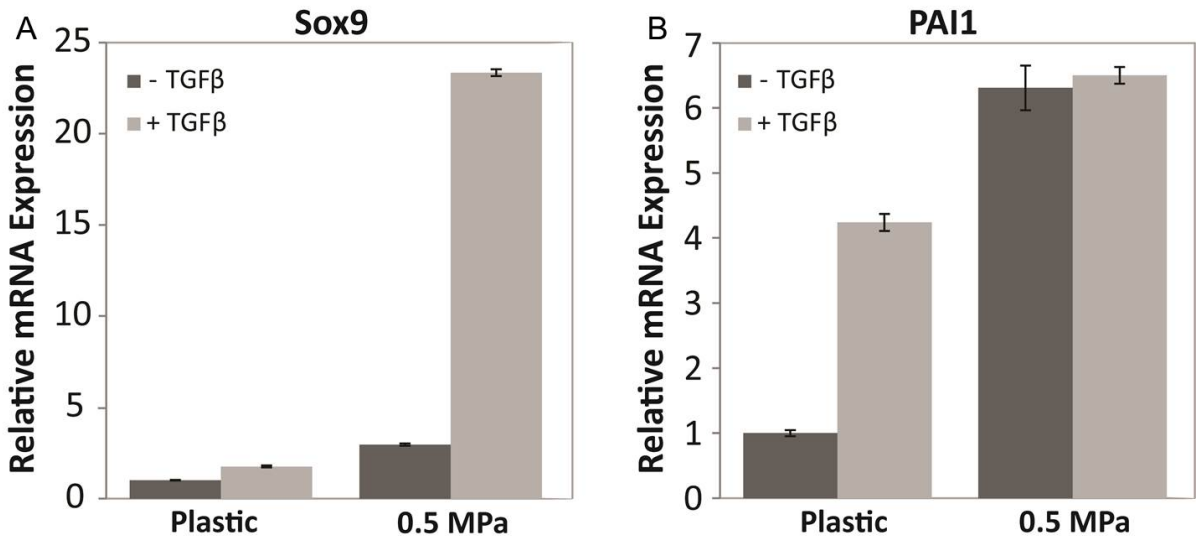

Figure 5.4. Synergy between ECM stiffness and TGFβ is specific for chondrogenic genes. Addition of TGFβ enhances Sox9 expression in hMSCs cultured on a compliant substrate (A). This synergistic response is specific for chondrogenic genes as PAI1, the classical TGFβ response gene, is not synergistically increased in the same conditions (B).

ECM stiffness regulates the nuclear localization of Smad2/3

In order to investigate the observed synergy between ECM stiffness and TGFβ, we examined the effect of substrate stiffness on Smad2/3 localization, as it is a key downstream effector in the TGFβ pathway in chondrocytes. Smad3 preferentially localizes to the nucleus in cells cultured on a 0.5 MPa substrate, relative to glass and a 0.2 MPa substrate, even in the absence of exogenously added TGFβ. The addition of exogenous TGFβ to these latter substrates leads to the nuclear localization of Smad3. To investigate what might be responsible for this stiffness-specific increase in Smad3 nuclear localization, we examined the effect of substrate stiffness on

TGFβ ligand expression. We found that TGFβ1 mRNA is induced 4.5 fold on the 0.5 MPa gel, relative to plastic.

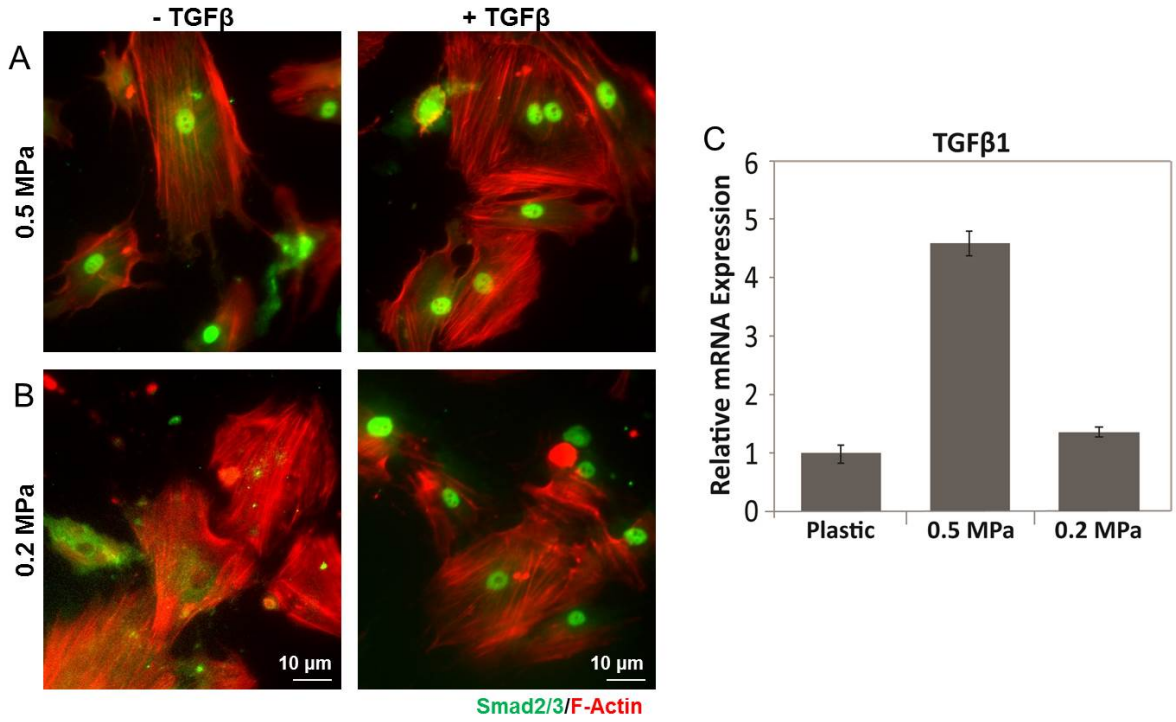

Figure 5.5. Nuclear localization of Smad2/3 is sensitive to ECM stiffness in hMSCs. Smad2/3 preferentially localizes to the nucleus on a 0.5 MPa substrate (A), even in the absence of exogenous TGFβ, relative to a stiffer or softer (B) substrate. The addition of TGFβ leads to Smad2/3 nuclear localization on all substrates (A,B). TGFβ1 ligand expression is specifically upregulated on the 0.5 MPa substrate (C).

Smad2/3 and JNK nuclear localization in primary human articular chondrocytes is sensitive to substrate stiffness

We also examined the localization of Smad2/3 and JNK in primary human articular chondrocytes (hACs) cultured on substrates of varying stiffness. Smad2/3 preferentially localizes to the nucleus in hACs cultured on 0.5 MPa substrates relative to softer 0.2 MPa substrates,

consistent with findings for hMSC and ATDC5 cells. Unlike hMSC and ATDC5 cells however, Smad2/3 also localizes to the nucleus in hACs cultured on glass substrates. This finding might suggest that hACs isolated from certain patients might have a decreased ability to sense and respond to physical cues in the environment.

Wnt signaling is important in chondrocyte differentiation and polarity. JNK is a shared effector between TGFβ and Wnt signaling, and here we find that the nuclear localization of JNK is sensitive to substrate stiffness. JNK preferentially localizes to the nucleus on a 0.5 MPa substrate, similar to the behavior of Smad2/3, relative to the localization in hACS cultured on glass or softer 0.2 MPa substrates. Furthermore, while TGFβ and Wnt5a can both lead to JNK phosphorylation, treatment with both ligands is required to maintain phosphorylation two hours later. It remains to be elucidated the extent to which JNK participates in the cellular response to cell tension and TGFβ, and how these roles potentially change from healthy to arthritic human articular chondrocytes.

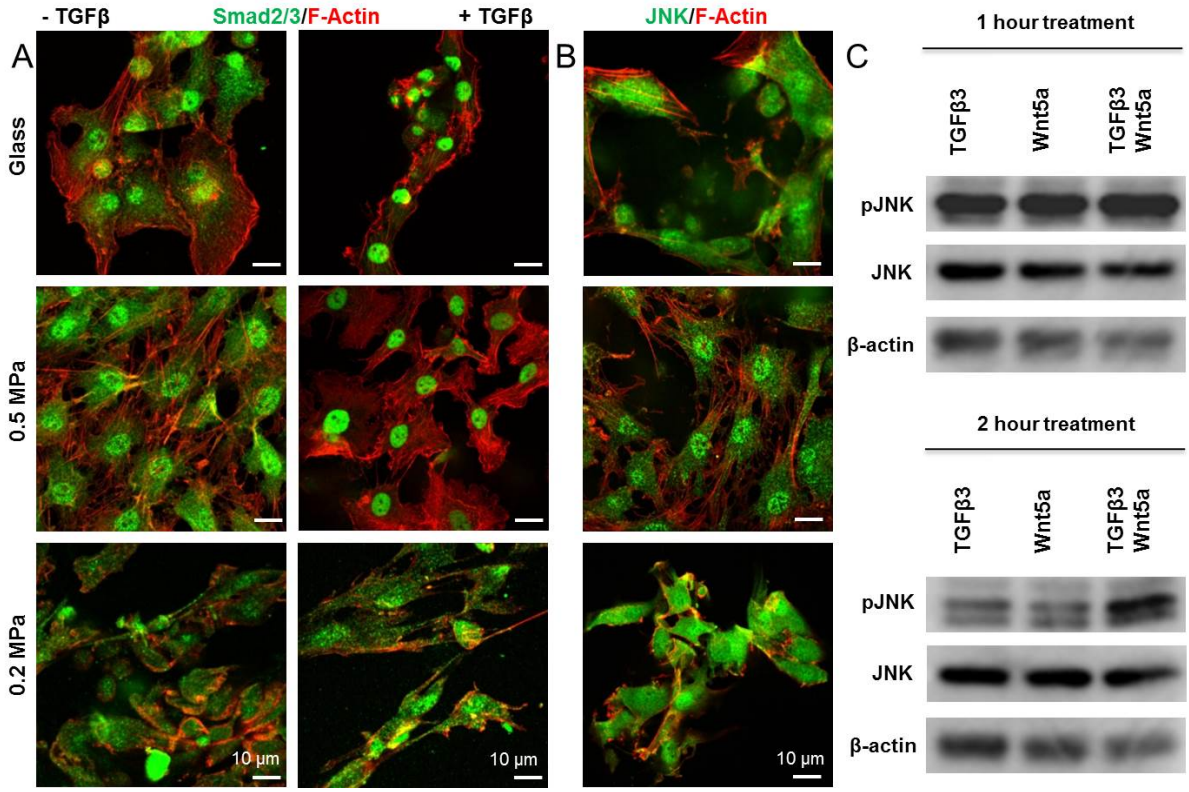

Figure 5.6. Nuclear localization of Smad2/3 and JNK in hACs is sensitive to ECM stiffness. Smad2/3 and JNK preferentially localize to the nucleus on stiffer substrates (A,B), even in the absence of exogenous TGFβ. The addition of TGFβ leads to increased Smad2/3 nuclear localization on all substrates (A). TGFβ and Wnt5a can both lead to JNK phosphorylation, and treatment with both ligands is required to maintain phosphorylation two hours later (C).

YAP localization in human cartilage corresponds to stiffness-sensitive YAP localization in primary hACs

YAP (Yes-associated protein) and TAZ (transcriptional coactivator with PDZ-binding motif) are nuclear relays of mechanical signals exerted by ECM stiffness and cell shape (7). This regulation is dependent on Rho activity and cell tension, and furthermore, YAP/TAZ are required for the differentiation of mesenchymal stem cells induced by ECM stiffness. Previous work has demonstrated that ECM stiffness and Smad3 have a shared ability to prime cells for chondrocyte

differentiation. This suggests a cooperative role in the control of transcription factors such as Sox9. One possibility for this role would be through YAP/TAZ, due to their cellular tension and TGFβ-sensitivity. Therefore, we examined the localization of YAP in human cartilage and hACs in response to varying substrate stiffness. Atomic force microscopy (AFM) maps are displayed alongside cartilage sections in Figure 5.7 to help visualize the variation in cartilage stiffness with increasing depth. Atomic force microscopy with a 15 μm diameter spherical tip was used to map the elastic modulus of ECM at five sites throughout the depth of an unfixed frozen OA human hip articular cartilage section. Modulus maps, in color scale, are superimposed on the phase contrast image of the analyzed tissue and AFM cantilever. Adjacent sections were stained for proteoglycan and for the mechanosensitive transcriptional coregulator YAP. Staining for proteoglycan content demonstrates matrix erosion in the superficial zones of osteoarthritic cartilage. In superficial cartilage with an average modulus of 0.2 MPa or in primary hACs cultured on 0.2 MPa polyacrylamide gel substrates, YAP localization is diffuse. In contrast, YAP is predominantly nuclear in deep chondrocytes or in primary hACs cultured on 0.5 MPa substrates. Although many factors vary with ECM stiffness and osteoarthritis, differences in the pattern of protein localization in equivalently stiff OA and healthy cartilage may indicate hAC-intrinsic defects in the response to cell tension.

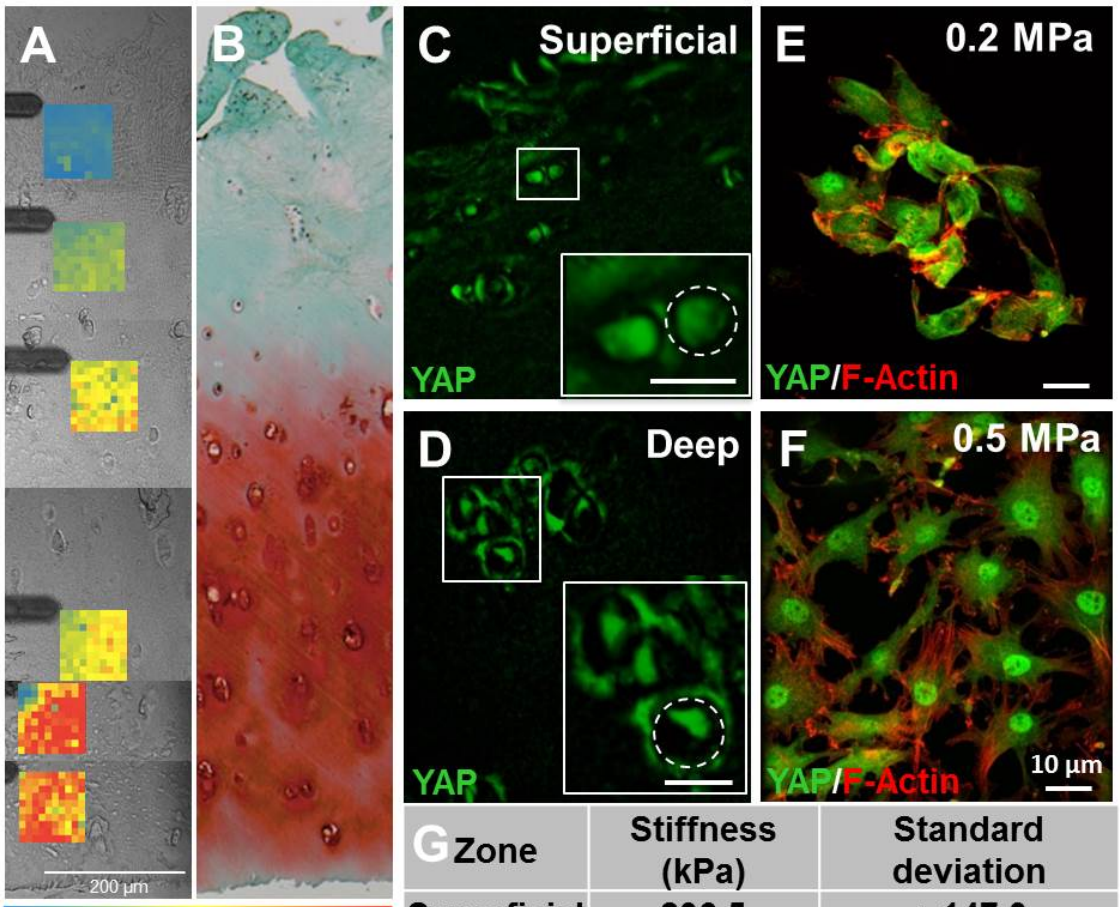

G

Zone	Stiffness (kPa)	Standard deviation
Superficial	236.5	± 147.3
Middle	410.4	± 94.7
Deep	767.0	± 14.1

Figure 5.7. Nuclear localization of YAP is sensitive to ECM stiffness in human cartilage and in hACs. AFM maps (A) and Safranin O staining (B) demonstrate the variations in cartilage stiffness and proteoglycan content with increasing cartilage depth. Relative to localization in superficial cartilage (C) and human articular chondrocytes on 0.2 MPa substrates (F), YAP is nuclear in deep chondrocytes (D) and in cells grown on 0.5 MPa substrates (E). AFM measurements for cartilage stiffness by zone shown in G.

Discussion

In summary, we found that hMSC shape, actin stress fiber formation, and chondrocyte differentiation are sensitive to substrate stiffness.

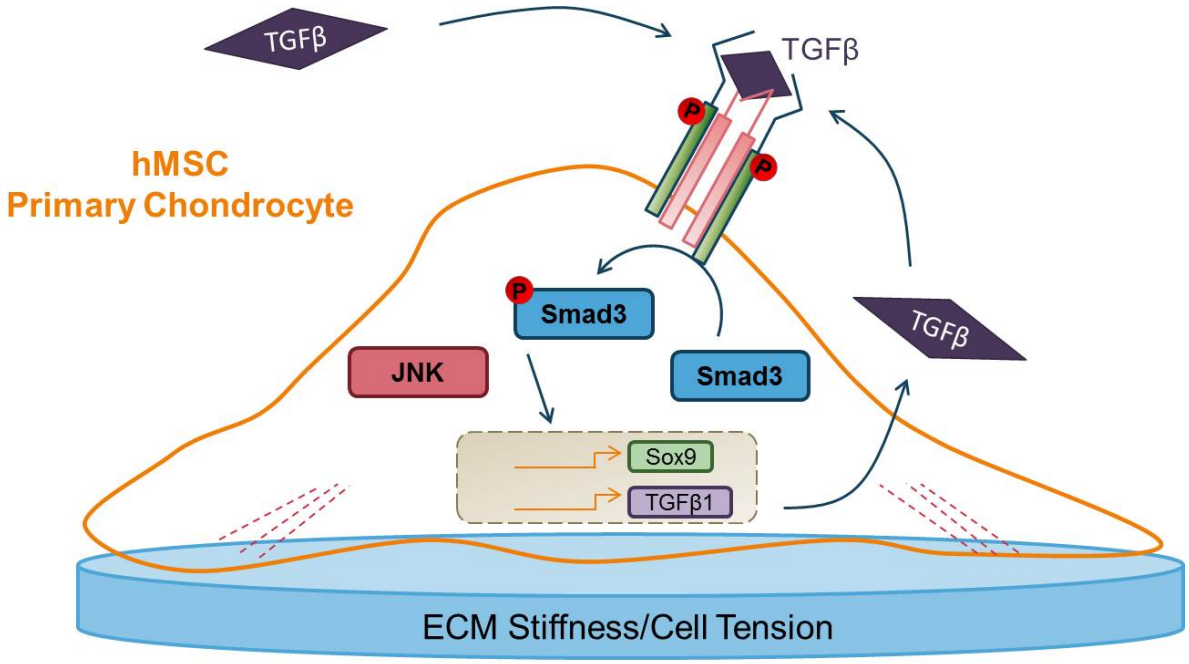

Figure 5.8. Proposed model for hMSCs and primary chondrocytes in response to ECM stiffness. hMSC shape, stress fiber formation, and Sox9 expression (chondroinductino) are sensitive to changes in ECM stiffness. In response to ECM stiffness, Sox9 and TGFβ1 expression are upregulated. ECM stiffness primes hMSCs for a specific and synergistic response to exogenous TGFβ. Smad3 and JNK nuclear localization is also sensitive to ECM stiffness in hMSCs and primary chondrocytes.

On a compliant substrate of 0.5 MPa, Sox9 expression and TGFβ1 expression are upregulated, relative to substrates that are more compliant or stiff. Furthermore, we demonstrated that substrate stiffness primes hMSCs for a synergistic response to TGFβ, and that this synergy is specific to chondrogenic genes. The upregulation of TGFβ1 is accompanied by and may be

responsible for an increase in Smad3 nuclear localization on this discrete substrate. Smad3 nuclear localization in hACs is also sensitive to substrate stiffness, exhibiting similar behavior to that of hMSCs. However, the nuclear localization of Smad3 in hACs cultured on glass substrates, not seen for hMSCs, suggests a possible impairment in the ability to properly sense physical cues. We also examined the localization of JNK, a common effector between TGFβ and Wnt signaling, and found that its nuclear localization in hACs is sensitive to substrate stiffness. Overall, understanding the mechanisms by which hMSCs integrate physical and biochemical cues might have implications for the understanding of cartilage development, disease progression, and regeneration.

References

1. Engler AJ, Sen S, Sweeney HL, Discher DE. Matrix elasticity directs stem cell lineage specification. Cell. 2006 Aug 25;126(4):677-89.
2. Paszek MJ, Zahir N, Johnson KR, Lakins JN, Rozenberg GI, Gefen A, et al. Tensional homeostasis and the malignant phenotype. Cancer Cell. 2005 Sep;8(3):241-54.
3. McBeath R, Pirone DM, Nelson CM, Bhadriraju K, Chen CS. Cell shape, cytoskeletal tension, and RhoA regulate stem cell lineage commitment. Developmental Cell. 2004 Apr;6(4):483-95.
4. Wang Y-K, Yu X, Cohen DM, Wozniak MA, Yang MT, Gao L, et al. Bone Morphogenetic Protein-2-Induced Signaling and Osteogenesis Is Regulated by Cell Shape, RhoA/ROCK, and Cytoskeletal Tension. Stem Cells and Development. 2012 May 1;21(7):1176-86.
5. Allen JL, Cooke ME, Alliston T. ECM stiffness primes the TGF beta pathway to promote chondrocyte differentiation. Molecular Biology of the Cell. 2012 Sep;23(18):3731-42.
6. Park JS, Chu JS, Tsou AD, Diop R, Tang Z, Wang A, et al. The effect of matrix stiffness on the differentiation of mesenchymal stem cells in response to TGF-beta. Biomaterials. 2011 Jun;32(16):3921-30.
7. Dupont S, Morsut L, Aragona M, Enzo E, Giulitti S, Cordenonsi M, et al. Role of YAP/TAZ in mechanotransduction. Nature. 2011 Jun 9;474(7350):179-U212.

Chapter 6

Discussion and future directions

The work detailed within this dissertation began as an exploration of stem cell differentiation and its sensitivity to substrate stiffness. This initial research was based upon previous findings that demonstrated that substrate stiffness primes the TGFβ pathway to elicit a synergistic response in chondrocytes. I set out to investigate whether this same synergy exists in human mesenchymal stem cells during chondrogenesis. We found that Sox9, a transcription factor and marker for chondrocyte lineage section, is upregulated on a discrete substrate. Furthermore, Collagen I, a marker for chondrocyte dedifferentiation, is downregulated in these same conditions. Unlike the work published by Allen et al. using chondrocytes, we were not able to see any induction of Collagen II. This indicates that although substrate stiffness alone is enough to initiate chondroinduction of hMSCs, it does not lead to chondrocyte differentiation. The addition of TGFβ to these substrates leads to a specific and synergistic induction of Sox9, such that PAI1, a classic TGFβ response gene, is not synergistically regulated. Interestingly, even with the addition of exogenous TGFβ, we did not see any increases in Collagen II expression. Future studies will explore conditions that promote chondrocyte differentiation by upregulating Sox9, Collagen II, and Aggrecan expression. These conditions might include a more expansive stiffness range, such as softer gels that mimic a stem cell environment and promote rounding and condensation, 3D substrates, or pellet culture of hMSCs.

Although the role of physical and biochemical cues in differentiation is fascinating, what really captured my attention was this unanswered question of how cells were able to sense and response to the multitude of cues in their microenvironment and then elicit one coordinated

response. Integrins act as a bridge between the external physical environment and the internal actin cytoskeleton, relaying cues and changes outside the cell to internal signal transducers. Therefore, I wanted to examine the potential interactions between integrins and TGFβ receptors, thus exploring the relationship between the receptors of the mechanotransudction pathway and the receptors of our key signaling pathway TGFβ.

In order to investigate the relationship between integrins and TGFβ receptors, we coupled the use of biochemical approaches with novel imaging techniques. The development and optimization of these microscopy tools unveiled an unprecedented view of TGFβ receptors at the surface of the cell that no one has reported. Specifically, we revealed a unique spatial organization in which TGFβ receptor subunits (TβRII and TβRI) are intimately and differentially involved at sites of adhesion. TβRII is excluded from these sites of adhesion, whereas TβRI is fully incorporated at these same regions. Through quantification we were able to demonstrate that both subunits of TβRI (Alk5 and Alk1) are significantly colocalized with integrin α2 relative to TβRII. It will be interesting to elucidate the precise domains of each receptor that yield the discrete localization patterns. One possibility would be to develop chimeric receptors with swapped domains to determine whether certain combinations of receptor domains lead to incorporation or exclusion at sites of adhesion. Another interesting approach would be to develop serial truncations of TβRII in order to examine the effect of receptor size on exclusion from adhesions.

Incorporating single-particle tracking PALM imaging provided further mechanistic insight into the dynamics of these receptors within these regions. Receptors experience decreased mobility near or within focal adhesions, indicating that these receptors are preferentially confined or trapped at these sites. Future experiments with sptPALM will examine the behavior and mobility

of single molecules that move from inside to outside or outside to inside of adhesions, revealing additional information on the confinement, interactions, and trafficking of TGFβ receptors at these sites. It would also be interesting to examine the mobility of these receptors relative to proteins involved in endocytosis pathways, such as studying colocalization with caveolae or clathrin, to determine if certain cues or stimuli regulate these processes. We also found that TGFβ receptors form a complex with integrin αV, suggesting that physical interactions might contribute to the observed decrease in mobility, especially for TβRI. Additional work is needed to identify whether these interactions are direct and which protein domains are involved. Mass spectrometry data provide insight into potential third party interacting proteins that could act as a bridge between the TGFβ and mechanotransduction pathways in this complex. Initial results implicate interesting proteins involved in this complex, such as cofilin and DYNLT1. Cofilin is an actin-binding protein that disassembles actin filaments, and its presence was confirmed via spectra analysis of TβR pulldowns. Interestingly, cofilin preferentially associates with TβRII relative to TβRI, as indicated through both mass spectrometry and co-immunoprecipitation experiments. This finding could shed light on the differential organization and dynamics between TβRI and TβRII. It will be interesting to examine the spatial organization of cofilin relative to these receptors, and to later knockdown cofilin expression and observe any effects on TβR interactions or spatial organization. For example, if cofilin links TβRII to integrins, then perhaps its knockdown will result in a decrease of integrin αV in TβRII pulldowns or in a change of TβRII organization at sites of adhesion. A full spectra analysis of DYNLT1 is currently underway, but this protein could be very intriguing as it acts as an accessory component of the cytoplasmic dynein 1 complex that is thought to be involved in the linkage between dynein and proteins that regulate dynein function. This complex plays a regulatory role in motility of

vesicles and organelles along microtubules. Although the precise proteins and mechanisms underlying this TβR-integrin complex remain to be elucidated, these novel findings provide essential insight into the proteins that link the TGFβ and mechanotransduction pathways. These links might underlie the ability of cellular tension to regulate the spatial organization and signaling of TGFβ receptors at focal adhesions. Disruption of cellular tension through ROCK or myosin leads to a rapid collapse of this highly ordered, discrete spatial organization. This releases the confined TGFβ receptors and allows for multimerization between TβRI and TβRII. Indeed, disruption of cell tension through ROCK inhibition and by culturing cells on compliant substrates drives TβRI/II heteromerization. Culturing cells on these compliant substrates also drives downstream signaling, upregulating levels of Smad3 phosphorylation. We find that the effect of exogenous TGFβ on Smad3 activity is dependent upon the substrate stiffness. This suggests that the cellular response to the combination of these cues is not linear, and that an optimum environment might exist for activating TGFβ signaling. This optimum likely acts as a gradient that shifts during a cell's life cycle and is undoubtedly different between cell types. It will be interesting to examine any variations in the spatial organization and the optimum environment during differentiation, homeostasis, and disease. Additional work is also needed to determine the exact mechanisms by which this spatial organization regulates cellular functions related to TGFβ signaling, such as cell motility and differentiation. It will be interesting to elucidate the role of this spatial organization in processes like EMT or stem cell lineage selection where the physical and biochemical cues are highly integrated and extremely important for regulating cell behavior. Overall, we discovered a novel spatial organization of TGFβ receptors at sites of adhesions that is regulated by cellular tension and has important functional implications for downstream TGFβ signaling and cell behavior.

Appendix

Table A.1: List of generated plasmids

Protein	Tag	Use
TGFβ receptor type II	mCherry, C	Fluorescence
	mCherry, N	Fluorescence
	mEmerald, C	Fluorescence
	mEmerald, N	Fluorescence
	mEos2, N	sptPALM
	mGeos, N	sptPALM
	pSNAPF, N	Quantum dots
	mNeonGreen, N	FRET
	mTurquoise, N	FRET
	PS-CFP2, N	STORM
TGFβ receptor type I, Alk1	mCherry, N	Fluorescence
	mEmerald, N	Fluorescence
	mEos2, N	sptPALM
	mGeos, N	sptPALM
	mNeonGreen, N	FRET
	mTurquoise, N	FRET
	PS-CFP2, N	STORM
TGFβ receptor type I, Alk5	mCherry, N	Fluorescence
	mEmerald, N	Fluorescence
	mEos2, N	sptPALM
	mGeos, N	sptPALM
	mNeonGreen, N	FRET
	mTurquoise, N	FRET
	PS-CFP2, N	STORM
Integrin α2	mCherry	Fluorescence
	mEmerald	Fluorescence
	mEos2	sptPALM
	mGeos	sptPALM
	pSNAPF	Quantum dots
	mNeonGreen	FRET
	mTurquoise	FRET
	PS-CFP2	STORM
Integrin αV	mCherry	Fluorescence
	mEmerald	Fluorescence
Integrin α1	mCherry	Fluorescence
	mEmerald	Fluorescence
Integrin α5	mCherry	Fluorescence
	mEmerald	Fluorescence
FAK	mCherry	Fluorescence
	mEmerald	Fluorescence
Vinculin	mCherry	Fluorescence
	mEmerald	Fluorescence
Paxillin	mCherry, C	Fluorescence
	mCherry, N	Fluorescence
	mEmerald, C	Fluorescence
	mEmerald, N	Fluorescence
Filamin	mCherry	Fluorescence
	mEmerald	Fluorescence
Caveolin	mCherry	Fluorescence
	mEmerald	Fluorescence

Publishing Agreement

It is the policy of the University to encourage the distribution of all theses, dissertations, and manuscripts. Copies of all UCSF theses, dissertations, and manuscripts will be routed to the library via the Graduate Division. The library will make all theses, dissertations, and manuscripts accessible to the public and will preserve these to the best of their abilities, in perpetuity.

Please sign the following statement:

I hereby grant permission to the Graduate Division of the University of California, San Francisco to release copies of my thesis, dissertation, or manuscript to the Campus Library to provide access and preservation, in whole or in part, in perpetuity.

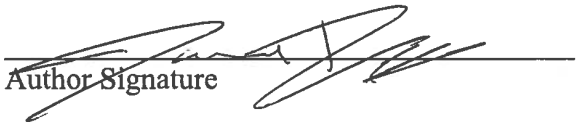

Author Signature

11/4/15

Date